NTNU – Trondheim
Norwegian University of
Science and Technology

Snaking Behavior of Umbilicals

Sharif Mohammad Moheudden

Abstract

Umbilical is a hardware element that connects the subsea systems to the top side systems of a floating production unit. During its manufacture, storage and installation, sometimes it shows behaviour like snake as found in three of the Aker Solution's umbilical Agbami, Droshky and kipper in three different situations.

An umbilical passes through many operations in the manufacturing plant like bundling, extrusion, reeling on and off the storage drum, transfer into installation vessel from storage reel. Different types of loading phenomenon may appear in these stages of operation. And from these loads even before being in the operation field, umbilical can experience different type of deformation in the manufacturing plant.

Curvature is the main source of umbilical deformation in the manufacturing field. Curvature may introduce directly in the umbilical from operation loads of straightener, creeping or squeezing effect in tensioner. Curvature may also arise from internal friction and unbalanced bending moment which arises from designs i.e. orientation, geometry and material property of the internal structural components.

To find the solutions of avoiding different deformations at the different stages of the manufacturing plant and to ensure desire comfortable handling, it is necessary to predict their behaviours correctly at different loading conditions. Exact analytical and numerical modelling is needed to find and predict the exact behaviours. In this thesis work, number of modelling and simulations have been done in software USAP and BFLEX to investigate the reason of snaking behaviour of three umbilicals, occurred in the manufacturing plant of Aker Solutions.

From the results of simulations it has found that umbilical Agbami experienced snaking when it was transferring from storage reel for installation work, due to having residual curvature from storage reel, gravity load and twisting rotation. The reason of residual curvature is creeping of its outersheath.

Umbilical Droshky showed snaking deformation because of having residual curvature in its component steel tubes. And, in umbilical Kipper snaking deformation arose because of developing internal friction in it.

In the different modelling of this work, PIPE31 element is used for the modelling of umbilical core pipe or outersheath and to model the inside helix elements HELIX231 element is used in USAP and HSHEAR353 element in BFLEX. The contact between pipe and helix element in BFLEX is modelled by HCONT453 element.

The software USAP and BFLEX has showed convergence problem in some cases of modelling. Improvement is needed to overcome these problems.

Scope of work as given by the Department of Marine Technology

MASTER THESIS SPRING 2014

for

Stud. tech. Sharif Mohammad Moheudden

Snaking behavior of Umbilicals
Buling av kontrollkabler

When an umbilical is manufactured and installed, it will be reeled on and off storage drums. In such cases the umbilical configuration at zero tension may change into a helix or other "snakelike" shapes. This project focus on identifying cases with respect to the parameters where this behaviour will occur and the evaluation of the resulting stresses.

1. Literature study including materials, manufacturing, mechanical performance and design.
2. Map the conditions where such behaviour has been observed.
3. Model an umbilical in USAP.
4. Identify critical input parameters (radial forces from insulation and outer sheeting, friction, lay angle, etc.)
5. Perform bending analyses of the Agbami umbilical cross-section at low tension with various assumptions related to friction and lay angle and including at least 3 pitch length reeling
6. For the cross-sections Kipper electric and Droshky, establish Usap models respectively using the following assumptions; that the helix elements are fixed by friction (Kipper), that the large diameter helix elements have a significant residual curvature (Droshky).
7. Perform parametric studies to with respect to residual curvature, friction and tensions and correlate the results in terms of snaking wave period to the in-field observations and pitch length
8. Potentially include more cross-sections and analyses to confirm hypotheses.
9. Conclusions and recommendations for further work.

The project assumes necessary inputs with regard to input data and cases where snaking behaviour has been observed are provided by Umbilicals Aker Solutions

The work scope may prove to be larger than initially anticipated. Subject to approval from the supervisors, topics may be deleted from the list above or reduced in extent.

In the thesis the candidate shall present his personal contribution to the resolution of problems within the scope of the thesis work

Theories and conclusions should be based on mathematical derivations and/or logic reasoning identifying the various steps in the deduction.

The candidate should utilise the existing possibilities for obtaining relevant literature.

Thesis format
The thesis should be organised in a rational manner to give a clear exposition of results, assessments, and conclusions. The text should be brief and to the point, with a clear language. Telegraphic language should be avoided.

The thesis shall contain the following elements: A text defining the scope, preface, list of contents, summary, main body of thesis, conclusions with recommendations for further work, list of symbols and acronyms, references and (optional) appendices. All figures, tables and equations shall be numerated.

The supervisors may require that the candidate, in an early stage of the work, presents a written plan for the completion of the work.

The original contribution of the candidate and material taken from other sources shall be clearly defined. Work from other sources shall be properly referenced using an acknowledged referencing system.

The report shall be submitted in two copies:
- Signed by the candidate
- The text defining the scope included
- In bound volume(s)
- Drawings and/or computer prints which cannot be bound should be organised in a separate folder.

Ownership
NTNU has according to the present rules the ownership of the thesis. Any use of the thesis has to be approved by NTNU (or external partner when this applies). The department has the right to use the thesis as if the work was carried out by a NTNU employee, if nothing else has been agreed in advance.

Thesis supervisors
Prof. Svein Sævik, NTNU
Specialist Engineer Technology Anne Marthine Rustad, Umbilicals Aker Solutions

Deadline: June 25th, 2014

Trondheim, January, 2014

Svein Sævik

Acknowledgments

Trondheim, June 2014   Sharif Mohammad Moheudden.

Notation

Abbreviations

3D	Three dimensional
B.M.	Bending moment
DOF	Degree Of Freedom
FEM	Finite Element Method
MBR	Minimum Bending Radius
MDPE	Medium-density polyethylene
M_e	Elastic bending moment
m_o	Master node of "o" element in USAP model
M_p	Bending moment, when plane section remains plane after loading
PVC	Polyvinyl chloride
PVD	Principle of Virtual Displacement
S_s	Slave node of "s" element in USAP model
STU	Steel Tube Umbilical
UMF	Umbilical manufacturers' federation
X-mas	Christmas

Characters

The Roman and Greek letters are used in this project work. All characters have explained in the main body when it has first introduced.

Roman

A   Cross sectional area

C_c Constraint coefficient for the master node number "c"

E   Modulus of elasticity

F_j Force along j axis

G   shear modulus of elasticity

I   Moment of inertia

I_t torsion moment of inertia

K_j Curvature about j axis

l length

M_i Moment about i axis

m_s distributed external torsion moment

R   Radius of curvature in curved beam

r_m Displacement of master node

r_s Displacement of slave node

S   Contact Force

s longitudinal direction in curved beam model of torsional instability

T   tension

w   distributed weight per unit length

Greek

α   Lay angle

δ   Downward displacement of simply supported beam

ε   Strain

Ө   Helix angle

$\kappa_{\eta r}$ Residual curvature about η axis

μ   Friction coefficient.

σ   Stress

η, ζ Transverse and vertical direction in curved beam model of torsional instability

υ Poisson ratio

Contents

Figures:

xiii

Tables:

Chapter 1 : Introduction

In this era of high energy demand around the world, people are exploring on subsea in search of new oil and gas resources. Many analysis, technology and instrument inventions are going on to make this journey efficient and easier. Umbilical is one of those important technologies whose are helping us to reach at seabed.

Norway is the fifth-largest oil exporter and third-largest gas exporter in the world. Oil and gas field are the biggest contributor in its economy. Most of the production units are in Sea bed and control of these subsea production units are very important for the efficient oil and gas production. Umbilical is the element which is used for the control of subsea production systems.

Aker Solutions ASA is one of the pioneer companies in the world, whose are working on designing and manufacturing of umbilical. They are continuing their research in the development of advanced umbilical system with well controlled production process.

The Department of Marine Technology at the Norwegian University of Science and Technology (NTNU) is the center for research and development of the marine engineering field in Norway. The department is providing solutions to the oil and gas companies regarding many of their practical field problems and taking initiatives for the advanced study and research in this area.

1.1 Motivation

Umbilical is used for the control of subsea oil and gas production unit. It is replacing rigid risers in the floating production system. Being flexible it provides number of facilities like not needing heave compensation for its stability in the operation field, easier to store and transfer in the manufacturing, installation and operation activities etc.

Because of flexibility, curvature develops easily in it; which is the main problem in flexible structure. In the manufacturing and installation activities regular and irregular helical or snakelike deformation (Figure 1.1) may arise because of this curvature. Such behaviour has experienced by few Aker umbilicals in some seldom cases which is the input of this work.

Umbilical is a group of functional components bundled together. Typical components of umbilical are Steel tubes, Electrical cables, Fibre optics, PVC conduits, Armouring, Outer sheathing etc. In the manufacturing process these component elements are first bundled up in a closing machine from their individual storage reel and then pass through the extruder to attach the outer sheath. The extruded umbilical through some turntables then pass onto the storage reel where it stored before it move to the installation vessel.

During these manufacturing and transferring activities in the manufacturing plant different types of loads may be applied in the umbilicals. From these loads curvature may arise in it. Like in the manufacturing plant construction of umbilical starts from the straightening machine where the curve on the component steel tubes are straighten by putting pressure and if insufficient pressure is put then curvature may remain in the component steel tubes which after bundling and extrusion may bring curvature in the whole umbilical structure.

During the extrusion process hot outersheath plastic is attached in the closed umbilical after which it is cooled by spraying chill water, so in this quick heating and cooling action permanent curvature can develop in the umbilical due to the metallurgical reasons.

After extrusion umbilicals are put in turntable. So if it bears curvature from the extrusion process and faces opposite curvature from turntable radius then irregularities may arise on its shape.

Before moving for installation umbilicals may stored for a period of time when it can be attacked by creeping load and plastic curvature may arise.

Also umbilical is needed to bend during storage and installation work. Excessive bending can result local buckling. So, umbilical has minimum bending radius (MBR) which defines its bending capacity and limit of bending.

Figure 1.1: Snakelike configuration in a deformed umbilical.

The design and orientation of internal structural component can also affect the snaking behaviour of umbilical. In umbilical numbers of components are bundled inside the umbilical structure, which come in contact and slide relative to one another when get contact load, so internal friction and stresses can develop, which can interrupt the structural integrity and stability. Also since inside elements have helical layout, so in high tension load they can tend to twist which can eventually introduce deformation in the whole umbilical.

Also when a helix element is put in tension radial force is generated and then bending moment can arise on it. Since the lay angle is not that much the radial force and subsequent bending moment magnitude will not such big to create snaking. But it can add some reason with the others. Low lay angle has also the advantage of providing high torsion stability.

When a flexible structure like umbilical behaves like snake, there could be challenges to handle it. Snaking causes problem in the installation and manufacturing work, it also introduce structural deformation in the umbilical which is not desired. So it is important to know the conditions or cases of this behaviour to discover the ways of controlling it.

Software modelling is a very efficient way of structural analysis nowadays. This not only reduces the time and complexity of doing physical test, but save a great amount of cost also.

USAP, SIMLA, UFLEX and BFLEX are the softwares developed by MARINTEK for the analysis of flexible structures, can be use for the analysis of umbilical. USAP and UFLEX are only for umbilical stress analysis. BFLEX is for flexible risers stress analysis and SIMLA is for the stress analysis of pipe. The elements of these softwares are established by comparing the results with corresponding physical model test, published in many paper and article works. Many companies are using these softwares in their design and analysis tasks.

The main focus of this thesis work has been on finding the reasons of the snaking scenarios occurred in the Aker's manufacturing plant. For this, software modelling of the possible snaking phenomenon will be performed by using different established features of the finite element software USAP[1, 2] and BFLEX[3, 4].

The knowledge for the study of this thesis work is a blend of three disciplines (Figure 1.2).
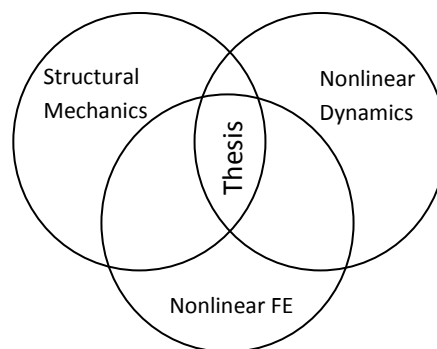
Figure 1.2: Competences needed in this work

1.2 Main Contributions

The simulations and results of the models developed in this work, mainly figure out the effect of friction and residual curvature on creating snakelike deformations in umbilical.

Three snaking events of three different umbilicals were chose as the task for this thesis work. Six modelling has been done in total to invent their snaking reasons. The description of this work, establish some approaches to model the snaking scenarios of umbilicals, considering the physical features of the snaking events. The model established will help in future to do the analysis of similar snaking events.

Comprehensive explanations of the deformation reasons have also been prepared connecting the related theories.

1.3 Organisation of the Thesis

Chapter 2: Brief introduction about umbilical, typical umbilical components and the manufacturing process of umbilical.

Chapter 3: Characteristics of the loads umbilical experiences and behaviour of umbilical under these loads

Chapter 4: Presentation of an analytical model formulates the torsional instability event and finite element formulations in USAP and BFLEX

Chapter 5: The input models has presented in this chapter. The possible phenomenon of snaking deformation of each model has described and defined, these phenomenons has eventually modelled in the modelling chapter.

Chapter 6: Modelling descriptions.

Chapter 7: Presentation of the results and their analysis.

Chapter 8: Conclusion of this work and proposals for the future work.

Chapter 2: Umbilical Technology

Umbilical is a link between the subsea production unit and a remote place from where power, communication and chemical services are provided into the unit. It (Figure 2.1) is a group of functional components bundled together. For making the bundle, usually one element is placed at the core of the umbilical – which may be a power cable, steel tube or a bundle of steel wires. The other components are placed around the core. Fillers are placed between the components to provide a stable construction. The bundle is armoured with thermoplastic polymer like MDPE (Medium-density polyethylene) to provide mechanical strength, protection and ballast to the bundle components.

Umbilical is a very hi-tech product. The design of umbilical is need to be highly reliable with high strength and safety. Any damage in the structure during operation may result in a disaster in the subsea oil and gas production system with a large economical effect.

Figure 2.1: Example of umbilical cross section, [5]

2.1 Umbilical Components

Umbilicals are used to supply necessary control, energy (electric, hydraulic) and chemicals to the subsea oil and gas production and installation unit. It is a combination of many different components with different functions.

Typical umbilical components are:

Fluid conduits: Umbilical contains fluid conduits for the transportation of chemical injection fluids. Two types of fluid conduits are used in umbilical, steel tubes (marked 1 in Figure 2.2) and thermoplastic hoses (Figure 2.3). Steel tubes are stiffer than thermoplastic hoses and have high tensile strength. One umbilical can have combination of both steel tubes and thermoplastic hoses for design or economical optimization. Different tubes are used for different applications like, hydraulic tubes are used for the transport of hydraulic fluids on the X-mas tree or manifold

for hydraulic control of valves. Chemical tubes are used for the injection of chemicals to the subsea production unit. Chemicals mainly injected are-

- Scale inhibitor: injected on X-mas tree or downhole, to prevent scale formation and remove scale deposits at the formation face and on downhole equipment.
- Corrosion inhibitor: injected on manifold, to prevent corrosion and reduce corrosion rate by forming a protective coating on metal surfaces.
- Gas: injected on downhole and lower riser end to increase the production rate by reducing wellbore flowing pressure.
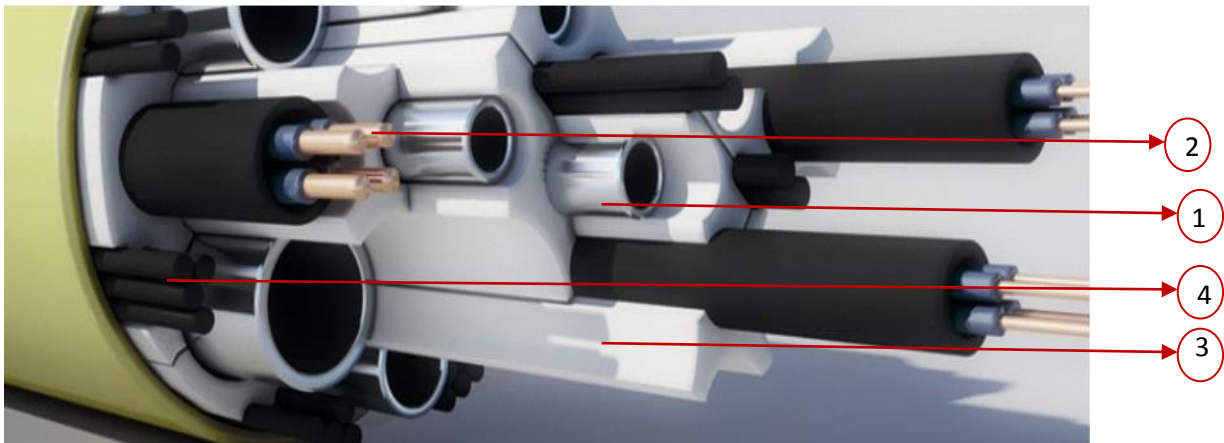
Figure 2.2: Components in an Umbilical, [5]

Weight elements:

- Steel wire: to increase the weight of the umbilical required for seabed stability.
- Steel tape: to increase seabed stability or for armoring.

Fibre optics: Transfer/receive signals to/from the subsea control module for monitoring purposes.

Electrical cables (marked 2 in Figure 2.2): For control and low voltage power supply. Power is required to operate the valves on subsea X-mas tree and through valves the stream of fluids from well is controlled.

Armouring (Figure 2.3): main functions

- Adding weight.
- Providing tensional balance.

PVC conduits (marked 3 in Figure 2.2): the main functions of this portion are

- Separating and spacing the components and letting them to move freely in their pockets.
- Protecting the internal components from impact loads by absorbing the impact energy through plastic deformation.
- Providing individual support to each of the internal components by preventing the build up of accumulated radial contact force.
- Providing capability of taking high loads in installation tensioner.

■ Providing high cross section lay-out flexibility.

Carbon fiber rod (marked 4 in Figure 2.2): To increase axial stiffness of the umbilical; required to face high strain in deep water application.

Outer sheathing (Figure 2.3):

■ To keep the umbilical bundle together.
■ To provide protection during handling and installation.
■ To have good visibility during installation.
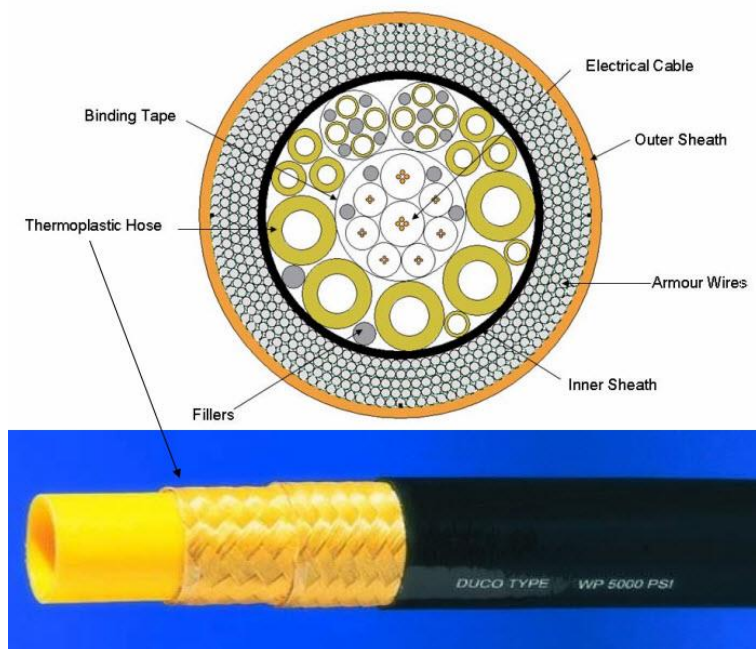
Figure 2.3: Umbilical cross section, [www.2b1stconsulting.com]

2.2 Types of Umbilical

Dynamic: Length of umbilical which is connected between host facility and seabed through the water column. Host facility could be a floating system or a fixed platform. So the dynamic umbilical faces dynamic loading from waves, currents and in case of a floater, the motions of the platform or vessel. The components of dynamic umbilical are normally manufactured by applying a helix configuration.

Static: Length of umbilical puts on sea bed, so faces static load only. Besides helix configuration, components of static umbilical may also be manufactures by Sz method which allows manufacturing of long lengths with a minimum of splices of high voltage cables. Sz method introduces transverse curvature along the initial curve path which is not done in helix method.

Static and dynamic lengths can be manufactured as one unit or as separate, which can be joined with a transition joint.

2.3 Manufacturing

All the components are brought together into a perfect bundle giving the cross section in a closing machine. This process is called CLOSING. After closing, the bundle passes through the extruder where a layer of polyethylene outer sheathing is melted around it. This process is called EXTRUSION. The extruded umbilical is then stored by spooling on the storage reel or transfer to the installation vessel.

Closing is done in two orientations:

1. Horizontal closing (Figure 2.4)
2. Vertical closing (Figure 2.5)

Picture of extruded umbilical has shown in Figure 2.6

Figure 2.4: Closing machine (horizontal), [6]

Figure 2.5: Closing (vertical), [7]

Figure 2.6: Closed (left) and Extruded (right) umbilical, [6]

Lay-up or the assembling of umbilical components into a bundle is done in two ways.

1. Planetary lay-up [8]:
   In this method the elements to be cabled together are continuously rotated in the same direction around the axis of the cabled product, such that the elements are incorporated in the form of continuous helices (Figure 2.7).

2. SZ or oscillatory lay-up [8]:
   In this method the elements to be cabled together are rotated around the axis of the cabled product, typically 360°-720°, followed by a reversal in the direction of rotation for a similar level of angular rotation, after which the rotation sequence is repeated (Figure 2.8).
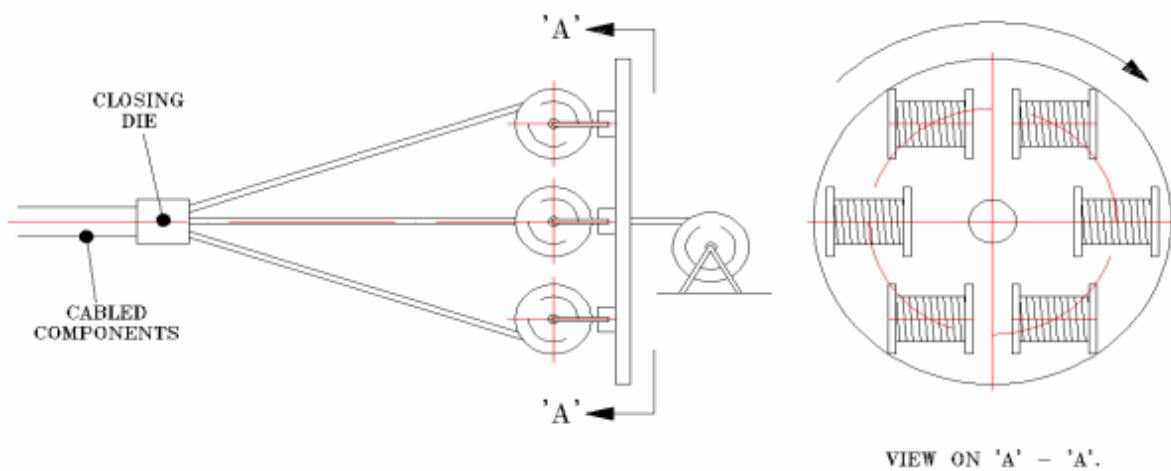
Figure 2.7: Planetary lay-up, [8]
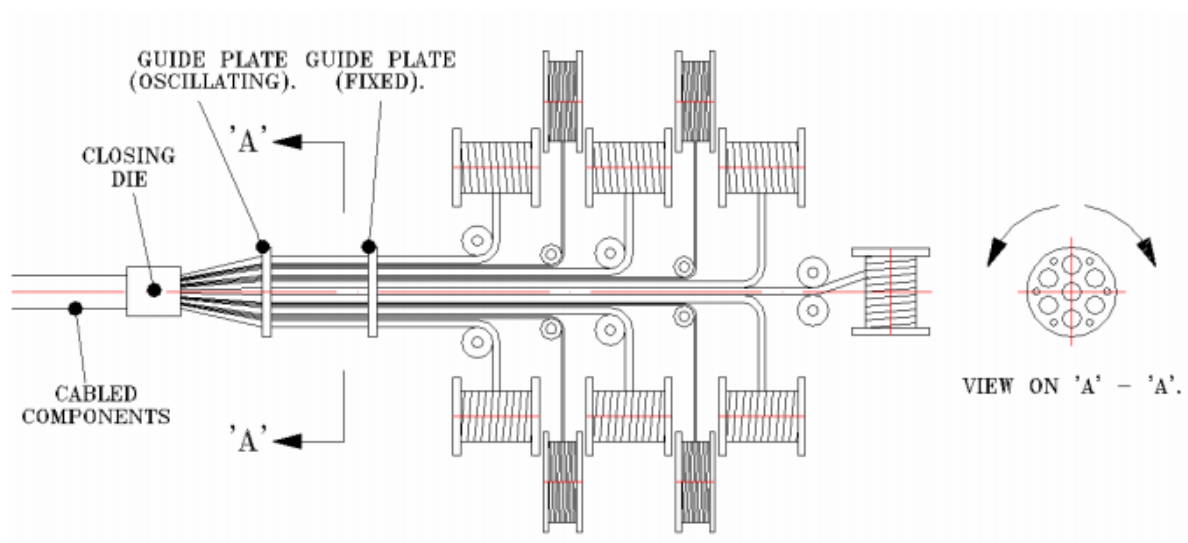
Figure 2.8: SZ or oscillatory lay-up, [8]

2.4 Straightening Process of Umbilical

In the straightening process umbilical faces plastic deformation of same amount as the curvature have in it, in opposite direction so that it become curvature free that is straight (Figure 2.9). Here point B indicating the residual curvature of umbilical at storage reel and point A is the curvature free point obtained after straightening action. So BA is the opposite curvature put on umbilical by straightener machine.
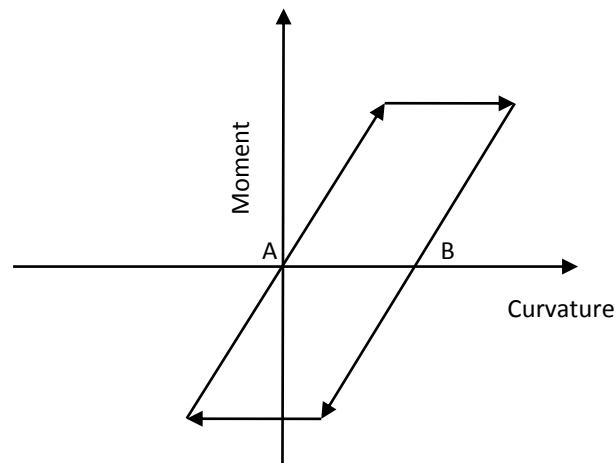
Figure 2.9: Straightening by putting opposite curvature

In a roller straightener umbilical passes through rollers, which roll eccentrically to the umbilical and put pressure on it [9]. Rollers provide bending support to the umbilical in the contact point to remove residual curvature from it. The setting of straightener is adjusted by changing the number of rollers, position of the rollers and the amount of pressure apply by these.
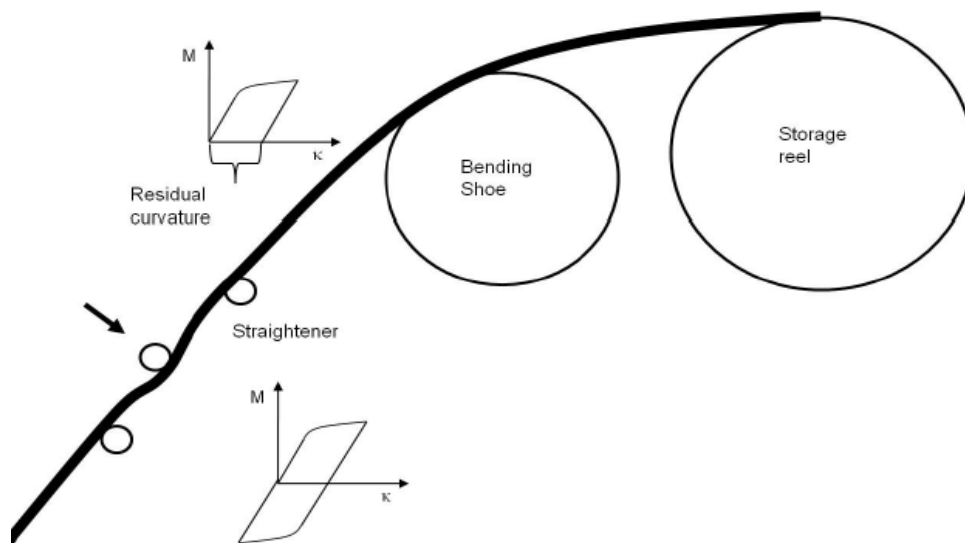
Figure 2.10: Straightening arrangement with bending shoe, [10]

An umbilical can have various amounts of curvatures along its length. But, straightener is set to provide a certain amount of opposite curvature. So curvature may remain in the umbilical in this case. To overcome this there need arrangement of bending shoe (Figure 2.10) in the straightening process. Bending shoe is placed before the straightener rollers. Bending shoe bend the whole umbilical with same curvature. So rollers only need to straight this curvature and there is no scope of remaining curvature in the umbilical. Figure shows three roller straightening arrangement with bending shoe. The mid roller is placed eccentrically at the top of the umbilical to bend it in the opposite direction of residual curvature.

Chapter 3: Mechanical Behaviour

To analyse the deformation nature of any structure it is important to know about its mechanical behaviour, that is the response of the structure against different loads. Mechanical behaviour of a structure depends on its geometrical and material properties. Umbilical is a cylindrical shaped flexible structure which is made strong and stiff against internal pressure, external pressure, tension and torque but it made deformable in bending so that it can wound around reel. Bending limit is defined by the parameter Minimum Bending Radius (MBR). This thesis work is concern about the loads on umbilical during manufacturing and installation work where these loads are present but in a minor severity. So it is necessary to know about the nature of these loads to understand the umbilical's behaviour under these loads. Different kinds of load that act on the umbilical and behaviour under these load has described in the proceeding of this chapter.

3.1 Type of Loads:

Umbilical is a bundle of elements covered by outersheath. Elements like tube, cable and wire have helix configuration and place with certain lay angle and pitch length inside the bundle. Loads act on umbilical during manufacturing and installation work are:

- Global curvature in reel and turntable
- Internal friction from sliding between the elements under transferring tension and curvature
- Creeping load from long storage time
- Residual curvature of the steel tube from straightener machine and on whole umbilical from creep load

Umbilical experiences elastic bending moment from the global curvature. It behaves as an Euler beam as long as plane surface remain plane that is until the shear stress at the neutral axis of bending exceeds the limit which is governed by the contact pressure and friction coefficient at each surface. Friction effect arises due to the sliding between the structural components which increases with the increase of tension. Contact pressure depends on the axial strain of the umbilical and residual elastic bending moment of helixes after manufacturing. Effects like dynamic tension and curvature gradient due to bending influence the contact pressure and create nonlinear helix stress, [11]
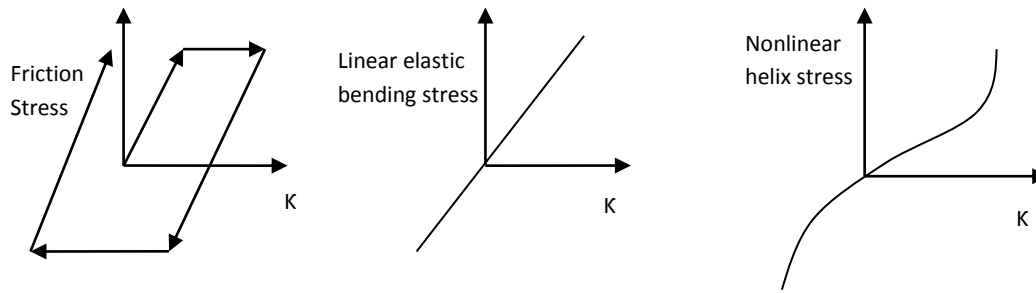
Figure 3.1: Dynamic stress contribution in umbilical, [11]

For the convenience of analysis and finite element formulation loads are divided into two categories:

Axisymmetric load: Load that only changes the length and diameter of a straight cylindrical pipe such as tension, torsion, internal and external pressure loads. Under this load, stresses related to the torsion and bending are not significant and stresses resulting from the axial load govern the deformation.

Bending loads: This will bend the straight cylindrical pipe. Axial, bending and torsion all are required for finding the bending deformation. For bending loads, the local bending moments and associated stresses are calculated from differential geometry by assuming either the geodesic or loxodromic curve path along the helix of a curved cylinder. Loxodromic curve represents the initial path which is obtained by considering the path as fixed relative to the cylinder surface. Geodesic curve represents the shortest distance between two points of a pipe, one on the tensile side and one on the compressive side of the pipe along the same helix.
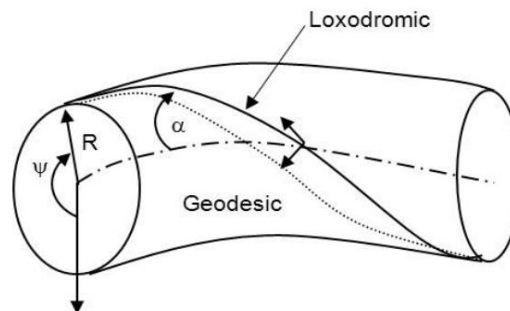
Figure 3.2: Definition of curve paths, [10]

3.2 Behaviour due to Axisymmetric Load:

With axisymmetric load the cylindrical straight pipe shape is kept during deformation. Steel tube in umbilical rest stress free in the helix configuration, this is done by involving plastic straining in their manufacturing process. According to Figure , the initial torsion K_1 curvature along the helix (K_2 and K_3) can be expressed by lay angle (α)and helix radius (R) as [10]

$$\kappa_1 = \frac{sin\alpha cos\alpha}{R} \tag{3.1}$$

$$\kappa_2 = \frac{sin^2\alpha}{R} \tag{3.2}$$

$$\kappa_3 = 0 \tag{3.3}$$

Here the Figure is for tendon wire having rectangular cross section. For steel tube the cross section will be circular and the torsion and curvature expressions will be same.

Long steel pipe character in axisymmetric load can be described curved beam theory. By using the equilibrium equation found from curved beam theory and considering axisymmetric load only the contact pressure line load in q_3 is obtained as, for details, see chapter 7.4 in [10]

$$q_3 = \kappa_2 Q_1 = \frac{sin^2\alpha}{R} Q_1 \tag{3.4}$$

Q_1 is the axial load.
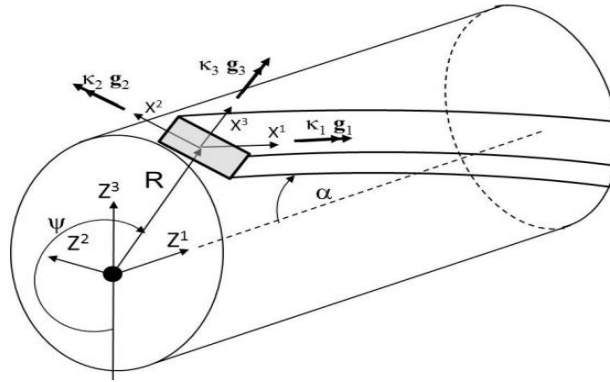
Figure 3.3: Initial torsion and curvature quantities, [10]

3.2.1 Finding Axial and Torsion Stiffness:

The axial stiffness of an umbilical having n number of steel tubes and considering no coupling with torsion, is found as, [10]

$$EA = \sum_{1}^{n} EAcos\alpha(\,cos^2\alpha - v_a sin^2\alpha) \tag{3.5}$$

Torsion stiffness of the same umbilical can be find as, [10]

$$GI_t = \sum_{1}^{n} EA\,R^2 sin^2\alpha\,cos\alpha \tag{3.6}$$

Excessive torsion can damage the umbilical structure. Application of axial tensile force will prevent torsional failure and for this it is important to know the torsional strength of umbilical.

15

3.3 Behaviour in Bending Load:

The behaviour of umbilical under bending loads is more complex phenomenon to analyse than the axisymmetric behaviour. Internal friction, global curvature, contact pressure these are the main contributors of umbilical's bending behaviour.

The bending behaviour of umbilical can be explained by the moment-curvature relation as in Figure 3.4. When the curvatures are small internal friction effect is dominant, results in a high initial tangent stiffness EI_p which is found by taking the sum of bending stiffness contributions of each component element taking plane surface remain plane as for standard beam theory.

When the friction moment is exceeded, the slope of the moment-curvature line is changes to the elastic bending stiffness EI_e which is the sum of elastic bending ($M=EI\kappa$) contribution from all the component elements. This stiffness is lower than the previous one.

Friction moment M_f is the moment needed to overcome the friction forces. Friction moment depends on contact pressure and consequently on the loads applied to the umbilical.
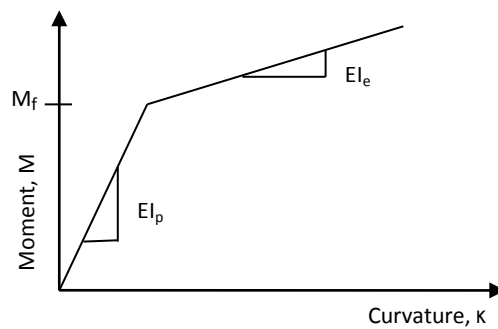
Figure 3.4: Typical moment curvature diagram of umbilical, [10]

3.3.1 Finding Bending Stiffness

When the amount of curvature is small, umbilical behaves as a rigid pipe according to the Navier's hypothesis and the assumption of plane surface remain plane is valid. The bending stiffness in this state, EI_p can be calculated as following:
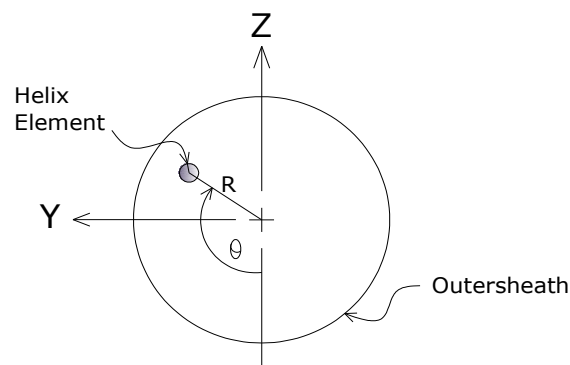
Figure 3.5: Umbilical cross section with orientation of a helix element.

Consider a helix element which is at R radius from the center with an angular position Ө with the negative Z axis as in Figure 3.5. Now if the element experiences a curvature κ, due to global curvature in the umbilical.

Strain develop at the helix element, $\varepsilon = \kappa.R\cos Ө$ (3.7)

So, bending stress is, $\sigma = E.\varepsilon$ (3.8)

Force, $F = \sigma.A$ (3.9)

Bending moment, $M = F.R\cos Ө = E.A.R^2. \cos^2 Ө.\kappa$ (3.10)

Also, moment, $M = E.I.\kappa$ (3.11)

From the above two equation bending stiffness contribution of one helix $EI_p = E.A.R^2. \cos^2 Ө$

(3.12)

Stiffness of whole umbilical will find by summing the contribution of each helix as

$EI_p = (E.A.R^2. \cos^2 Ө)$ (3.13)

This expression has dependency on Ө which changes along the length for each element due to the helical configuration of the element according to

$$\theta = \theta_0 + \frac{L_s}{L_p} \times 2\pi$$ (3.14)

Where, L_s is the distance of the considering section from the section where it has $Ө_0$ angular position and L_p is the pitch length of the helix element. Value of Ө will be calculated from above equation considering its limit between [0 to 2π].

So the expression of EI_p of Equation 3.13 is the bending stiffness on a certain section of the umbilical along its length and the stiffness value will differ along the length.

3.4 Friction Moment Development in an Umbilical During Reeling

For the reeling action of an umbilical a certain tension is needed. The moment development can be observed by following the reeling of a certain section of the umbilical.

Before reaching the reel only tension load acts on the umbilical elements, which introduce sliding between the elements and as a result internal friction develops.

When the umbilical reach the reel, then curvature starts to increase. It experiences contact pressure beside the tension load from the contact with reel. This contact pressure increases as it reel more according to the equation next page,

$S = S_0 e^{\mu \Theta}$ (3.15)

Here,

S_0 = contact pressure at B

S = contact pressure at B

Θ = angle between A and B at roller center.

μ = friction coefficient.
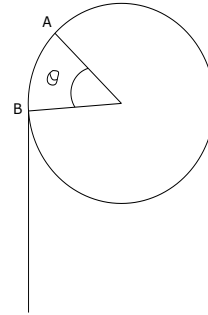
So with the increment of reeling amount elastic bending moment increases due to curvature increment according to Equation (3.11) and friction moment increases due to increase of contact load according to Equation (3.15).

During reeling off elastic bending moment and contact load decreases according to Equation (3.11) and (3.15). So the total moment decreases. But the moment decrement line during reeling off do not follow the same line of moment increment during reeling on and hysteresis appear in the process as in Figure 3.6 below.
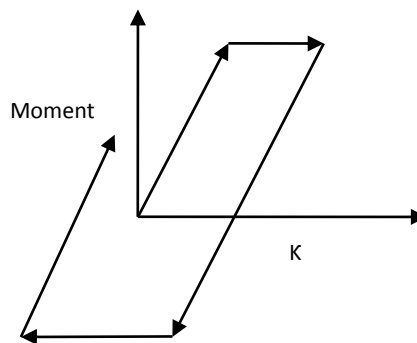
Figure 3.6: Moment-curvature hysteresis.

Due to hysteresis umbilical have curvature at zero moment which is the stage when umbilical has left the reel. So the umbilical will not be straight when reel off depending on the hysteresis from friction effect. Friction originates from the sliding between the internal elements. Sliding amount proportionally depends on the lay angle of the helix elements.

This friction moment dissipate energy from the section. The area under this loop is the amount of energy dissipates from the section due to development of friction.

The internal friction between the umbilical components deviate the elastic relationship of moment and curvature. Larger the hysteresis area, more friction is involved in the process and more nonlinearity in the moment-curvature relationship is observed.

For an umbilical which has positive X axis along its length, total moments at any section of umbilical are found by summing the moment contribution from all element groups as:

$M_x^{total} = \Sigma\ (M_x + F_x.R.sin\alpha)$, total moment about X axis

$M_y^{total} = \Sigma\ (M_y - F_x.R.cos\Theta)$, total moment about Y axis $\qquad$ (3.16)

$M_z^{total} = \Sigma\ (M_z - F_x.R.sin\Theta)$, total moment about Z axis

Here, M_x, M_y, M_z are the torsion moment contribution due to twisting of the section.

$F_x.R.sin\alpha$, $F_x.R.cos\Theta$, $F_x.R.sin\Theta$ are the torsion moment contribution from the eccentricity of the applied force, due to lay angle (α) and helix angle (Θ) of each helix. R and Θ have defined in Figure 3.5 and Equation 3.14.

3.5 Second order helix effect:
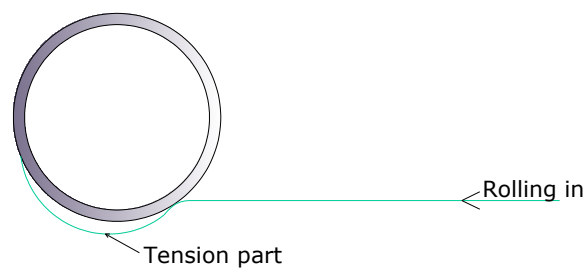
Figure 3.7: Tension part in an umbilical, when it is rolled in.

Second order helix effect is a very important cause of internal friction generation. When an umbilical is spooling in, then a tension part is created as in Figure 3.7 due to second order helix effect and this tension part pull the lower part of the umbilical. This pull created sliding between the helical umbilical components and due to this sliding internal friction is generated in the umbilical. Second order helix effect proportionally depends on lay angle.

3.6 Creeping

Creep is a time-dependent plastic deformation which severity mainly depends on the magnitude and duration of the applied stress and temperature (Figure 3.8). It can occur as a result of long-term exposure to high levels of stress that are still below the yield strength of the material because of the accumulation of strain for a long time.
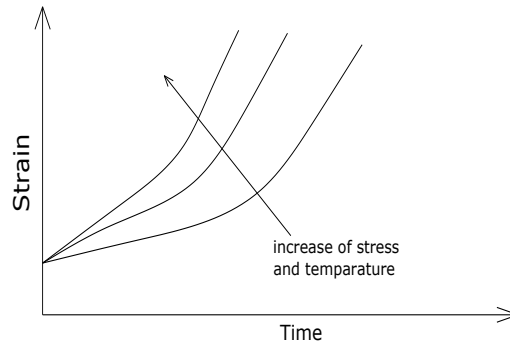
Figure 3.8: creep curve, [12]

Creep is more severe in materials that are subjected to heat for long periods, and generally increases, when the temperature is near their melting point. Low-melting-temperature metals can begin to creep even at room temperature.

The outer sheath material of the umbilical (Agbami) is made of Medium-density polyethylene (MDPE), which material properties are:

Density range	$0.926–0.940$ g/cm^3
Young modulus	172–379 MPa
Tensile strength	12.4–19.3 MPa
Specific heat	1.916 kJ/kg.K
Crystallinity	70% -80%,
Brittleness, low temperature	-118 °C
Elongation	50% -60%
Heat distortion temperature (at 0.46 MPa)	49-74 ° C
Melting temperature	126-135 ° C

Table 3.1: Material properties of MDPE, [13]

Although MDPE has good flexibility but due to its low melting point and poor thermal properties it has relatively poor creep resistance.

When umbilical is in the storage reel for long time, then it is residing with constant bending stress due to the curvature from the storage reel. So umbilical may have creep deformation and consequently may experience plastic curvature which magnitude will vary along its length depending on its wounding radius on the reel. This process will also be affected by the temperature of the storing time.

So when the umbilical will unreel, then it will come out with residual curvature and will have helical or snakelike deformation.

Chapter 4: Literature Review

At the beginning of this chapter an analytical model will present which can describe the criterion of appearing torsional instability in umbilical. In finding the snaking behaviour of Agbami, a numerical model will develop following this analytical model.

In the remaining parts of this chapter finite element formulation and solution procedure used in USAP and BFLEX computer programmes will present.

4.1 Analytical Model of Torsional Instability

When a straight cylindrical structure like umbilical which has the nature of ideal elasto plastic material like in Figure 4.1(a) is reeled off from the storage reel, the moment curvature relation will take the form as shown in Figure 4.1(b). In the storage reel the umbilical may be exposed to plastic strains. Amount of strain is governed by the radius of curvature of the storage reel rather than external load.

M_y is the yielding moment, the curvature at this moment is K_o which is fully elastic. If the moment applied M_1 is larger than yielding moment, then the part of total curvature (K_1) at this moment will be elastic (K_e) and the other part will be plastic (K_r) due to plastic strain. This plastic curvature will not removed from the umbilical and will reside on it, even when the applied moment M_1 is removed and this is called residual curvature. So if the umbilical is bent to the value M_1 in the storage reel as indicated in the figure 4.1(b) residual curvature will result as unreeled to M=0, which means the umbilical is no longer straight when it is out of the storage reel.
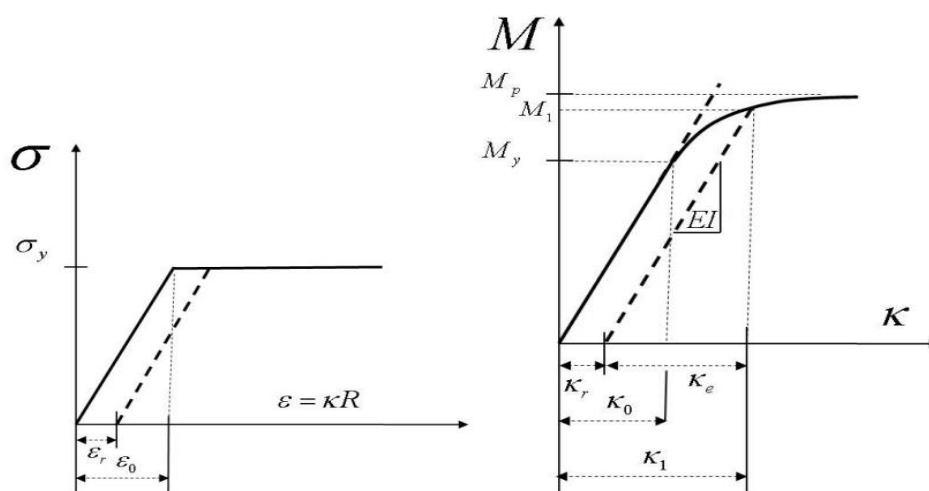
(a) Ideal elastic-plastic material   (b) Residual curvature from plastic bending

Figure 4.1: Moment-curvature relation, [10]

This residual curvature in the storage reel may also appear from creeping as described in Chapter 3.6.

In the installation vessel when the umbilical transfers from storage reel, it crosses an unsupported portion between the storage reel and installation chute. Where, due to gravity load umbilical will curve in the downward direction as in Figure 4.2 below, like a simply supported beam with uniformly distributed load (w).
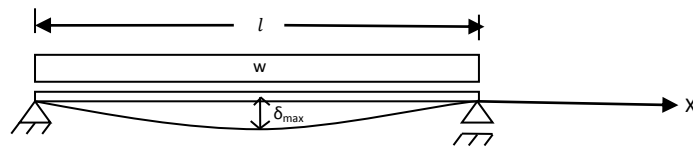
Figure 4.2: Simply supported beam, representing the unsupported umbilical length under gravity load.

The maximum magnitude of this curve is at the center,

$$\delta_{max} = \frac{5wl^4}{384EI} \tag{4.1}$$

But in the installation process there will be some tension along X direction, so the above expression will be modified as

$$\delta_{max} = \frac{5wl^4}{384EI} \left[\frac{1}{\left(1 + \frac{Tl^2}{\pi^2 EI}\right)} \right] \tag{4.2}$$

So the umbilical have curvature from gravity load and may have residual curvature from the storage reel. Now, if the residual curvature is in the opposite direction of δ then torsional instability can occur.

The criterion for occurring torsional instability due to a curvature on an opposite curvature, has described by S. Sævik in [10], which has presented here:

The criterion for torsional instability can be evaluated from the differential torsion equation of a curved beam as shown figure 4.3.

$$\frac{\partial Ms}{\partial s} - \kappa_\zeta M_\eta + \kappa_\eta M_\zeta + m_s = 0 \tag{4.3}$$

Where, M_s, M_η, M_ζ are the moment about s, η and ζ axis.

M_s is torsion moment and M_η is Bending Moment

κ_ζ and κ_η are the curvature about ζ and η axis respectively in an arbitrary equilibrium state.

m_s is distributed external torsion moment which is neglected here.
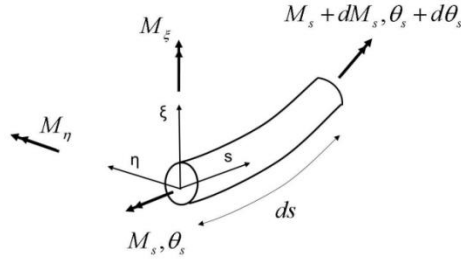
Figure 4.3: Curved beam coordinate system and curvatures

The moments and curvatures are taken positive when the components are associated with a positive rotation when moving a small positive distance along the s axis. Neglecting the deformations in the ζ direction and by taking the residual state characterised by its curvature $\kappa_{\eta r}$ as the reference state, the moment about z axis can be expressed as

$$M_\zeta = EI(-\Delta\kappa_\eta)sin\theta_s \qquad (4.4)$$

This means, the moment potential available to cause torsion instability increases as the pipe is being straightened by an increment of the $\Delta\kappa_\eta$ from the $\kappa_{\eta r}$ state. By introducing Equation 4.4 and St. Venant torsion expressed by:

$$M_s = GI_t \frac{\partial\theta_s}{\partial s} \qquad (4.5)$$

Into Equation 4.3 and neglecting m_s, the following differential equation is obtained

$$GI_t \frac{\partial^2\theta_s}{\partial s^2} - \kappa_\eta EI(\Delta\kappa_\eta)sin\theta_s = 0 \qquad (4.6)$$

Writing $\kappa_\eta = \kappa_{\eta r} - \Delta\kappa_\eta$ from Figure 4.4

$$GI_t \frac{\partial^2\theta_s}{\partial s^2} - EI(\Delta\kappa_\eta)(\kappa_{\eta r} - \Delta\kappa_\eta)sin\theta_s = 0 \qquad (4.7)$$

If θ_s is small, then $sin\theta_s \approx \theta_s$. So Equation 4.7 is modified into a standard second order differential equation as:

$$\frac{\partial^2\theta_s}{\partial s^2} - \frac{EI}{GI_t}(\Delta\kappa_\eta)(\kappa_{\eta r} - \Delta\kappa_\eta)\theta_s = 0 \qquad (4.8)$$

Solution of the above equation depends on the sign of $(\kappa_{\eta r} - \Delta\kappa_\eta)$

If the umbilical still have a positive total curvature i.e. $(\kappa_{\eta r} > \Delta\kappa_\eta)$ then the solution will have hyperbolic functions. If $(\kappa_{\eta r} - \Delta\kappa_\eta)$ is zero i.e. $(\kappa_{\eta r} = \Delta\kappa_\eta)$, then there is no residual curvature and the umbilical is straight. A linear function of θ_s will be the solution in this case. Now, if the umbilical is in a stage where the total curvature is negative i.e. $(\kappa_{\eta r} < \Delta\kappa_\eta)$, the general solution will given by trigonometric functions as:

$$\theta_s = C_1 cos\kappa s + C_2 sin\kappa s \qquad (4.9)$$

Where κ is found from the coefficient of Θ_s in Equation 4.8, as:

$$\kappa = \sqrt{\frac{EI}{GI_t}\left(\Delta\kappa_\eta(\Delta\kappa_\eta - \kappa_{\eta r})\right)}$$ (4.10)

Introducing the boundary conditions that, Θ_s=0 at s=0 and s=l, a non-trivial solution requires that

$$Kl = \pi$$ (4.11)

From the above two Equations

$$\kappa^2 = \frac{EI}{GI_t}\left(\Delta\kappa_\eta(\Delta\kappa_\eta - \kappa_{\eta r})\right) = \frac{\pi^2}{l^2}$$

Or, $\Delta\kappa_\eta = \frac{1}{2}\kappa_{\eta r}\left[1 + \sqrt{1 + \frac{(2\pi)^2}{\frac{EI}{GI_t}(l.\kappa_{\eta r})^2}}\right]$ (4.12)

So, when the reversed curvature is larger than the initial curvature then, torsional instability is resulted. For a beam of length l and having curvature of amount $\kappa_{\eta r}$, the required amount of reversed curvature will be found from Equation 4.12. The ratio of bending stiffness (EI) and torsional stiffness (GI$_t$) is depends in the material property of the beam. Introducing $G = \frac{E}{2(1+v)}$ and I$_t$=2I the expression of reversed curvature becomes:

$$\Delta\kappa_\eta = \frac{1}{2}\kappa_{\eta r}\left[1 + \sqrt{1 + \frac{(2\pi)^2}{(1+v)(l.\kappa_{\eta r})^2}}\right]$$ (4.13)

When l tends to infinity, then$\Delta\kappa_\eta = \kappa_{\eta r}$. So the torsional instability will occur for any negative total curvature i.e. when$\Delta\kappa_\eta > \kappa_{\eta r}$. Curvatures amount has shown in Figure 4.4 below
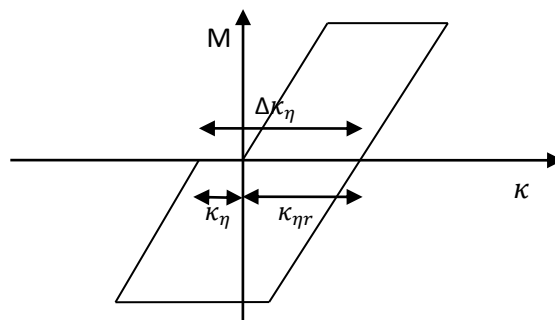
Figure 4.4: Curvatures

$\kappa_{\eta r}$ = initial or residual curvature about η axis.

$\Delta\kappa_\eta$ = curvature applied in direction opposite to the $\kappa_{\eta r}$

$(\Delta\kappa_\eta - \kappa_{\eta r})$ = magnitude of opposite curvature when $\Delta\kappa_\eta > \kappa_{\eta r}$

From Equation 4.13, it can say that for a model of certain length, shorter the residual curvature($\kappa_{\eta r}$), larger the reversed curvature ($\Delta\kappa_\eta$) required to get torsional instability; again for a model having certain residual curvature, shorter the model, larger the reversed curvature ($\Delta\kappa_\eta$) required to get torsional instability.

S. Sævik [10] has done a test modelling in USAP to check Equation 4.13, with a model of 1000 meter suspended length. Where residual curvature ($\kappa_{\eta r}$, column 2 of Table) has applied as initial curvature and opposite curvature κ_η (column 5 of Table) from Equation 4.13 has applied by bending moment (M=$EI\kappa_\eta$) at the ends of model. A fixed-pinned boundary condition was applied from the ends. Then a restart was carried out where all end DOFs were defined fixed in the local coordinate system except the torsion at one end where a prescribed rotation was introduced.

Case	$\kappa_{\eta r}$ (1/m)	Required $\Delta\kappa_\eta$ From Eq. 4.13 (1/m)	Required $\kappa_\eta = \frac{1}{\frac{1}{\Delta\kappa_\eta} - \frac{1}{\kappa_\eta}}$ (1/m)	Applied κ_η(1/m)
1	0.003	0.005	0.0016	0.0005
2	0.003	0.005	0.0016	0.0012
3	0.0020	0.004	0.0019	0.0008
4	0.0020	0.004	0.0019	0.0022
5	0.001	0.003	0.0023	0.0020
6	0.001	0.003	0.0023	0.0025

Table 4.1: Roll numerical study data, [10]

Torsion moment at different twisting is found as in Figure 4.5 below. Model 2, 4, 6 cross the zero moment line i.e. they have zero torsion moment configuration which means without any moment applied they can show a certain twisting rotation, which is the torsional instability.

Case 4 shows the highest drop in torsional stiffness for which largest reversed curvature ($\Delta\kappa_\eta = \kappa_\eta + \kappa_{\eta r}$, summation of column 5 and 2) has applied. For Case 1 opposite curvature applied is less than the requirement of Equation 4.13 so it showed no drop in torsional stiffness. But the case 2 and 5 is not showing expected behaviour.

Calculation of Table 4.1 has attached in Appendix C
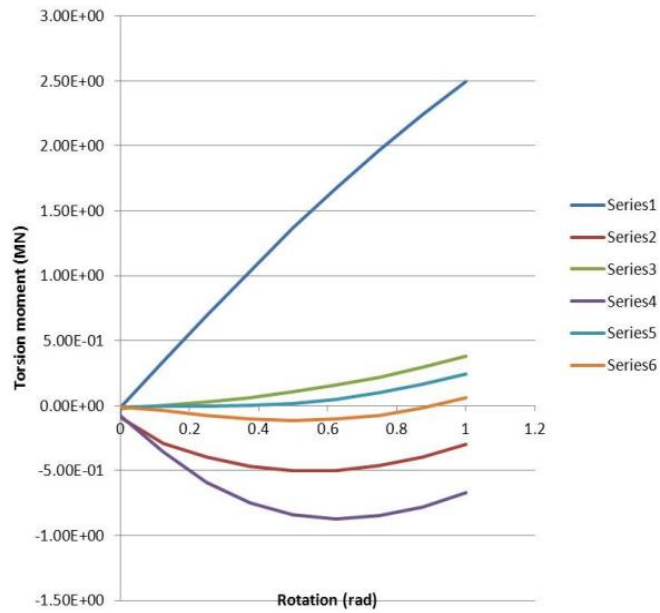
Figure 4.5: Torsion moment versus torsion rotation.

For the umbilical case as mentioned above, the amount of curvature $(\Delta\kappa_\eta)$ from gravity load is fixed for a certain model. So if the reversed residual curvature $(\kappa_{\eta r})$ from storage reel is smaller than this, then criterions of appearing torsional instability will be reached (Figure 4.6).
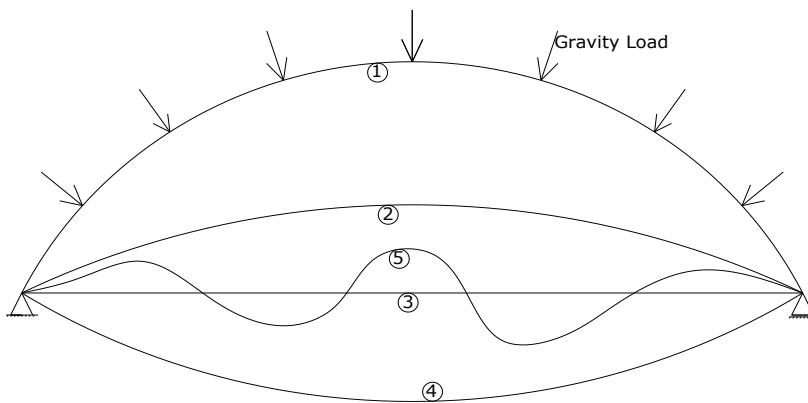
1. Initial residual curvature $(\kappa_{\eta r})$
2. $\Delta\kappa_\eta < \kappa_{\eta r}$
3. Straight configuration $\Delta\kappa_\eta = \kappa_{\eta r}$
4. $\Delta\kappa_\eta > \kappa_{\eta r}$
5. Possible buckled configuration due to torsional instability.

Figure 4.6: Creation of torsional instability phenomenon from residual curvature and gravity load.

4.2 Finite Element Method

The fundamental concepts of Finite Element Method in structural mechanics are, [10]:

1. Kinematic description: A relation between the displacements, rotations and strains at a material point.
2. Material law: Relation of strain and resulting stresses. The relation is either elastic or elastic-plastic. In simplified spring models non-linear elastic in combination with elastic-plastic models is applied.
3. Energy principle: it is based on the Principle of Virtual Displacement (PVD) to formulate stiffness matrix.

Finite element formulation and solution procedure of USAP and BFLEX will present here,

4.3.1 Stress and Strain in Umbilical

Slender structure like umbilical has small strains. So Green strain tensor in combination with 2nd Piola Kirchoff stress is applied for the strain and stress measure here, since they always referring back to the initial unreformed configuration. For uniaxial case as shown in Figure 4.7,

Green strain, $E = \frac{L^2 - L_0^2}{2L_0^2}$ $\qquad\qquad\qquad\qquad$ (4.14)

$\Delta E = \frac{L\Delta L}{L_0^2}$ $\qquad\qquad\qquad\qquad$ (4.15)

2nd Piola Kicchoff stress, $S_{11} = \frac{L_0}{L}\frac{F}{A_0}$ $\qquad\qquad\qquad\qquad$ (4.16)
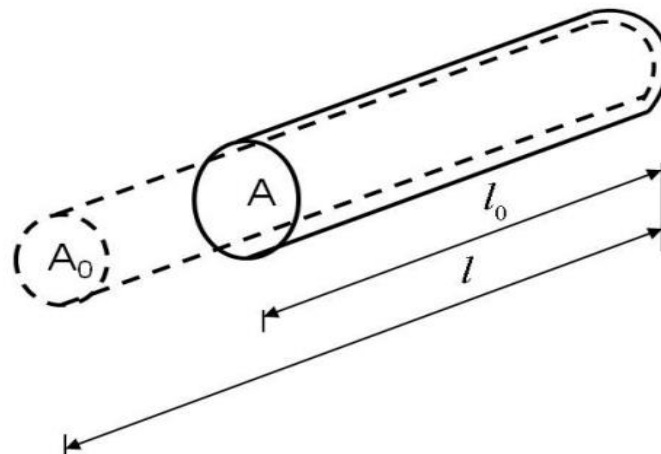
Figure 4.7: Deformed and unreformed configuration, [10]

4.3.2 Non linear Finite Element Formulation

To formulate a finite element problem it is need to establish the stiffness matrix of the problem. In USAP and BFLEX the basis of stiffness matrix is the incremental form of the principal of virtual displacement (PVD). In PVD an infinitesimal change in system coordinate is assumed keeping the time constant. The work is calculated on a set of kinematical admissible displacements and strains. The differential equation is formed on an average form not by point wise. Error produced from this virtual work is eliminated by equalling the error introduced from assumed weight function of external work and the error from internal work.

In an arbitrary equilibrium state of a body, the principle of virtual work is

$$\int_V \boldsymbol{\sigma} : \delta\varepsilon dV_o - \int_S \boldsymbol{t} \cdot \delta\boldsymbol{u} dS_o = 0 \tag{4.17}$$

Here, V is deformed volume, S is deformed surface, $\boldsymbol{\sigma}$ is Cauchy stress tensor, $\boldsymbol{\sigma_0}$ is the initial stress tensor, $\boldsymbol{\varepsilon}$ is the natural strain tensor, $\boldsymbol{t}$ is the surface traction, $\boldsymbol{u}$ is the displacement vector.

In case of the non-conservative loading, the resulting load will change as a function of the area change and the above equation is need to be formulated to allow equilibrium iterations to be carried out. Equation of incremental stiffness for an infinitesimal increment Δ is

$$\int_V \boldsymbol{C} : \Delta\varepsilon : \delta\varepsilon dV_o + \int_V \boldsymbol{\sigma} : \delta\,\Delta\boldsymbol{E}\, dV_o - \int_S \Delta t dS_o = 0 \tag{4.18}$$

Here, first term gives the material stiffness matrix and second term gives the geometric or initial stress stiffness matrix, where **E** is the Green strain tensor.

To demonstrate how a point in a material deforms, Lagrangian formulation is used in finite element analysis, which is divided in two types depending on the choice of reference configuration. In the Total Lagrangian (TL) formulation all variables are referred back to the initial (C_o) configuration. In the Updated Lagrangian (UL) formulation variables are referred to the current (C_n) configuration.

To improve the computational efficiency, rigid body motion is separated from the local or relative deformation of the element by attaching a local coordinate system to the element which translates and rotates with the element during deformation. To separate the nonlinearities of large displacement from the nonlinearities of element, Co-rotated Total Lagrangian formulation (CTL) is used in both USAP and BFLEX. In CTL formulation stress measure and strain tensor are used to define the equilibrium equation with respect to the to the initial (C_o) configuration.

Finite element equations are developed by applying the above two equilibrium equations (4.17 and 4.18) in combination with the material law and displacement interpolation function.

For USAP, kinematics and material models are described in [1, 14, 15]

For BFLEX, kinematics and material models are described in [4, 16]

The finite element equations are solved numerically by using Newton-Rapson iterative method.

4.3.3 Co-rotated Total Lagrangian Formulation (CTL)

CTL formulation is appropriate for the analysis of slender structure experiencing moderate strains and it is the basis for RIFLEX, BFLEX, USAP and SIMLA.

CTL is formulated in reference to the initial undeformed configuration. So Green strain tensor, in combination with 2nd Piola Kirchoff stress is applied. CTL is not suited for large strain problems and higher order components of the Green strain tensor can be neglected when updating both the stiffness and stress matrix.

In CTL a local coordinate system is attached to each element from which the element deformations and forces are referred, as illustrated in the Figure 4.8 below.
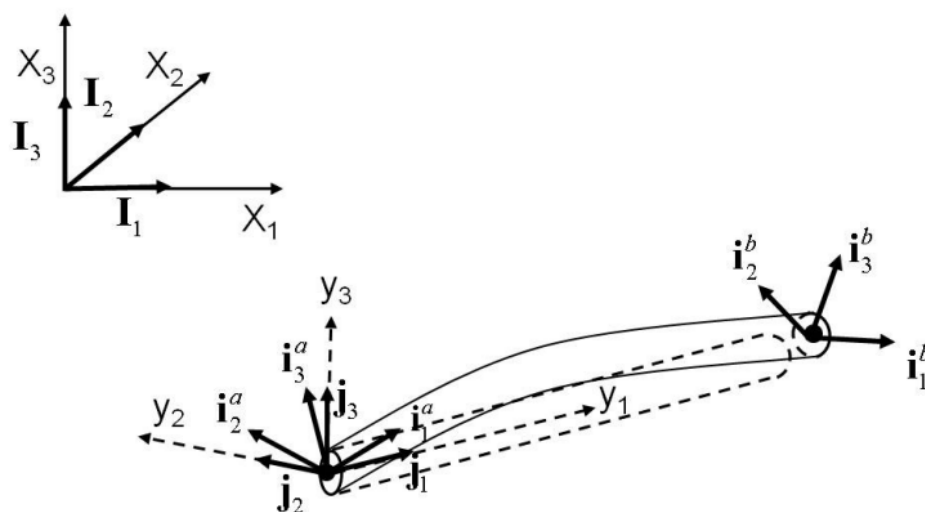
Figure 4.8: 3D beam element in CTL formulation, [10]

Where, j_i is the element reference system.

i_i^a and i_i^b are base vector of the element end node a and b.

j_i is obtained by combining the tangent vector connecting the two nodes at the updated coordinate position with the current orientation of i_i^a and i_i^b . The element rotational deformation at each end is the relative difference between i_i^a , i_i^b and j_i systems.

The element reference system do not deform, it follows the element throughout whatever the rigid body motion is. Large deformations and rigid body motions are taking into account by continuously updating the element orientation, node orientation and end coordinate positions and then transforming to the global system. To capture large motions large stress and stiffness matrix expressions are formulated.

The axial strain is calculated directly from above equation of uniaxial Green strain. Bending deformation is computed by measuring the relative deformation between undeformed and co-rotated coordinate system.

4.4.4 Solution Procedure:

The aim of all structural analysis is to get equilibrium between external forces (R_{ext}) and internal mass ($M\ddot{r}$), damping ($C\dot{r}$) and response forces (Kr).

$$R_{ext} - R_{int} = 0 \tag{4.19}$$

$$R_{ext} = M\ddot{r} + C\dot{r} + Kr \tag{4.20}$$

There are many procedures available for the solution of above equations.

Static case:

In static case, change of response with time is not so much that can create velocity and acceleration of the response. So there will be no mass and damping forces here.

$$R_{ext} - R_{int} = f(R_{ext}, r) \tag{4.21}$$

The solution can be achieved by applying any of the load incremental or iterative methods. The method which is used for the solution of static analysis in USAP and BFLEX is combination of both. External load is applied in stepwise increments and in each load step equilibrium is achieved by doing iteration with Newton-Rapson method. The iteration equation at load step k is

$$r_k^{i+1} - r_k^i = K_{T,k}^{-1,i}(r_k^i)(R_{ext,k+1} - R_{int,k}^i) \tag{4.22}$$

Or, $\Delta r_k^{i+1} = K_{T,k}^{-1,i}\Delta R_{k+1}^i) \tag{4.23}$

Here, i is the iteration number. The basic principle of the iteration has illustrated in Figure where ΔR is the load increment from R^I (load at equilibrium state I) to R^{II} (load at equilibrium state II), Δr is the displacement between two consecutive iterations in a load step and δr is the displacement from the beginning of load step to the end of any iteration in that step. So the load increment ΔR results in a displacement increment Δr_{k+1}^0 at iteration 0 in any load step (k+1). The internal load and stiffness matrix is updated and iterations are continued until convergence is achieved (i.e. δr is zero).
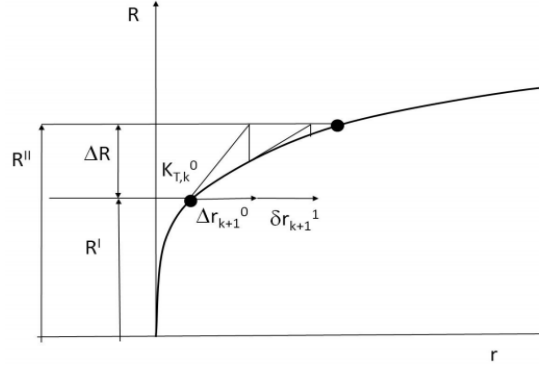
Figure 4.9: Newton-Rapson (NR) method, [10]

Dynamic case:

$$R_{ext} - R_{int} = f(R_{ext}, \ddot{r}, \dot{r}, r) \tag{4.24}$$

In dynamic case, displacement, velocity and acceleration all are present in the equation of motion. So direct time integration is needed in this case. HHT-α and Newmark-β are the two time integration method can be used.

In dynamic analysis response of low frequency modes are described with high accuracy than the high frequency modes. So it is required to describe the lower modes with good accuracy and remove the higher modes. In the Newmark-β method medium modes can be damped out by increasing damping ratio or introducing Rayleigh –damping but the lower and higher modes remain unaffected [17]. By performing numerical damping higher modes can be damped out but this will reduce the accuracy of the method.

HHT-α method can damp out the high frequency modes without any reduction in the accuracy [[17]]. In BFLEX HHT-α method is used in the time integration scheme. HHT-α is an implicit time integration method. So displacement of the next time step will depend on the information of the current step and next step. The modified equilibrium equation for the system is

$$M\ddot{r}_{k+1} + (1+\alpha)C\dot{r}_{k+1} - \alpha C\dot{r}_k + (1+\alpha)R_{k+1}^I - \alpha R_k^I = (1+\alpha)R_{k+1}^E - \alpha R_k^E \tag{4.25}$$

Subscript k+1 denote the next time step and k denote the current time step.

Total damping matrix, $C = C_o + \alpha_1 M + \alpha_2 K$ (4.26)

Displacement, velocity and acceleration are found as outlined in [4], using incremental time integration scheme. But these solutions will not fulfil Equation 4.25, equilibrium; iterations are needed, which is done by using Newton-Rapson iteration scheme. The governing iteration equation is as follows [18]

$$\widehat{K}_k^i \delta r_{k+1}^{i+1} = (1+\alpha)\left[R_{k+1}^E - R_{k+1}^{I,i} - C\dot{r}_{k+1}^i\right] - M\ddot{r}_{k+1}^i - \alpha\left(R_k^E - R_k^I - C\dot{r}_k^i\right) \tag{4.27}$$

Tangent stiffness matrix ($\widehat{K}$) is updated at each iteration cycle so that the convergence rate is improved.

In BFLEX mass matrix is set as consistent type i.e. interpolation function of mass matrix and stiffness matrix is same. Damping is proportional to both mass and stiffness matrix (Equation 4.26), but here damping is considered as proportional to the strain velocity. So it is proportional to the stiffness matrix only. Mass proportional damping factor α_1 is zero and stiffness proportional damping factor α_2 is positive. For the modelling of this work the value of α_2 is taken as 0.09.

Value of α of the HHT-α time integration method is taken as negative 0.05. When α=0, then HHT-α method is coincide with Newmark-β method.

$$-\frac{1}{3} \leq \alpha \leq 0 \qquad (4.28)$$

$$\gamma = \frac{1}{2}(1 - 2\alpha) \qquad (4.29)$$

$$\beta = \frac{1}{2}(1 - \alpha^2) \qquad (4.30)$$

Convergence criterion:

Iteration is stopped by means of a vector norm when equilibrium at a given tolerance level is reached. A norm based on total displacements given by Mathisen [19]

$$\left\| \delta r_{k+1}^{i+1} \right\| < \in_D \left\| r_{k+1}^{i+1} \right\| \qquad (4.31)$$

Explanation is refer at [19]. Accuracy of the solution is governed by $\in_D$ parameter which is usually in the order of 10^{-2} to 10^{-6}. In both USAP and BFLEX a predefined number of iterations are performed first and if the equilibrium is not achieved, the time step will be divided before a new trial is initiated. It is also possible to use norms in terms of energy or forces. Displacement norm has been used in here.

4.3 USAP

USAP [1, 2] is a computer programme which has developed for the stress analysis of umbilical structure. It is based on finite element approach and it can analyse each helix elements separately which is wound around a central core and subjected to tension, pressure, temperature, friction or residual strain during reeling, installation or operation. USAP focuses on longitudinal helix behaviour by considering uneven bending gradients and friction during bending.

In USAP Helically wound armours and tubes are formulated by a combination of curved beam kinematics and thin shell theory. Interaction of the contact between structural components is handled by a penalty parameter contact formulation. The contact between elements needs to be address precisely for correct prediction of the friction. It also includes the material and geometrical nonlinearity from gap and lateral contact between individual bodies of umbilical. Finite element equations are formulated by applying principal of virtual displacement.

The program modules of USAP used in this work are:

- USAP module: perform stress analysis by reading and controlling input data.
- XPOST: for presenting results.
- USAPPOST: for post processing of results.

4.4.1 Finite Element Formulation of HELIX231

HELIX231 is a 3D, elastic helix pipe element. A helix can be represented by a space curve wound around a cylinder with constant radius. This element is able to describe uneven curvature gradient effects, friction and elastic bending effects along arbitrary curve paths in space.

The total degree of freedoms required to describe one helix element attached to a beam element has shown Figure. During axisymmetric loading transverse and longitudinal DOFs of each structural element can be described by a common DOF and helix is allowed to move individually in the radial direction. For bending loading axisymmetric strains and bending strains are assumed as uncoupled and separate transverse and longitudinal DOFs are required to avoid shear locking and unstability due to coupling between axisymmetric and bending load effects.
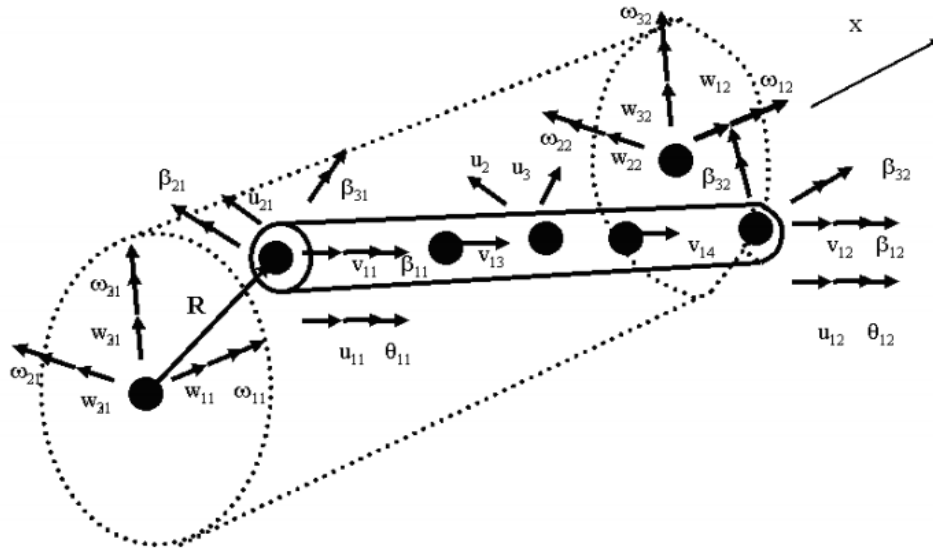
Figure 4.10: DOFs of helix element, [19]

The supported pipe is a two nodded element. It has three linear (w) and three rotational (ω) DOFS at each node. Same number of linear (u) and rotational (β) DOFs are required for the helix element also (Figure 4.10). But for HELIX231 only 13 DOFs are required for the formulation of finite element equations by using the linear constraint equations [15] as defined below and applying only one degree of freedom along u_3 direction. Here u_2 DOF is not required and 4 v-DOFs are required in addition to consider the bending friction. So HELIX231 need 17 DOFs in total.

$$\theta_{1i} = T_{11}\omega_{1i} \tag{4.32}$$

$$u_{1i} = T_{11}w_{1i} + T_{21}R\omega_{1i} \tag{4.33}$$

$$u_{2i} = u_2 - T_{11}R\omega_{1i} \tag{4.34}$$

$$\boldsymbol{\beta = T_\beta \omega} \tag{4.35}$$

Here, T_{ij} are the relevant components of the transformation matrix and $\boldsymbol{T_\beta}$ is the curvature transformation matrix obtained from differential geometry.

The kinematic quantities of this helix element has formulated by Sævik in [15].

4.4 BFLEX

BFLEX [3, 4]is a computer programme for the nonlinear static and dynamic analysis of flexible pipe. It has been developed based on Finite Element Methods. It can model the cross section such as carcass, pressure, tensile layers and do detailed cross sectional analysis of fatigue and extreme loads.

In this thesis work BFLEX has used to do the structural analysis of umbilical, since umbilical and flexible pipe both has the same mechanical behaviour. Flexible pipe has armour tendon on it; umbilical has helix tube inside it. The formulation of tendon wire behaviour on flexible pipe is same as helix tube behaviour inside umbilical. So same element and material property of BFLEX is used in both modelling. Several phenomenon of umbilical like reeling, torsional instability, friction development has modelled with BFLEX for the analysis of this thesis work.

HSHEAR353 and HCONT453 are Bflex elements which have been developed to model the behaviour of tendon wires over flexible pipe and the contact with the tendon. These two elements have used in the umbilical modelling of this thesis work to model helix inside a core and contact between them, since the physical phenomenon and principals are same in both models.

4.5.1 Finite Element Formulation of HSHEAR353:

HSHEAR353 is an elastic helix element includes both transverse and longitudinal slip. It is the improved version of HSHEAR352 element which only included the longitudinal slip by considering the axial relative displacement between core and wire. Transverse slip has included by including the torsion, radial and transverse degree of freedoms of tendon wire. Two main features of the HSHEAR353 element are,

1. Assumption of plane surface remains plane.
2. Inclusion of motion, relative to the plane surface.

The basis of HSHEAR353 is its internal virtual work expression [20], which has the form:

$$Wi = \int_0^1 [EA(\beta_{1,1} + u_{1p,1})\delta\beta_{,1} + GI_1(\omega_1 + \omega_{1p})\delta\omega_1 + EI_2(\omega_2 + \omega_{2p})\delta\omega_2$$
$$+ EI_3(\omega_3 + \omega_{3p})\delta\omega_3 + \beta.c.\delta\beta]dX^1 \qquad (4.36)$$

Here, β is the bi-directional relative displacement between tendon and core, along helical path of sandwich beam theory. c is a two-dimensional shear stiffness tensor. c is determined by stick-slip condition between layers, it is zero in the slip-domain. ω_{ip} represent the torsion and curvature quantities, considering plane surface remain plane, see [20]. ω_i are the torsion and curvature quantities resulted from curved beam theory because of the relative sliding

from the reference loxodromic curve, see [16]. ω_i include the coupling terms between the current torsion, curvature, displacement and rotation of the centreline Here strain, torsion and curvature quantities of tendon wire are described by the loxodromic curve quantities.

The assumption, description and the explanations of the kinematic quantities of HSHEAR353 has formulated and described by Sævik in [16, 20].

The finite element model of standard two nodded beam element is normally described by taking six degree of freedoms per node. In the finite element formulation of HSHEAR353 element additional nodes has introduced to describe both standard beam quantities and the relative deformations resulted from slip. It includes total 26 degree of freedoms in 4 nodes, among which 12 are standard beam DOFs of the core pipe centreline to describe the global strain quantities and 14 are to describe local displacement of the tendon wire relative to the core. Among 14, 6 helical DOFs are at each end of the corresponding helix and 2 internal DOFs are for accurate description of the longitudinal slip process.

Hence, the cubic interpolation is possible in all direction and so the membrane locking phenomenon from curvature coupling terms. Degree of freedoms of HSHEAR353 has illustrates in the Figure 4.11 below,
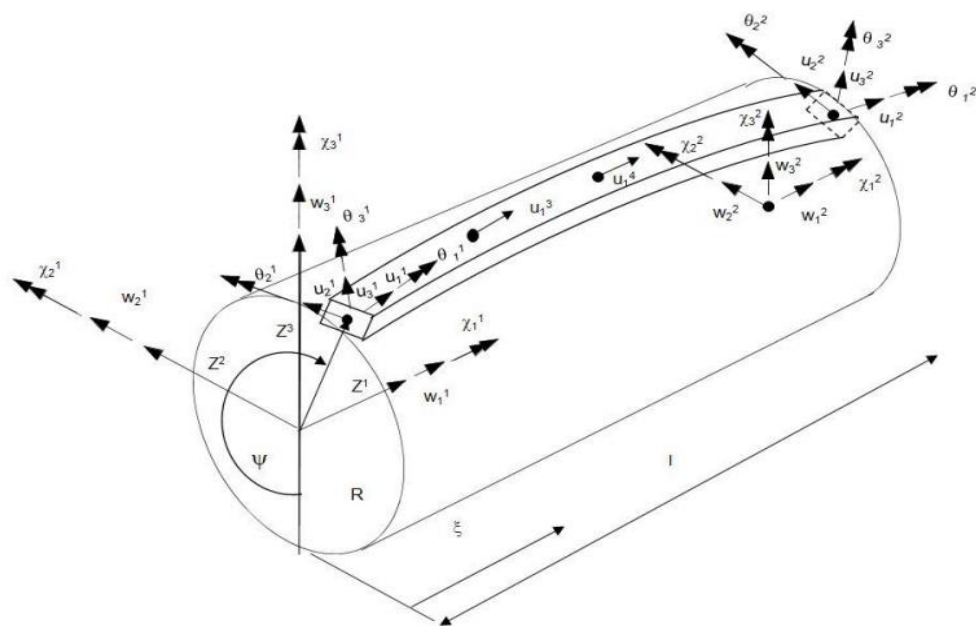
Figure 4.11: DOFs of HSHEAR353, [20]

4.5.2 Finite Element Formulation of HCONT453:

HCONT453 is a 4 nodded hybrid mixed contact element (Figure 4.12) with 24 DOFs. It describes the interaction between layers by taking interlayer contact forces and friction from relative displacement into account. This contact element has been developed to describe the same quantities as have in HSHEAR353. The displacements of each of the two beam elements A, B of Figure are described by 10 DOFs with the same convention as HSHEAR353 beam element has, along both the longitudinal X^1 and transverse X^2 and X^3 directions. So the contact element has in total 20 DOFs matching the corresponding beam DOFs. Taking 4 dummy torsion DOFs, the contact element HCONT453 is implemented with 24 DOFs for making a match of standard 6 DOFs at each node.

HCONT453 is based on a Hybrid Mixed formulation, described in [20]. The basis of this formulation is the concept of incremental potential, which is formulated as:

$$\Delta\pi = -\int_{S_c} (q_3 + \Delta q_3) \cdot u_3 ds - \frac{1}{2c_n} \int_{S_c} \Delta q_3^2 \, ds - \int_{S_c} q_t \cdot \Delta\beta ds - \int_{S_c} \Delta q_t \cdot \Delta\beta ds \qquad (4.3)$$

Here, q_3 is the distributed normal reaction.

q_t is the distributed tangential reaction assuming a bi-directional friction model.

c_n is the penalty stiffness parameter.

The finite element of HCONT453 has the following two key features [20]

1. Describing contact between layers of crossing tensile wires.
2. Enabling easy description of the resistance against wire rotation from other layers by including torsion coupling terms.
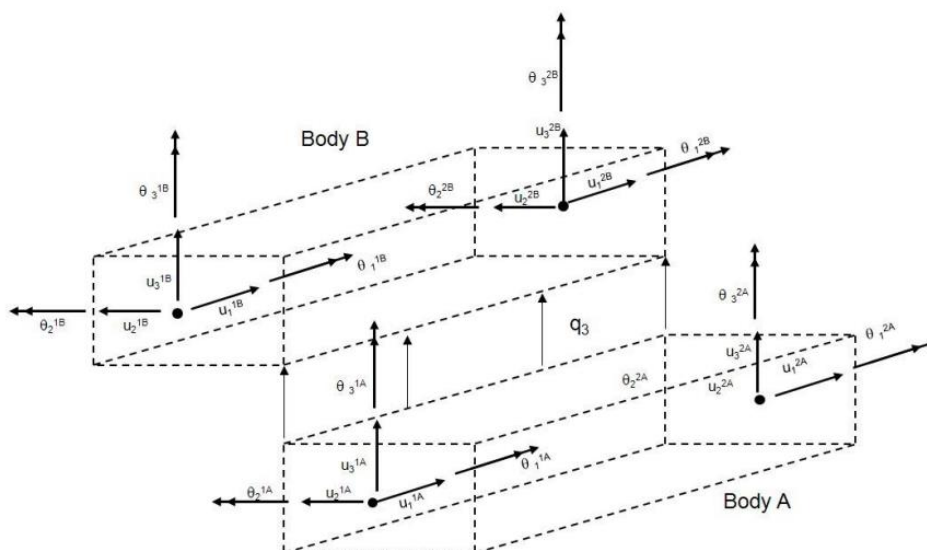
Figure 4.12: DOFs of HCONT453, [20]

Chapter **5**: Presentation of the Models

The problem this thesis work is dealing has provided from Aker Solutions. Three of their umbilicals, where snaking behaviour has been seen, are presented in the Table 5.1 below. Agbami is the heaviest umbilical among these three. It has radius of 89 mm and weight (in air) of 370 Newton per meter. Also it is stiffer than other two and it has higher axial, bending and torsional stiffness. That's why it has larger bending radius (MBR operation and installation) and pitch length. They have same Minimum Bending Radius (MBR) storage, as they have manufactured in the same plant.

The outersheath of all the umbilicals are made of Medium Density Polyethylene (MDPE) and they have almost same thickness. The umbilical Agbami is of dynamic type, that is it will face dynamic wave load when it will be in operation, whereas Kipper and Droshky will not, so they are of static type. Also because of being dynamic, Agbami has much higher tension capacity than the other two. All of these umbilicals have very low lay angles. The advantage of having low lay angle is, small amount of internal friction is generated when the umbilical is put in tension, which is very good for its structural stability.

Umbilical Name	Agbami	Droshky	Kipper
Type	Dynamic	Static	Static
Outer radius (mm)	89	57.5	41.5
Thickness(mm)	5	5	4.5
Pitch length (m)	11.5	7	6
Lay Angle (degree)	2.8	2.96	2.5
Weight in air, empty hollows(N/m)	370	154	106
Weight in water, empty hollows(N/m)	170	72.1	54
Weight in water, filled hollows(N/m)	200	85.3	51
Relative specific weight compared with sea water	1.79	1.81	2.0
Axial stiffness(N)	4.62E8	1.99E8	1E8
Bending stiffness (Nm^2)	2.68E4	0.858E4	0.549E4
Torsional stiffness(Nm^2)	2.06E4	0.66E4	0.1E4
Tension capacity, installation(KN)	1010	497	252
Tension capacity, operation(KN)		298	151
MBR in storage (m)	2.5	2.5	2.5
MBR in operation (m)	12	6.2	1.9
MBR in installation (m)	7.1	4.7	1.9

Table 5.1: Properties of umbilical models.

The components of umbilical, their number and orientation can be seen from its cross section. The components in an umbilical and their number depend on their service purposes. The cross section of the models and their deformation scenarios have been discussed here.

5.1 Agbami

Agbami is quite densed with many structural components. The arrangement and orientation of the component elements is symmetric about vertical plane. It has 26 steel pipes among which four are big and rest are smaller. Big tubes carry larger curvature so residual curvature in big tubes is more dangerous for umbilical deformation than the smaller ones. Agbami has nine copper power cables, copper has high modulus of elasticity so high stiffness. .
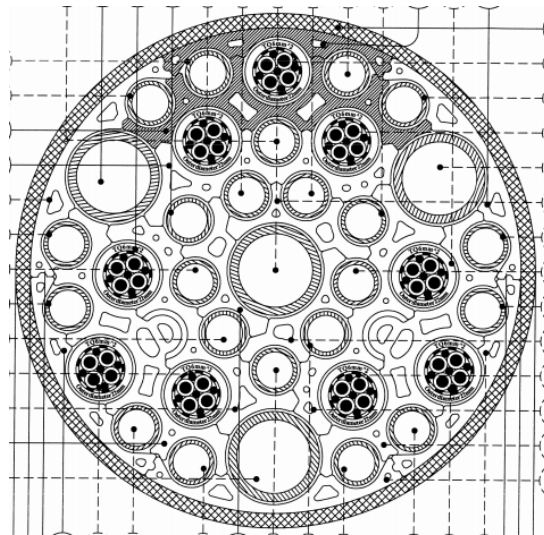
Figure 5.1: Agbami cross section

Snaking found in Agbami when it was transferring from storage reel to installation vessel. The snaking was very big (Figure 5.2)with pitch length of about 11 meter which is very near to the bundling pitch length of umbilical and double amplitude is about 2.5 meter.

5.1.1 Sources of Curvature
Curvature is the main reason of snaking in umbilical. Curvature can appear in an umbilical from three sources:

1. From the curvature of component steel tube: If the component steel tubes of umbilical bundle has curvature then they will introduce bending moment in the umbilical structure which will produce helical or snaking deformation. Curvature can remain in steel tube due to the improper action of straightener machine as mentioned in Chapter 2.6. But this case is not here, since snaking found in Agbami in the installation vessel, if residual curvature of steel tube would be the reason than snaking would appear in the manufacturing plant but that did not happened.

2. Friction moment development during reeling: The snaking of Agbami has been found when it was spooling out from the storage reel and due to sliding between the internal elements friction moment develops in umbilical during the reeling, which eventually produce curvature. So reeling of Agbami in the storage reel is a probable source of its curvature. This phenomenon of developing curvature from friction moment has described in Chapter 3.4.

3. Creeping of outersheath: Agbami was stored for a long period of 10 months before installation. So creeping and consequently plastic curvature can develop in the outersheath because of the reasons mentioned in Chapter 3.6. This is also a very probable source of curvature in Agbami.

5.1.2 Possible Snaking Scenario:

In the installation process, when umbilical is transfer from reel then the length of umbilical between reel and installation chute is appeared as unsupported where snaking can appear due to the phenomenon described in Chapter 4.1. Also the end of umbilical over chute is free to twist so torsional instability can develop according to the analytical model of Chapter 4.1. The deformation pattern of Figure 5.2 can be from torsional instability.

Installation chute

Coming off from Reel
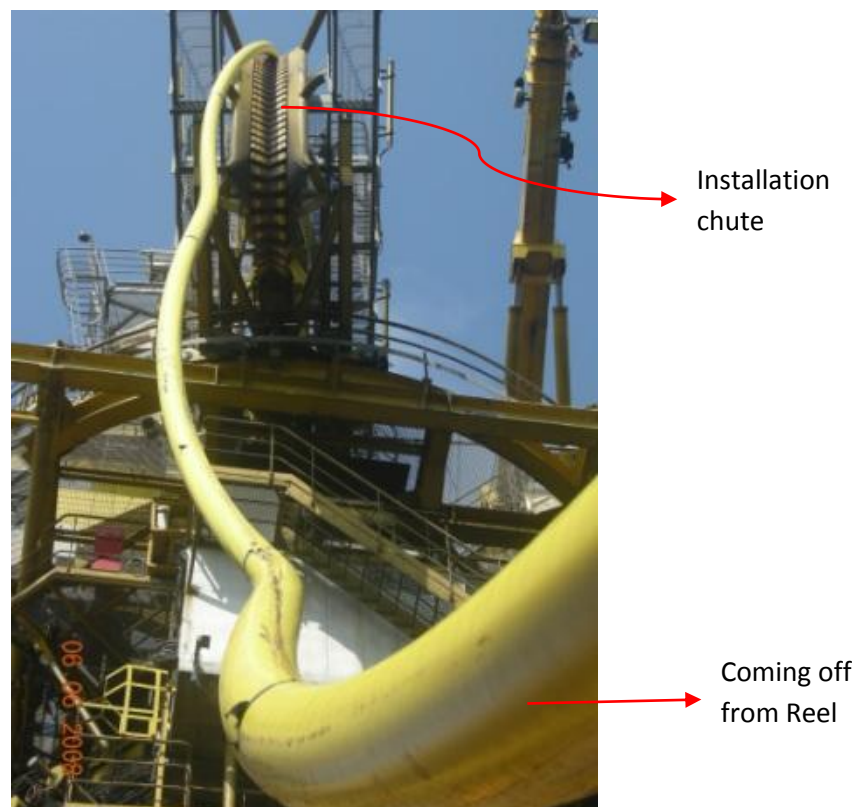
Figure 5.2: Snaking picture of Agbami

In the installation process, snaking can arise in umbilical without any impact of curvature also and from the installation mechanism. During installation when umbilicals are drop from vessel to water, they pass through tensioner, which drive the umbilical into water with control. The belt of tensioner compresses the umbilical and drives it into water. But in tensioner, accidently, one or more internal elements of umbilical may not get the compression. For example if one

steel tube does not get the compression, then due to its downward position and from the action of gravity load, it will move faster than the other elements of the bundle (Figure 5.3). The tube will experience a backward load from its weight from the water depth and will push its length behind. Because of this, the umbilical length behind tensioner that is over chute and before may get helical deformation with the same pitch length as the helix element.

Steel tube, not feeling the compression and moving fast under gravity load

Tensioner belt, compressing and driving the umbilical into water
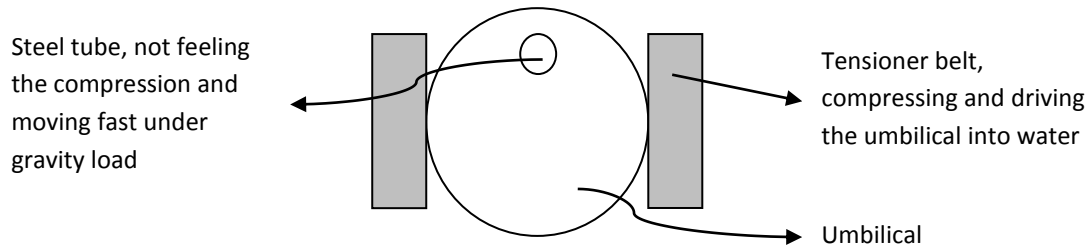
Umbilical

Figure 5.3: Umbilical in tensioner of installation vessel.

Since the pitch length of deformation is almost similar to the pitch length of umbilical. So this reason is also very probable here.

5.2 Droshky

Droshky has lots of steel tubes, five big and seven small (Figure 5.4). The orientation of the steel tubes is symmetric neither about center horizontal plane nor about center vertical plane. So unbalanced bending moment (M=EIk) may be generated from the curvature in the tubes and can create snakelike deformation of the umbilical structure.
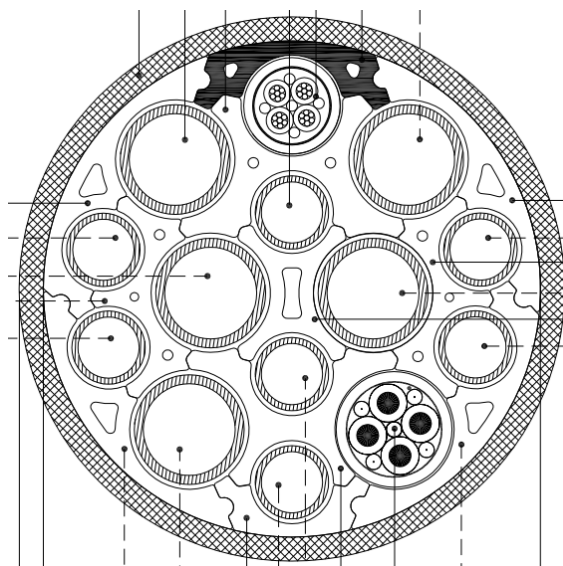
Figure 5.4: Droshky cross section

41

Droshky has showed snaking just after its extrusion (Figure 5.5). The snaking pattern is quite regular and there is no twisting. The pitch length and double amplitude of the deformation is about 4.5 meter and 150 millimetres respectively.

In the extrusion process before bundling each steel tube pass through the straightener machine from their individual storage reel. But curvature may remain in the tubes in a certain extent if it is straightened by applying a fixed pressure in the roller straightener and not using bending shoe as mentioned in chapter 2.4.

Figure 5.5: Snakelike deformation of Droshky

The curvature amount depends on the radius of the reel. The sections stored on the outermost layers have larger radius than the inner layers. In a reel which has r_i inner dia and r_o outer dia the umbilical section which wound first in the in the roller will have r_i radius of curvature. On the other hand the section which is wound last in the roller will have r_o radius of curvature and the portion of umbilical in between outer and inner radius of roller will have different amount of curvature depending on their wounding radius on the reel (Figure 5.6).

Umbilical reeled, in between inner and outer radius

Inner radius, r_o

Inner radius, r_i
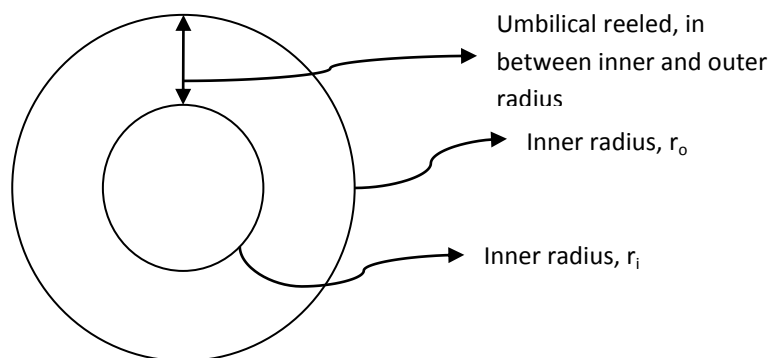
Figure 5.6: Turntable

So, now if the umbilical passes through a straightener which is tuned to a certain amount of curvature then the sections having same amount of curvature as the straightener will be straight but the sections which have different amount of curvature than the straightener will go with curvature from the straightener. Suppose the straightener is set to make a curvature of r_o radius. Then the umbilical from outermost layer will be straightened but innermost will have curvature of (r_o-r_i) amount (Figure 5.7).
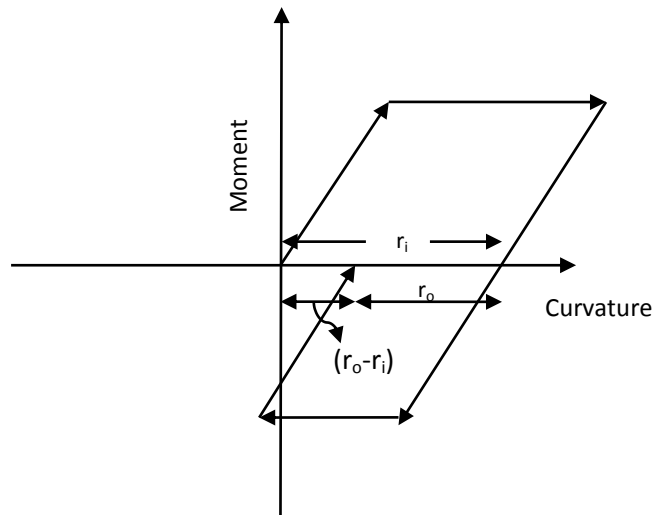
Figure 5.7: Curvature from straightener

Now if some tubes carry considerably bigger amount of residual curvature from the straightener and they have unsymmetrical orientation in the cross section like Figure 5.8 then unbalanced bending moment will generate and snake shaped deformation of umbilical will happen.
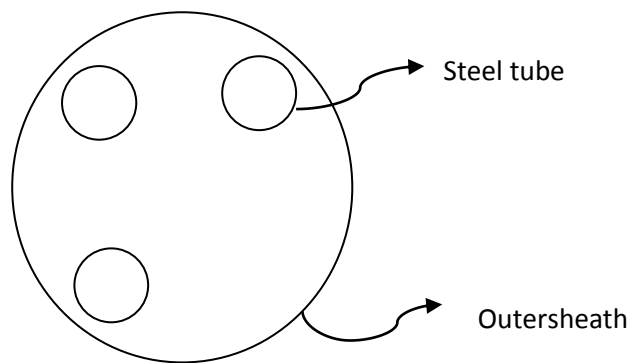
Figure 5.8: Probable asymmetric orientation of steel tubes, having residual curvature

The snaking picture (Figure 5.5) says, residual curvature of tubes is the possible reason of this snaking and this will consider in modelling.

5.3 Kipper

Kipper is a quite unorthodox type of umbilical having no tubes but some electrical wires of steel and it has no gap between the wires and PVC profiles (Figure 5.9). So during reeling when contact load will apply on the structure, steel wires and PVC profile will come into contact and high internal friction will generate. If the friction amount is so much that it can modify the moment curvature relation and considerable amount of curvature found at zero moment (Chapter 3.4) then helical or snakelike deformation will appear.

Kipper has three bundles of wires. The biggest bundle is at the center consists 19 closely packed wires. The other two bundles have 7 wires on each, situated at two side of center vertical plane. Three copper wires are located in each of upper and lower half of center horizontal plane. The element orientation in kipper cross section is symmetric both about horizontal and vertical plane. Although symmetry of plane is not maintained during the movement, as umbilical rotate in the circumferential direction.
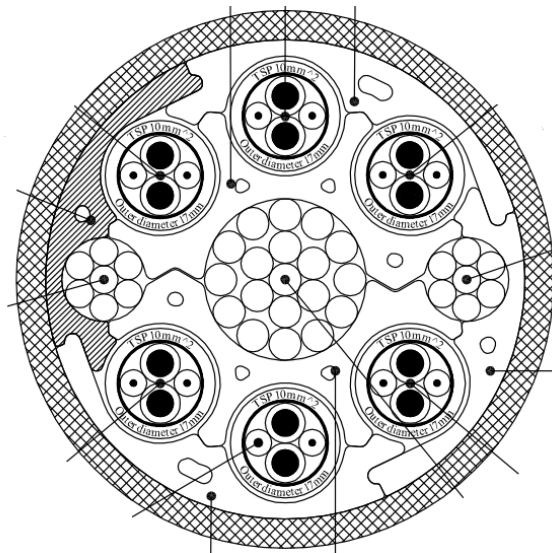
*Figure 5.9: Cross section of Kipper*

It has showed some minor irregularities (Figure 5.10, up) when it was kept on the turntable after extrusion and also when put on installation carousal. The severe form of deformation which has snakelike configuration, it has showed when it was spooling off from the storage reel. As it can be seen from the picture below (Figure 5.10, below) some serious twisting is also happening with snaking during spooling off. It is quite hard to say about the amplitude and pitch length of the deformation from the picture. It is having three pitch lengths in the picture with an average length of about four meter and double amplitude of about half a meter.

Development of friction due to having no gap between the steel wires and PVC profile could be the reason of snaking of Kipper. The reason of twisting could be the low torsion stiffness of Kipper, whereas the reason of deformation on the turntable could be its low bending stiffness. These will be investigated in the analysis part of Kipper in the relevant chapters.
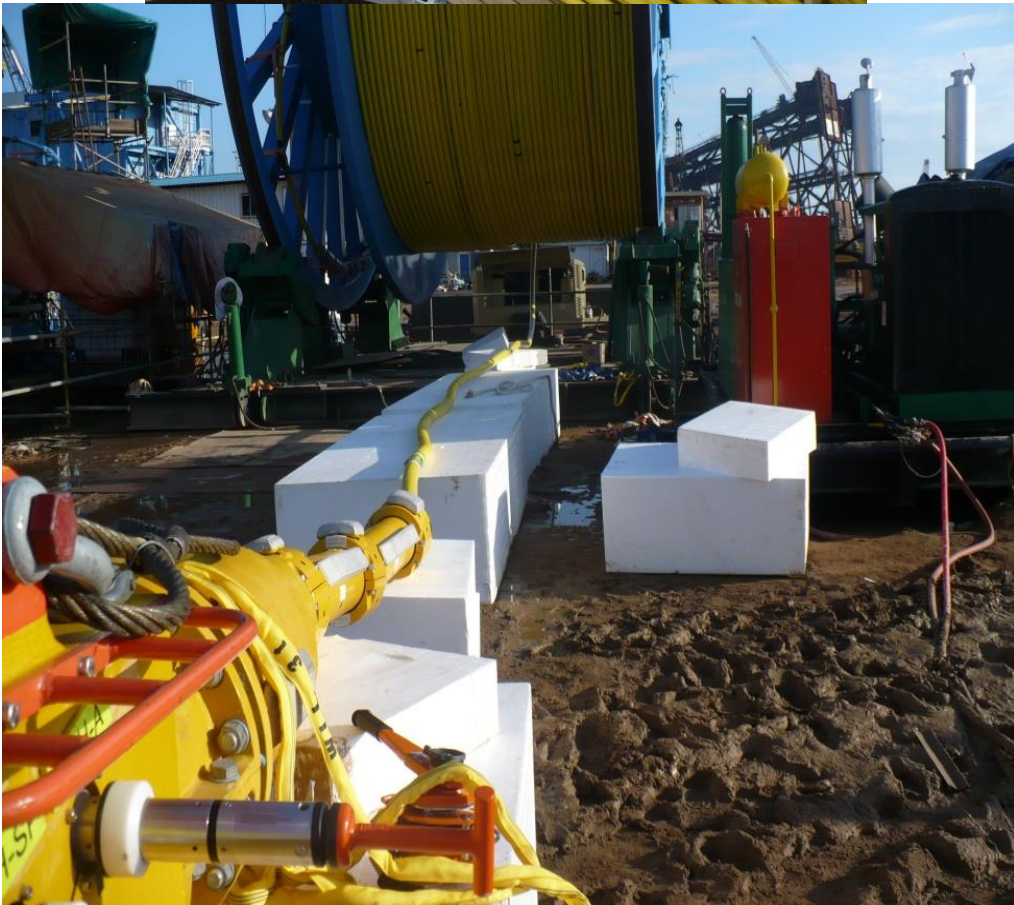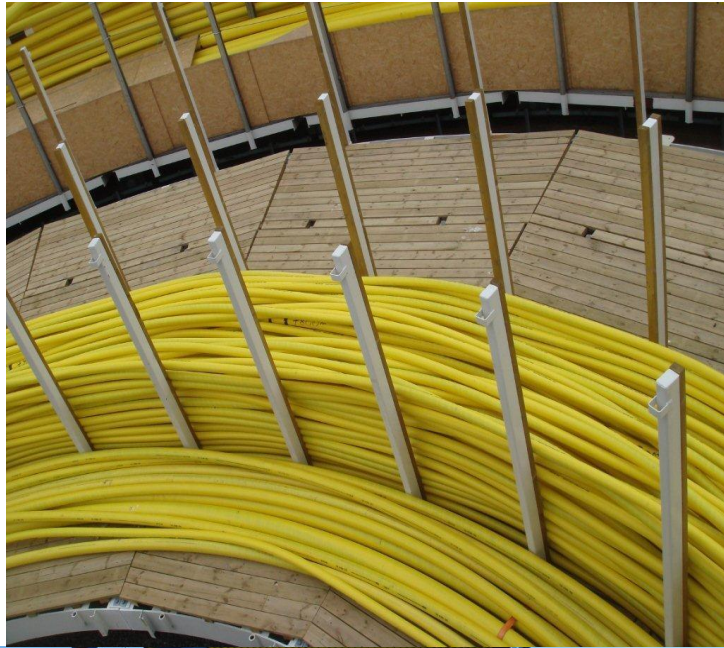
Figure 5.10: Real deformation pictures of Kipper.

The properties and parameters related snaking picture definition is presented briefly in Table 5.2 below.

Umbilical Name	Agbami	Droshky	Kipper
Initial symmetry of cross section	Symmetric about vertical plane	Asymmetric about both plane	Symmetric about both plane
Snaking seen	Under installation, coming off from reel	After extrusion	On turntable and installation carousal and when spooling off from reel.
Double Amplitude (m)	2.5	0.15	0.5
Pitch Length (m)	11	4.5	4

Table 5.2: Snaking properties of umbilical models.

Chapter **6**: Modelling

Modelling was very important part of the analysis of this work. Model of the umbilicals were established on the basis of their snaking deformation scenarios by selecting proper element type, material property, loadings, boundary conditions in software USAP and Bflex. For some cases exact physical phenomenon was not possible to model, in that case model of equivalent mechanical behaviour has established.

The main strategy of the analysis has been doing the simulations of the established model for finding the exact deformation picture as showed in Chapter 5. Because then it is possible to know the reason of the deformation. It is also possible to know the parameters that have effect on the deformation, intensity of their effect and also the possible solutions of not having the deformation. Simulations have been performed by changing the geometry, material property, loadings and boundary condition of the models. The analysis strategy has presented briefly in Figure 6.1 below,

Figure 6.1: Strategy of the analysis in brief.

6.1 Agbami

Four modelling has been done for Agbami:

1. Agbami Reeling: Reeling on and off to check the amount of friction develops.
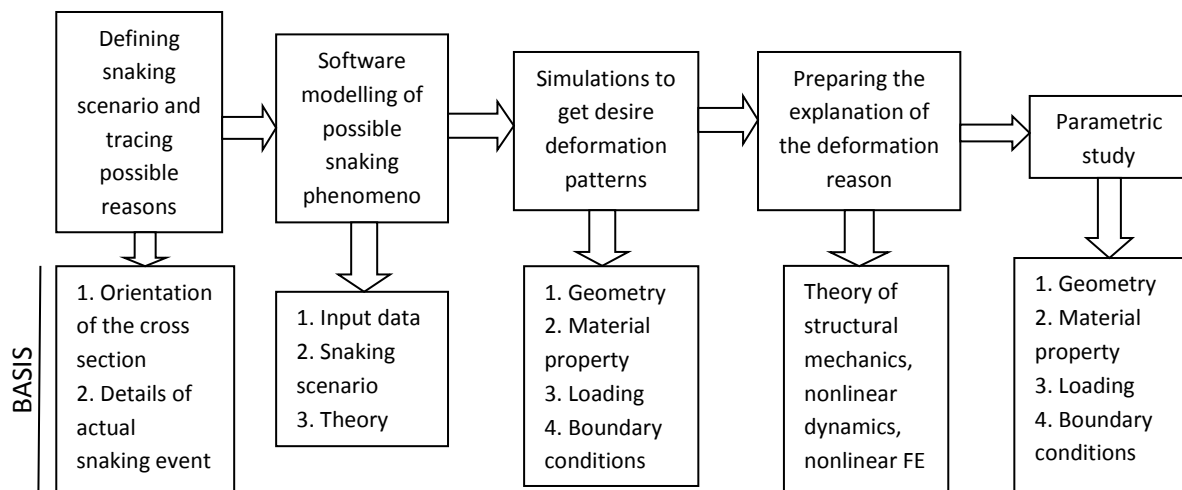2. Agbami Residual Curvature: Applying residual curvature on the whole umbilical to check whether deformation pattern matches with Figure 5.2 or not.
3. Agbami Torsional Instability: Modelling the analytical model of Chapter 4.2 to check whether the deformation of Agbami (Figure 5.2) is from torsional instability or not.
4. Agbami Tensioner Effect: Modelling the tensioner effect on snaking, by applying axial strain in one helix and checking the deformation picture with Figure 5.2.

6.1.1 Agbami Reeling

The umbilical Agbami showed snaking, when it was spooling out from the storage reel and transferring for installation. Friction moment development during reeling process is the reason of snaking, considered in this modelling. That's why the phenomenon modelled for the Agbami here is, spooling on and off in a reel of 2. 5 meter radius which is the minimum storage bending radius of Agbami.

The model of umbilical Agbami (Figure 6.2 and 6.4) is comprised of 26 steel pipes, one of which is core pipe and others are helix at different helix angle and helix radius. Helixes are modelled with HELIX231 element; outersheath and the core pipe are modelled with PIPE31 element in USAP. PIPE 31 and HELIX231 are linear elastic elements, modelled by LINEAR material card.

Helix elements need contact material to describe their radial stiffness and longitudinal friction properties. The aim of this model is to find the effect of friction on Agbami snaking and friction stress analysis is carried out in the model by choosing proper friction stress control parameter.

Contact material is described by three material curves along three directions. For reeling, rotation will be applied about local x axis; that is why material curve along x axis has selected as very soft with elastoplastic material and material curve along y and z axis has modelled as very stiff with hyperelastic that is nonlinear elastic material.

The modelled length of the umbilical is 35 meter and 200 elements have taken along the length. So, length of each element is 175 mm. The global and local both coordinate systems have taken, according to the right hand rule. The center of the global coordinate system is at the center of the spool, positive X is towards the spool width (Figure 6.4). In the local coordinate system of umbilical, positive X is taken along the element length (Figure 3.2) which means the coordinate system is rotated 90 degree clockwise about the global Y axis. The local coordinate system of spool center elements and helping elements are such that, it is rotated 90 degrees counter clockwise about the global Z axis.
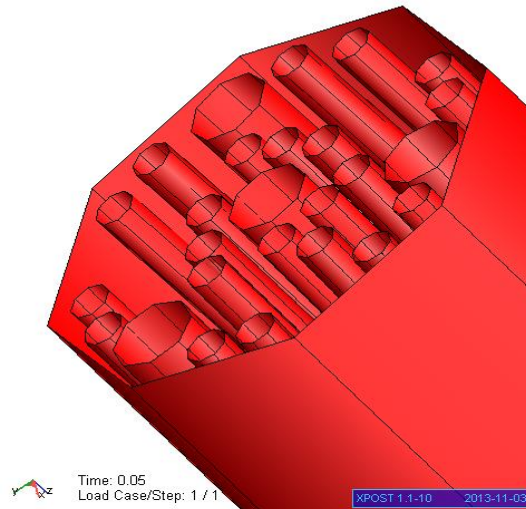
Figure 6.2: Agbami cross section modelled in USAP

The simulation of reeling phenomenon in USAP is performed by master-slave technique. The outersheath of umbilical only contains master node, except the first node, which is a salve of the spool axis. Each master node of outersheath ($m_{outersheath}$) has corresponding slave node in the spool (S_{spool}); this slave follows the rotation of the master in the spool and located under its master in the outersheath. The local coordinate system is always normal to the spool as indicated in the Figure 6.3. When contact between an outersheath node and the spool occurs the displacement normal to the spool is locked to the slave node of spool.

(a) View from side.   (b) View from top.
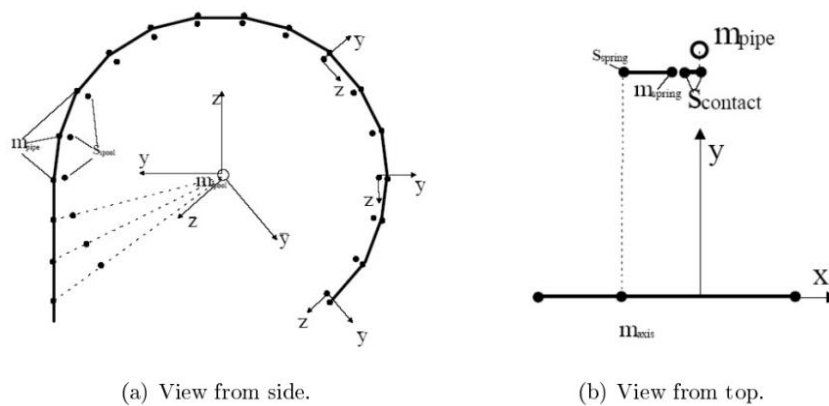
Figure 6.3: Reeling, [1]

To monitor the contact force and have a criterion for disconnecting, a helping element is introduced, which is comprised of slave and spring element (ordinary beam). One node of slave or contact element is connected to S_{spool} and another node of slave is locked to m_{spring} (Figure 6.3). The contact force for each point can then be found as the shear force (local y-direction) of the beam. For a given negative contact force limit (or zero) the $m_{outersheath}$ disconnects from the slave node and the slave node connects to the m_{spring}.

49
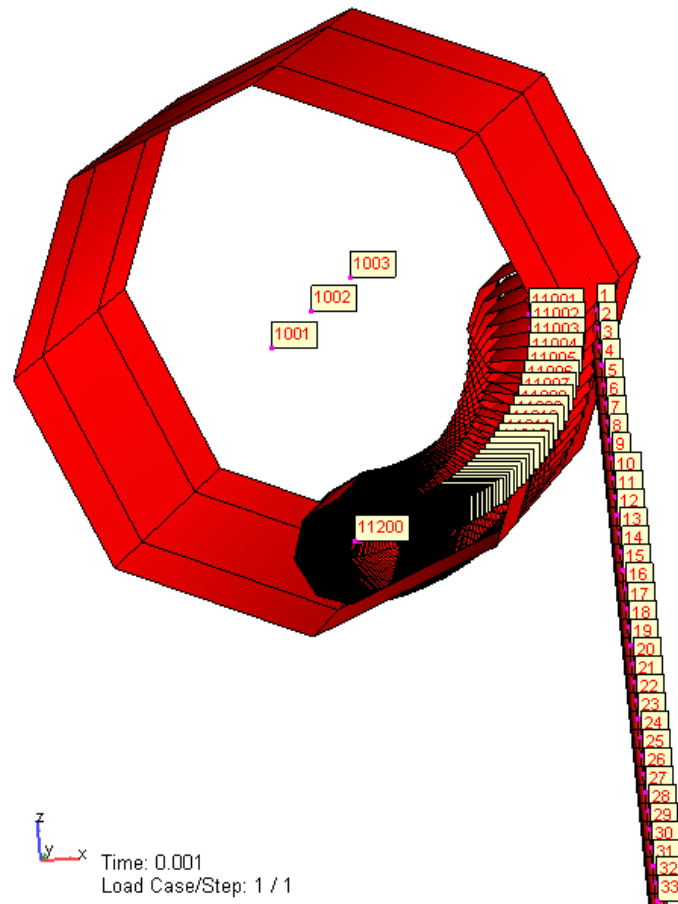
Figure 6.4: Agbami reeling, modelled in USAP, with element numbers.

In this model, four nodes (1001 to 1004) have taken on spool axis. Two hundred elements have taken on each of the spring element and slave i.e. contact element. For reeling of Agbami, rotation is applied at the spool center which is transferred to the umbilical outersheath nodes through spring and slave elements. The location of S_{spool} underneath the $m_{outersheath}$ is governed by a constraint equation between the S_{spring} and m_{spool}.

A linear constraint equation has the form; $r_s = C_o + C_1 r_{m1} + C_2\ r_{m2} + ...$ (5.7)

Here, C_o is the constraint displacement and C_1, C_2 are the constraint coefficient for the master node number 1 and 2.

The connection between spool center and outersheath pipe has been made with four sets of local constraint equation

1. Between S_{spring} nodes (11001 to 11200) and spool center (node 1002), along all degrees of freedom.
2. Between m_{spring} nodes (12001 to 12200) and S_{slave} nodes (13001 to 13200), along all degrees of freedom.
3. Between m_{spring} nodes (12002 to 12200), S_{slave} nodes (14002 to 14200) and $m_{outersheath}$, along the degree of freedom 1 and 2.
4. Between S_{pipe} and spool center (node 1003).

The number of elements required on the spring and slave elements for making target reeling, depends on the perimeter of the reel, umbilical is covering. Suppose for 270 degree rotation, perimeter of reel is 11775 millimetre which is equivalent to 68 elements of outersheath, since length of each element is 175 millimetre. So at least 68 elements are required on the helping elements (slave and spring) for 270 degree reeling.

6.1.2 Agbami Residual Curvature

As creeping can create plastic curvature in the whole umbilical, so in this model the whole umbilical (Agbami) has modelled as a single pipe element of 34.5 meter length (3 pitch length) with 200 PIPE31 elements along the length (Figure 6.5). The material property of whole umbilical has lumped into the pipe, so that the mechanical behaviour of umbilical is represented by this.

Both end of the model are free in rotational DOFS. First end has kept fixed along all translations and other end is free to translate along X axis only.

Time: 0.01
Load Case/Step: 1 / 1

XPOST 1.1-10   2014-06-
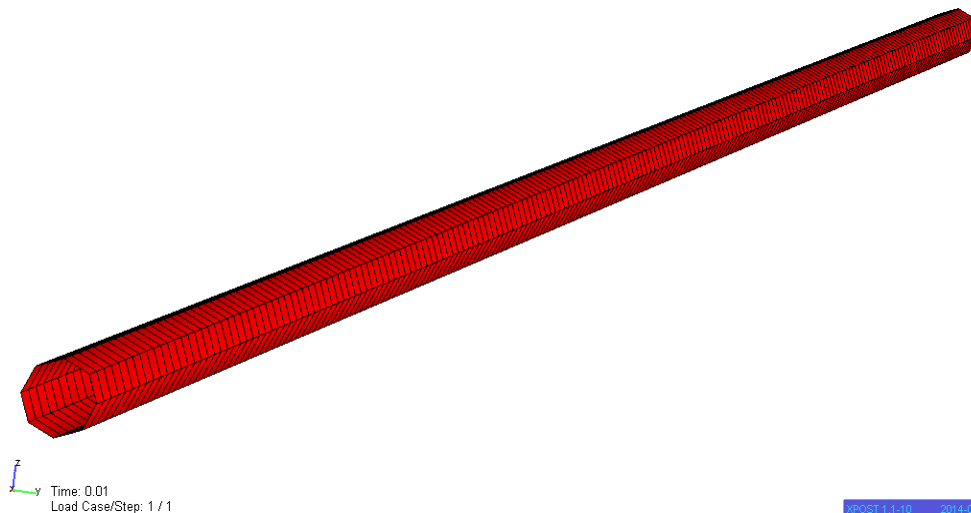
Figure 6.5: Agbami model for residual curvature analysis.

The only load here is bending curvature in the pipe; it has applied in a very smooth way like a half cosine shape by RAMPCOS time history (Figure 6.6), so that it reaches its maximum amplitude very slowly.

In normal time history load increases linearly from the beginning, so load has relatively high rate of growth in the beginning seconds which can stimulate acceleration since it is dynamic analysis and mass load is active in the whole process. Numerical stability of the simulation will be hampered if mass load is activated, so there can be convergence problem. To avoid this smooth increase of load is used by RAMPCOS time history.

Figure 6.6: Load history

Also 2 KN tension has applied, as it exist in the real installation process.

6.1.3 Agbami Torsional Instability

As mentioned in the analytical model in Chapter 4.1, umbilical will have curvature from gravity load and could have opposite curvature from residual curvature of storage reel when transferring from reel for doing installation. So torsional instability phenomenon might happen here. This will be checked in Agbami, by the following model.
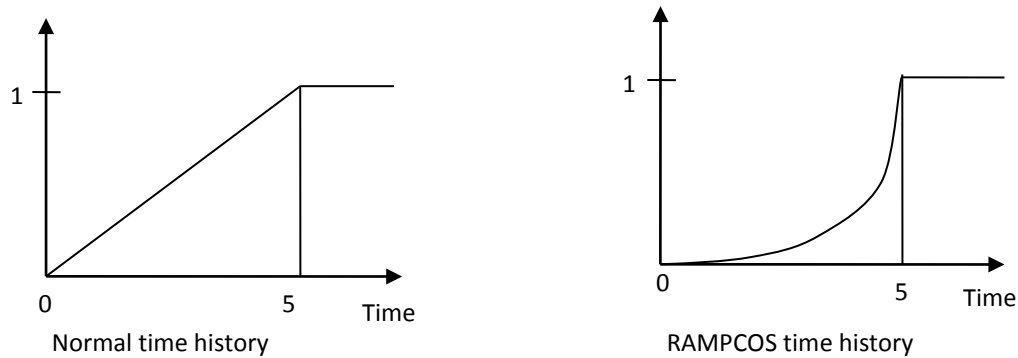
The model has same geometry and material property as the residual curvature model of Figure 6.5. But the loading and boundary condition is different here.

The length of model 34.5 meter has taken as the approximate distance between storage reel and installation chute. One end of the model is kept fixed in all DOFs and the other end is allowed to make axial displacement and twisting rotation.

To simulate the same transferring phenomenon of Agbami from storage reel through installation chute as in real field, a tension of 2 KN has applied in the model. The end of Agbami over chute is free to twist (Figure 5.2). So twist rotation has applied in one end of the model. Storage reel has MBR of 2.5 meter, so residual curvature can have the minimum value of 2.5 meter radius.

Simulation has run for 50 seconds. Sequence of loading (Figure 6.7) is also important to model the phenomenon properly. Residual curvature has activated from the first second, which develops in the umbilical when it is in the storage reel. When the curvature has reached its full magnitude at 10th second, tension and gravity has started to apply, which means that umbilical has started to move from storage reel to installation vessel. Gravity load is acting from 11th second when the Agbami has start to feel unsupported in the in between space of storage reel and installation chute. Twisting has applied at last from 31st second.
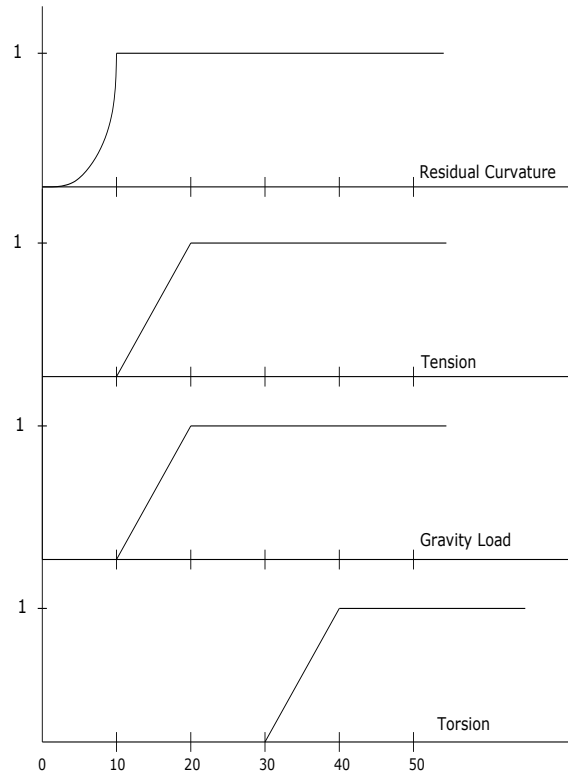
Figure 6.7: Loading sequence

53

6.1.4 Agbami Tensioner Effect

This is quite hard to model the exact physical phenomenon, described in Chapter 5.1.2 (Figure 5.3). The phenomenon of one helix tube not finding compression in tensioner and moving faster than the other elements of bundle is modelled by considering axial strain in that element. Because when one helix tube in an umbilical has axial strain, it can introduce helical deformation in the whole umbilical of its own pitch length. So the model will be able to show same physical behaviour.

Modelling has done in Bflex and the model consists of one helix tube inside a core pipe (Figure 6.8). The core pipe has modelled with PIPE31 straight beam element. The steel tube has modelled by HSHEAR353 helix element. The contact between core pipe and helix tube has modelled by HCONT453 contact element. Contact elements are introduced for numerical stability of the simulation and they kept fixed in all degree of freedoms at each nod along the length. The mechanical properties of all other components except the helix steel tube have lumped into the core pipe. Calculation of the material properties of helix tube and core pipe has shown in Appendix A.
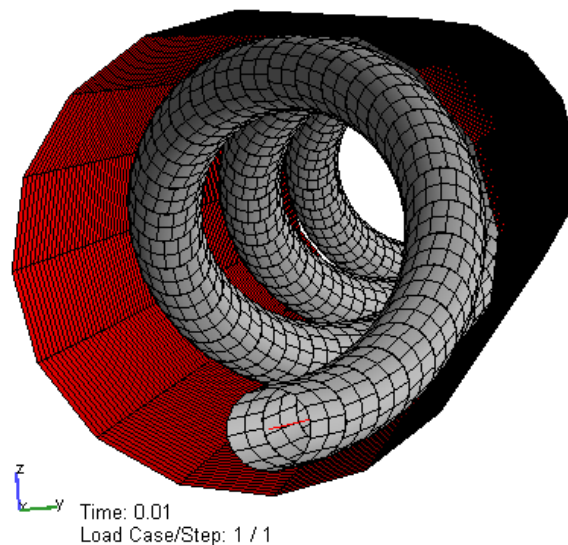
Figure 6.8: Agbami modelled with one helix, to investigate the effect of tensioner.

Axisymmetric and bending quantities are taken into account in the model. The shear coupling between axial and torsion quantities has avoided. So no instability from shear coupling or shear locking will happen and the shear stresses between helix element and contact element will only occur as a result of bending.

The friction between helix element and contact element has turned on in the model.

The only load here is axial strain in the helix tube; it has applied in a very smooth way like a half cosine shape by RAMPCOS time history, so that it reaches its maximum amplitude very slowly.

Also 2 KN tension has applied, as it exist in the real installation process.

Steel tube modelled has 2 kg/m mass and it was installing in 1460 meter water depth.

So, load from water due to own weight = $2 \times 9.81 \times 1.460 = 28.6$ KN

Moreover there is 2KN tension in the installation process of Agbami. So from water steel tube will get a backward load of total 30.6 KN.

Features of all the models of Agbami has presented in Table 6.1 below

Models	Component	Element Group	Element Type	Element Property	Material Type
Reeling	Outersheath	Outersheath	PIPE31	PIPE	LINEAR
	Helix tubes	Helixtube1 to Helixtube26	HELIX231	HELIX	LINEAR
	Contact material		CONTACT		
	Reel	Spool1	PIPE31	PIPE	LINEAR
	Spring	Spring1	PIPE31	PIPE	LINEAR
	Slave	Slave1	PIPE31	PIPE	LINEAR
	Core pipe	Centertube	PIPE31	PIPE	LINEAR
Residual curvature and Torsional instability	Umbilical	Umb1	PIPE31	PIPE	LINEAR
Tensioner effect	Core pipe	core	PIPE31	PIPE	LINEAR
	Helix tube	Helix1	HSHEAR353	SHEARHELIX	ELASTIC
	Contact between core and helix	Contact1	HCONT453	LAYERCONTACT	ISOCONTACT

Table 6.1: Summery of Agbami models.

6.2 Droshky

Droshky has unsymmetrical cross section and showed snaking when it had finished the extrusion process so the residual curvature of component steel tubes is the probable reason in this case.

Any steel tube in the bundle can have residual curvature. Here for the Bflex modelling three out of five big tubes has taken, having unsymmetrical orientation in the cross section (Figure 6.9). Big tubes have large contribution in bending moment than the smaller. So only the bigger tubes has considered here. Due to asymmetric position of the 3 tubes the resulting bending load (M=EIk) from the residual curvature of the tubes could introduce helical deformation in the whole umbilical by creating asymmetric bending moment. Position of the tubes has fixed by setting exact helix angle and helix radius as in the physical model.
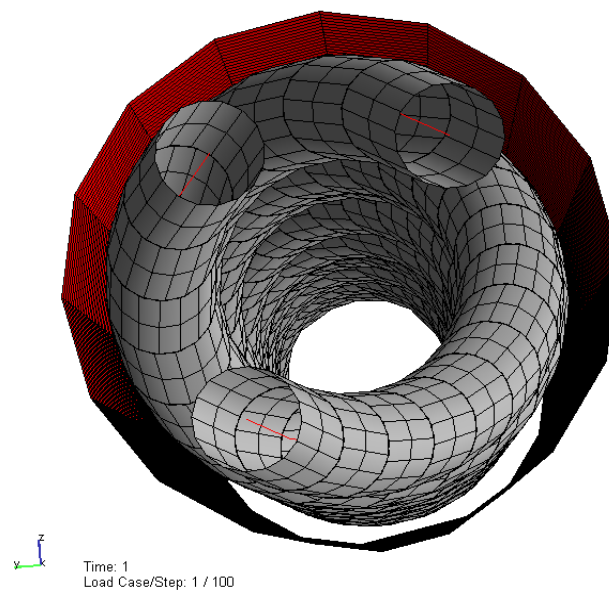

Figure 6.9: Cross section of Droshky, modelled in Bflex.

Droshky has bundling pitch length of 7 meter. In this modelling four pitch lengths has been taken that is the length of the model is taken as 28 meter and 100 elements has taken along the length in each of the tubes and core pipe.

The core pipe has been modelled as a straight cylindrical beam with PIPE31 beam elements. Core pipe has the same element property as the outersheath and in the material property the properties of whole umbilical except the three tubes which have modelled separately has lumped in the core pipe. Calculation of the material properties of helix tube and core pipe has shown in Appendix A.

Axisymmetric and bending quantities are taken into account in the model. The shear coupling between axial and torsion quantities has avoided. So no instability from shear coupling or shear locking will happen and the shear stresses between helix element and contact element will only occur as a result of bending.

Steel tubes within the core pipe have been modelled with HSHEAR353 curved beam elements, taking tubular cross section. Element property of helix element is of SHEARHELIX type.

The contact of each helix tube with core pipe has modelled by HCONT453 contact element. Element property of contact element is of LAYERCONTACT type and material property is of ISOCONTACT type. The material curve along Z direction has taken as very stiff for proper contact between helix tube and core pipe, modelled with HYCURVE material type.

The contact interface between core and helix is controlled by master-slave technique, taking the core as master element group and helix as slave element group.

The friction between helix element and contact element has turned on in the model.

Contact elements are introduced for numerical stability of the simulation and they kept fixed in all degree of freedoms at each nod along the length. Helix elements are kept fixed at all nodes along the length with respect to translation along Z and rotation about X and also at end nodes with respect to translation along X and Y axis. Allowing the curvature about Y and Z axis only.

Each simulation has run for 40 seconds. For smooth increase of residual curvature it has applied from third second in RAMPCOS load shape

Mass load has acted throughout the whole simulation time also a tension load of 1 KN since it is engaged during the real extrusion process.

Dynamic analysis has run to obtain the numerical stability of the simulation. With static analysis convergence problem is appeared in the simulation. Dynamic analysis is run with physical timing, which means timing is as it is in the actual field. Static analysis is not related with the physical timing so load step is the only feature to care in it.

In the extrusion process of umbilical, component elements are bundled together and the outersheath is put on it. Before coming to the extrusion process from storage reel, each steel tube is straightened in the straightener. After straightening they are again spooled in reels from where they are send to the bundling machine.

In the bundling process each reel rotate in a certain rotation speed around the bundling machine and at the same time tubes passes from their individual reel to bundling machine. So the curvature changes along the length in a harmonic motion. Curvature about Y axis change by sine function and about Z axis by cosine function, as

$$\kappa_y = \kappa_0 \sin\left(\frac{2\pi x}{L_p}\right) \qquad (6.1)$$

$$\kappa_z = \kappa_0 \cos\left(\frac{2\pi x}{L_p}\right) \qquad (6.2)$$

κ_0 = Curvature at the first end of steel tube, entering in extrusion

x = Length from the first end

L_p = Pitch length of steel tube

The storage reel of steel pipe has inner dia of 1.8 meter and outer dia of 2.9 meter. Suppose the straightener machine is tuned to straight the curvature of outer wound lengths i.e. to straighten 2.9 meter radius, then the inner wound lengths will bear curvature of $2 \times \left(\frac{1}{1.8} - \frac{1}{2.9}\right) = 0.42$ per meter. This curvature will change along the length harmonically due to the rotation of reel. So the κ_0 value in above two equations is 0.42.

Simulations have also performed to straighten the deformed umbilical. For this RESTART has done after 40 seconds of simulation and only tension has applied to make the umbilical model straight.

Component	Element Group	Element Type	Element Property	Material Type
Core pipe	Core	PIPE31	PIPE	LINEAR
Helix tube	Helix1, Helix2, Helix3	HSHEAR353	SHEARHELIX	ELASTIC
Contact between core and helix	Contact1, Contact2, Contact3	HCONT453	LAYERCONTACT	ISOCONTACT

Table 6.2: Summery of Droshky Bflex modelling

6.3 Kipper

Here the modelling of Kipper is done to investigate the effect of friction in its reeling process. The phenomenon which has modelled here is, an umbilical is rolling on in a reel (turntable E of the Aker manufacturing plant) and then rolling out from the reel. Friction effect has introduced by applying residual axial strain which will squeeze the umbilical and will bring the internal elements in contact. Tension has also applied both in rolling on and off for smooth and successful rolling.

Dia of turntable E is 15.8 meter. To make one round on it length of the model need to be longer than its perimeter 49.64 meter. A 60 meter model of kipper which is ten pitch lengths has taken with 200 elements along the length. The umbilical consists of a core pipe and two helix tubes on it. The element and material properties of core and helix elements of kipper are same as that for Droshky.
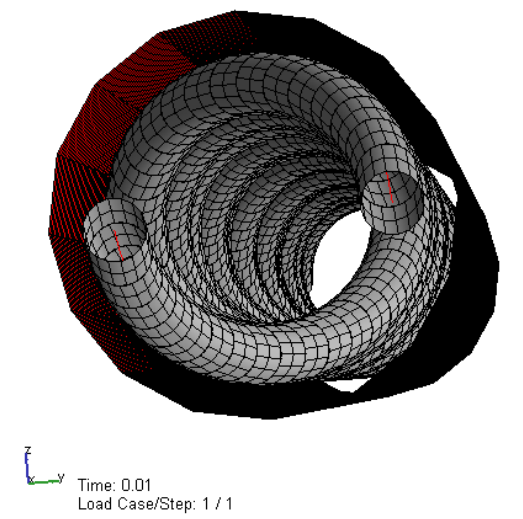

Figure 6.10: Kipper Model

Kipper has three bundles of wires, one at the center and other two are at two side of it. Kipper is modelled in Bflex with a core pipe having two helix tubes on it (Figure 6.10). The properties of the bundle at the center, cables and conduits and outersheath are lumped in the core pipe. The two bundles at two side of the center have modelled as helix tube having the same outer radius as wire bundle. The steel tube has modelled with the same mechanical properties as the wire bundle so that the mechanical behaviour will be same.

The reel is consists of 24 equally spaced rollers (Figure 6.11), which are modelled by CONT164 elements. Each roller element have two nodes, one coincide with spring node which is fixed in all DOF other is positioned at the roller center. The position of the rollers with respect to center is fixed by setting the eccentricities using STINGER type of elements.
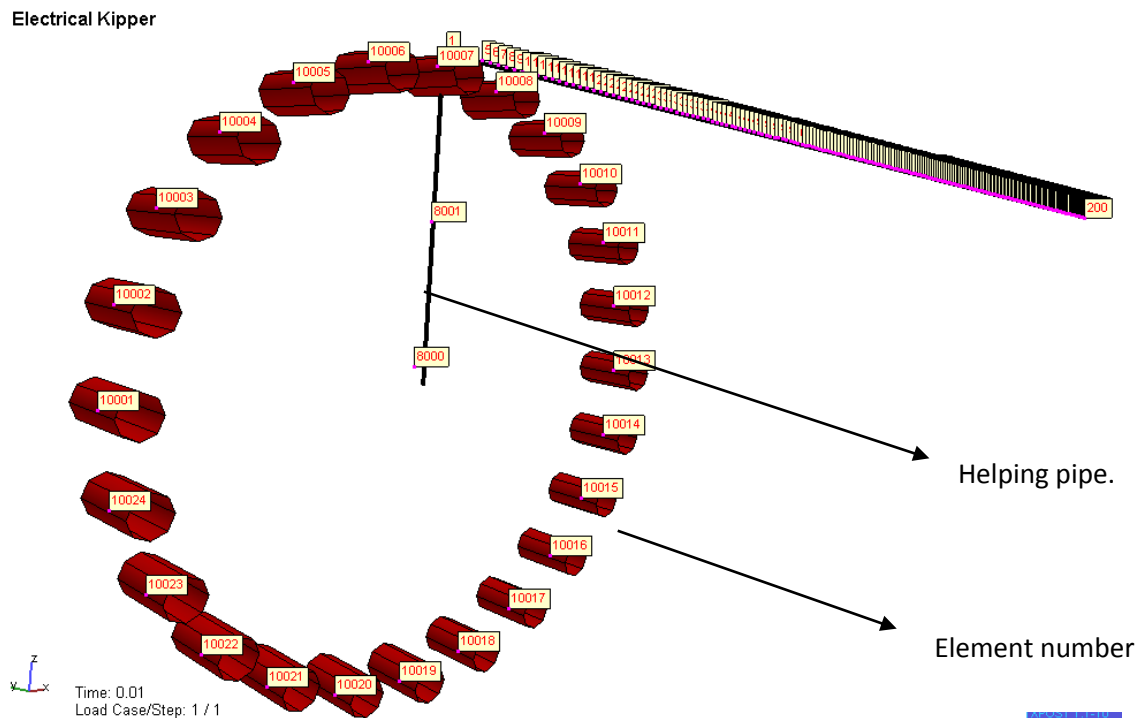
Figure 6.11: Rolling of Kipper, modelled in Bflex.

To obtain the rotation of the umbilical along the reel a spring element (SPRING137) has placed at the center. The spring is a very stiff two nodded element having the same coordinates. One node of the spring is fixed in all DOFs and other one is allowable to rotate about Y axis only. The material of the spring is of GENSPRING type which is fixed by setting six springs along six degree of freedoms. Since the spring node is provisioned to move in direction 5 only, so dummy spring materials have provided in all directions except 5 where a very stiff spring material has been set. Dummy spring is for numerical stability.

To make the umbilical follow the rotation of reel center a connection has set between them by a two nodded pipe element modelled by PIPE31. This pipe is modelled as a very stiff element having high axial, bending and torsional stiffness by LINEAR material card, so that any possible distortion of the roller end does not transfer in the spring end. The roller end of the pipe is connected with umbilical by four constraint connecting equations along directions 1, 2, 3 and 6. The other end of pipe is placed at reel center, have same coordinate as spring nodes. Contact interface of each roller has been set with all nodes of the umbilical core so that umbilical rotate along the rollers. The other end of umbilical has kept fixed for displacement along Y and Z axis and along X axis kept free for the application of tension.

The reeling action is performed by applying rotation at the spring node which is free to rotate only about Y axis. This rotation is transferred to the rollers by a connecting pipe element. Due to the connection of umbilical core with rollers, the umbilical rolls with the rollers rotation. Here a rotation of 360 degree has modelled. To obtain a smooth rotation, it has timed by RAMPCOS loading. A certain amount of tension has also applied at the free end of the umbilical core for a controlled reeling action. Tension has increased in stepwise with time to get numerical stability. Maximum tension applied is 70 KN for this model. Tension is also need to apply when the

umbilical spool off. Here around 500 KN tension has applied to spool out, which is unrealistic. But for the convergence of the model in Bflex this high amount of torsion has required. As mentioned earlier, to investigate the friction effect, residual axial strain has imposed on the two helixes of kipper from the beginning of simulation that is before the starting of rolling and in this case axial strain level is 0.02%.

The total spooling in and out simulation was for 60 seconds. The rolling action has started after the development of full axial strain at 11th second. Kipper has given 30 seconds for rolling in and 20 seconds for rolling out. To run the simulation with physical timing DYNAMIC type analysis was chose. Mass load was also acting from the beginning.

The global coordinate system has taken at the center of the reel (Figure 6.11), which is also the local coordinate system center of the reel. The center of the local coordinate system of umbilical is at its center (Figure 6.10).

Calculation of the material properties of helix tube and core pipe has shown in Appendix A.

Component	Element Group	Element Type	Element Property	Material Type
Core pipe	Core	PIPE31	PIPE	LINEAR
Equivalent helix tube of the wire bundle	Helix1, Helix2,	HSHEAR353	SHEARHELIX	ELASTIC
Contact between core and helix	Contact1, Contact2,	HCONT453	LAYERCONTACT	ISOCONTACT
Reel	Rolcontact1 to Rolcontact24	CONT164	ROLLER	CONTACT
Spring at reel center	Spring	SPRING137	GENSPRING	GENSPRING
Helping pipe	Rotpipe	PIPE31	PIPE	LINEAR

Table 6.3: Summery of Bflex modelling of Kipper

Chapter **7** Results and Analysis

Total six models were established to investigate the concerned snaking scenarios. Deformation pattern they show will figure out in this chapter. By comparing the resulted deformation pattern of the models with the real deformation pictures of Chapter 5, the reason of each models deformation will fixed out. Some parametric study will also do to identify the nature of the snaking deformations.

7.1 Agbami

Four modelling were done for Agbami, the first modelling did to figure out the friction effect in creating curvature of Agbami. The other three models did to trace out the reason of snaking happened in Agbami.

7.1.1 Agbami Reeling

The moment and curvature values of each component element of umbilical can be found from the USAPPOST, once the umbilical is modelled in USAP. Taking these values, plot can be made by doing few hand calculations using equation (3.16). The detail calculation has been attached in Appendix C.

Here, in the USAP model of Agbami, the whole model has divided into 200 elements and figure can be plotted by observing the moments and curvature development at any element. Here moment and curvature values have been find out for the element 15 (Figure 6.4).
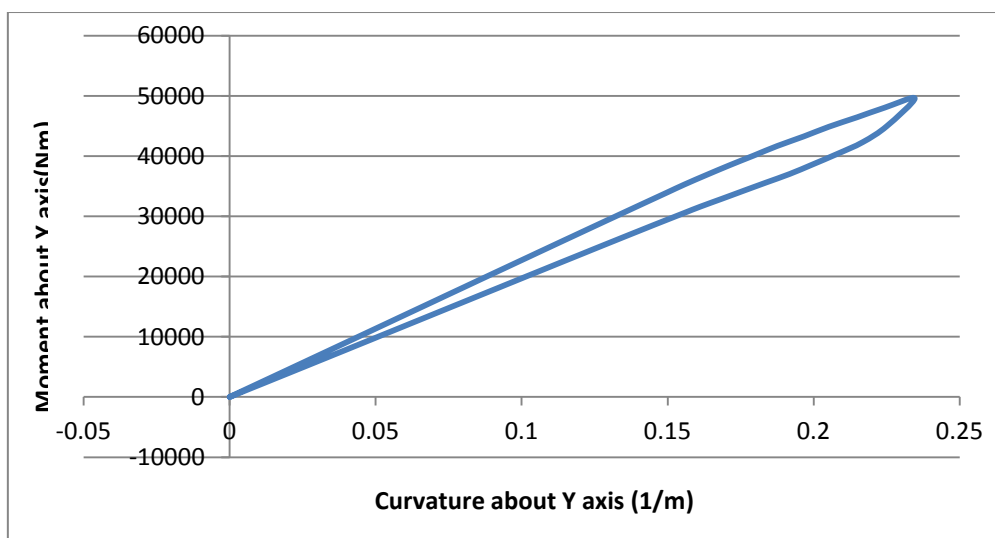

Figure 7.1 (a): Moment curvature plot about Y axis for 90 degree reeling.
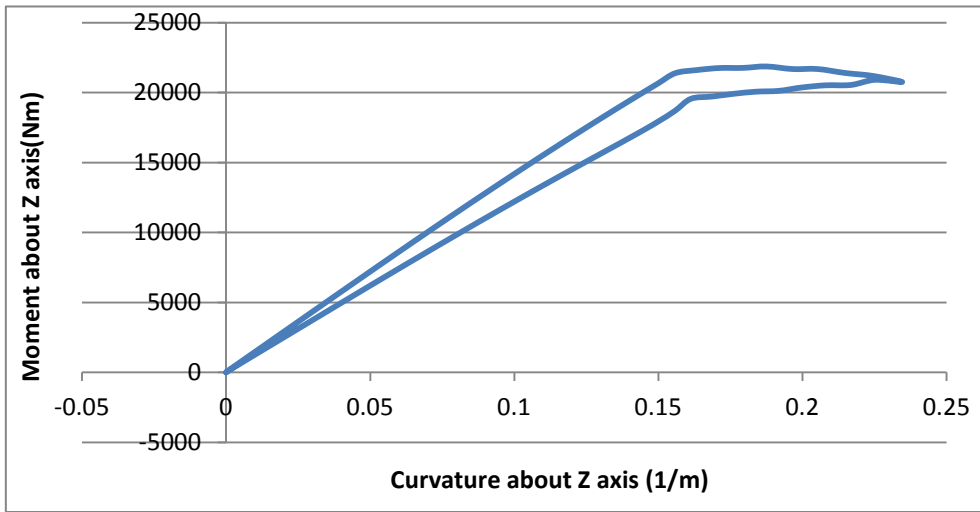
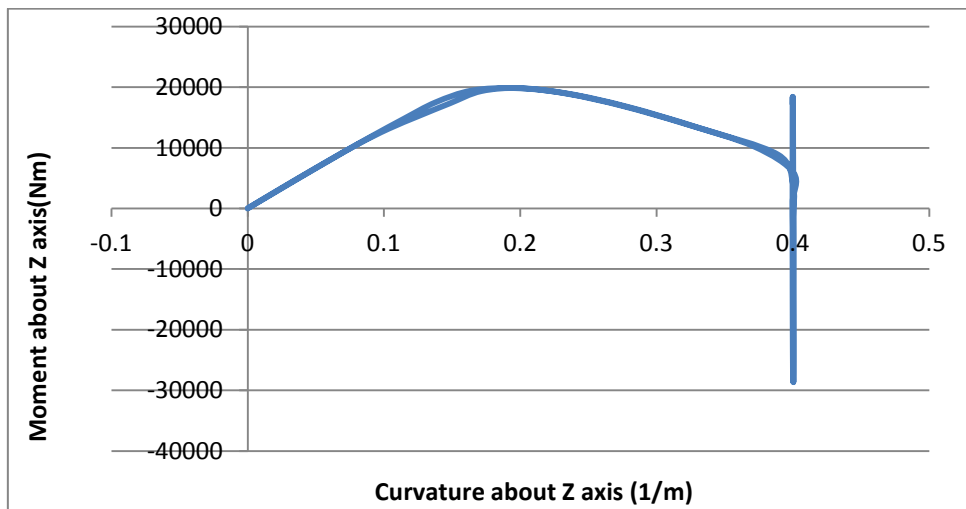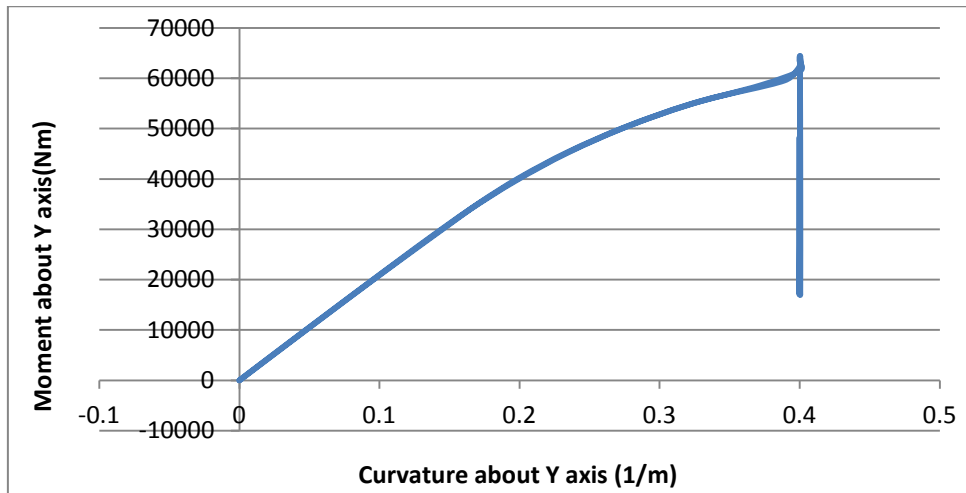*Figure 7.1 (b): Moment curvature plot about Z axis for 90 degree reeling.*

Figure 7.2: Moment curvature plot for 360 degree reeling.

The moment curvature plot has been developed for four different amount of angular reeling amount. Plot for 90 and 360 degree has been shown in figure 7.1 and 7.22 respectively. Plot for 180 and 270 will found in Appendix B. But none of the plot showed any sign of hysteresis, every plot is coming back to zero after spooling off. The plot for 90 degree reeling (Figure 7.1) shows some loop but no hysteresis. In the plot of other reeling, the development of moment with curvature decrement i.e. spooling off follow the same path as for curvature increment i.e. spooling on. So no loop or hysteresis is formed.

Highest possible curvature is 0.4 per meter, as the radius of reel is 2.5 meter. For 360 degree reeling, at 0.4 curvature that is at the end of spooling on and at the start of spooling off, the moment curvature plot become almost vertical. This is because; for very small change is curvatures large variation of moment is happening. Same happens for 180 and 270 degree reeling.

This behaviour is very strange and not expected. And according to moment curvature relation described in Chapter 3.4 this tells that, no curvature will appear in the umbilical due to friction, when it will spool out from the reel, it will remain straight as it was before start of reeling.

So friction moment is not the reason of residual curvature in Agbami and the other effect, which is creeping, is the reason of residual curvature in Agbami. Creeping is very possible as Agbami was stored for long period of 10 months.

The physical reason of getting this low hysteresis is the low lay angle (2.8 degree) of the Agbami. Due to low lay angle, there is less sliding between the helical umbilical components, when it experienced contact load in reeling. And because of this less sliding, less friction is generating in the process, so the low hysteresis.

Also due to less friction, change of contact pressure is not so high. As, contact pressure increases during rolling in according to $S = S_0 e^{\mu\Theta}$ and decreases during rolling out according to $S_0 = S e^{-\mu\Theta}$, where, μ is the friction coefficient. So, amount of moments during rolling in is not that much higher than the moments during rolling out and so the shape of the loop is found very tiny.

Low hysteresis; also indicate that, there is no second order helix effect developed in this umbilical during its rolling on the roller. That is when it is rolls in to the reel; no tension part will create as in Figure 3.7 which can pull the helixes from below and causes snaking like shape in umbilical.

7.1.2 Agbami Residual Curvature

Snakelike deformation has found on the model for 4.5 meter residual curvature radius as shown in Figure 7.3 below. But the pitch length of the deformation is very higher from the expected 11 meter pitch length of Figure 5.2.
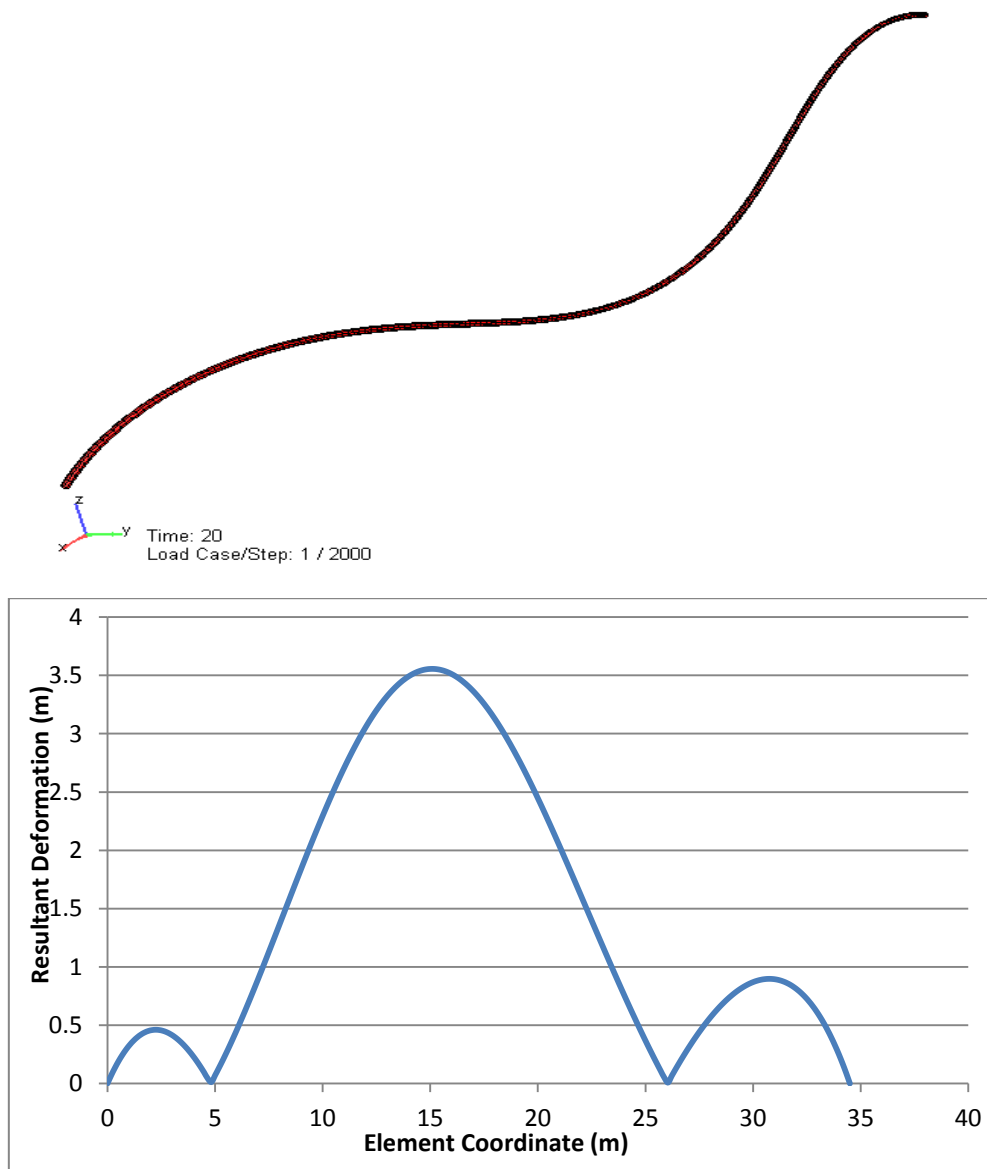

Figure 7.3: Deformation of 34.5 meter model with 4.5 meter residual curvature radius.

The maximum curvature that can be applied is the curvature with radius of 2.5 meter, as this is the MBR storage of Agbami. But the deformation under this curvature is very severe and the model is coiling (Figure 7.4). This tells that inner wound lengths of a storage reel experiences the most severe deformation from creeping than the outer wounds.
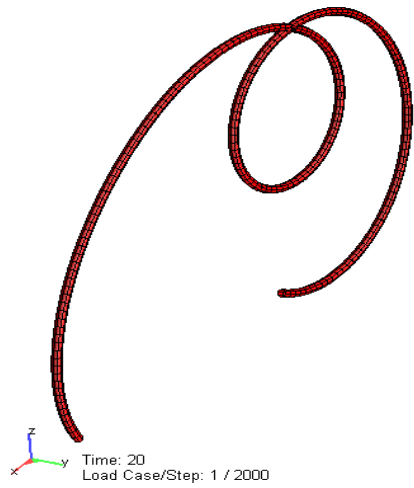
Figure 7.4: Deformation of 34.5 meter model with 2.5 meter residual curvature radius.

To observe the effect of change of model length two other simulations has done by changing the length from 34.5 meter and with 4.5 meter radius of curvature as shown in Figure 7.5 and 7.6.
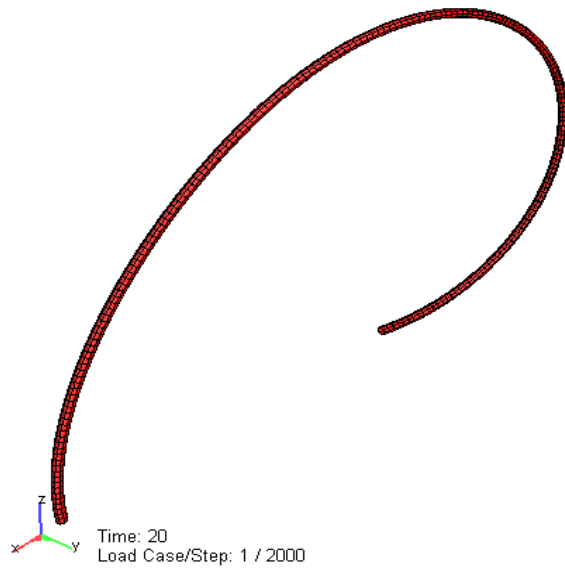

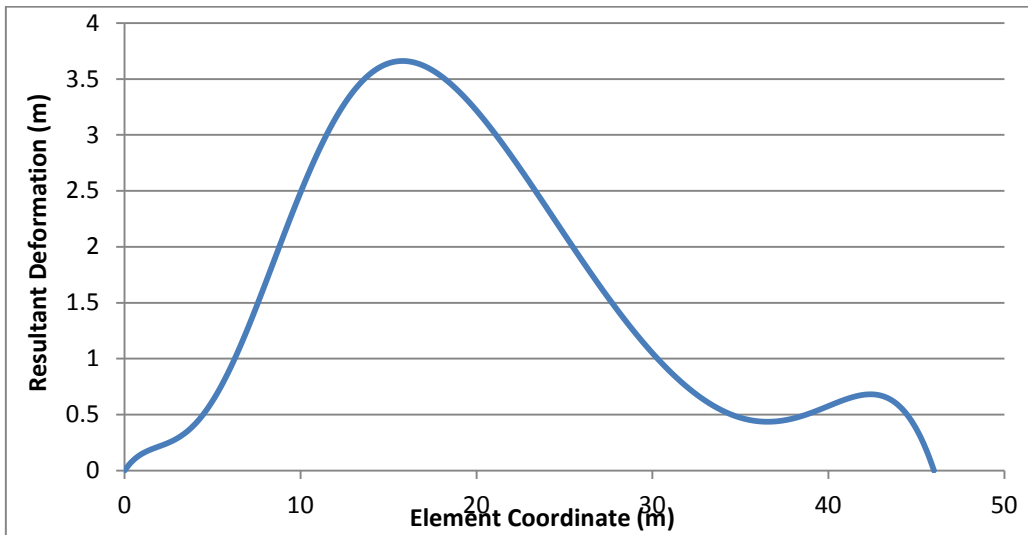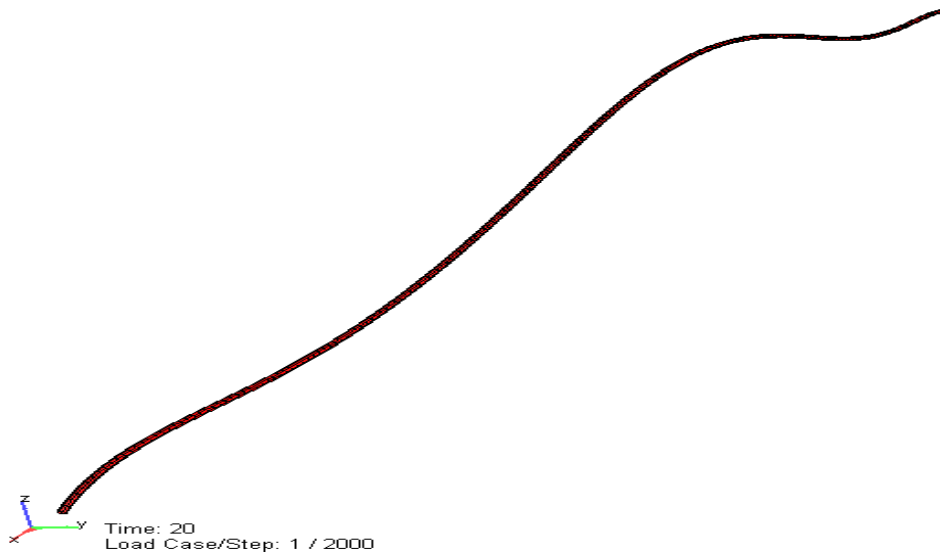*Figure 7.5: Deformation of 23 meter model with 4.5 meter residual curvature radius.*

Time: 20
Load Case/Step: 1 / 2000

Figure 7.6: Deformation of 46 meter model with 4.5 meter residual curvature radius.

Figure 7.5 and 7.6 suggests that, Increment or decrement, none of the length changing brings the deformation with 11 meter pitch length. Many other simulations have also done by changing both curvature and model length, but the desired deformation pattern (Figure 5.2) has not got. So it has been confirmed that, though residual curvature can create deformation but the deformation of Figure 5.2 is not because of residual curvature.

7.1.3 Agbami Tensioner Effect

The modelling has done, taking axial strain in one helix tube. But which strain is equivalent for 30.6 KN load, this is unknown. So simulations of the model have done by changing the axial strain amount and checking back what is the load developed for that strain.

For 0.075% axial strain, 32 KN loads develops (Figure 7.7) which is in the range of required 30.6 KN. But this does not create any deformation, as can see from Figure 7.7 the model remain straight after applying axial strain. Because 32 KN load one helix tube is not enough loads to create snaking in the whole umbilical. The very low lay angle (2.8 Degree) of helix tube is also the reason engaged here.
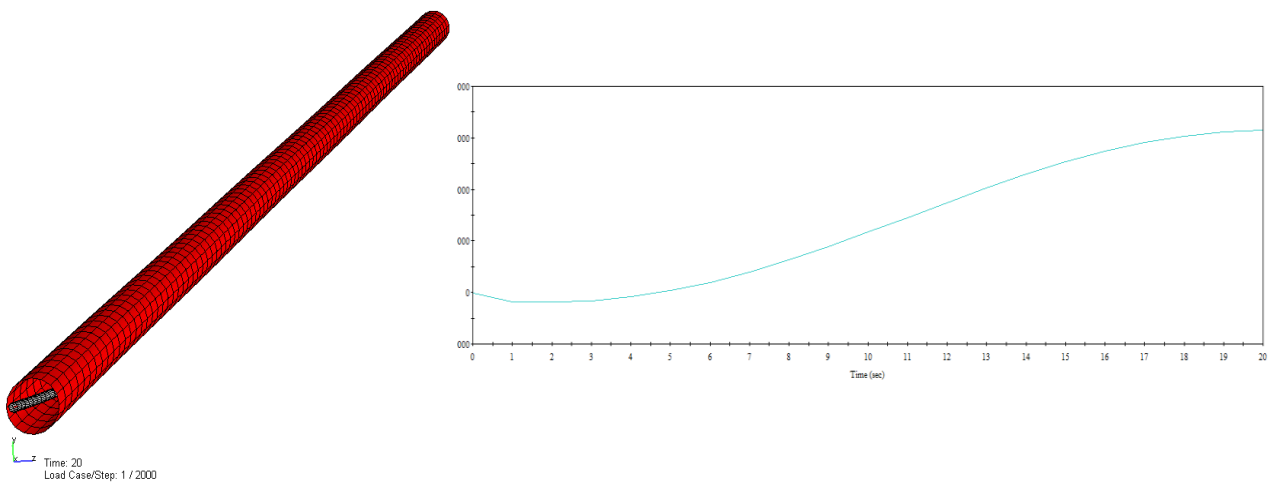

Figure 7.7: Deformation pattern and axial force, developed from 0.075% axial strain.

For 2.0% axial strain, snaking deformation of 6 meter pitch length and 0.1 meter double amplitude is found (Figure 7.8). But the axial load develop in this case is 820 KN which is unacceptable. Also since yield strain of steel is 0.2% so deformation with 2.0% is from plastic yielding not from the expected load generation phenomenon.
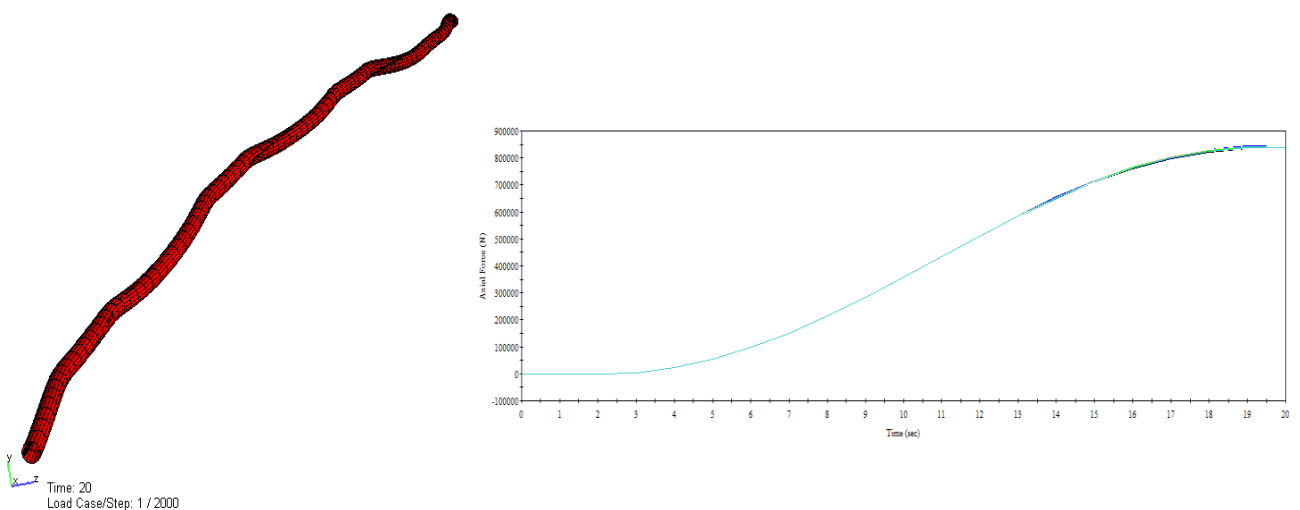

Figure 7.8 (a): Deformation pattern and axial force, developed from 2.0% axial strain.
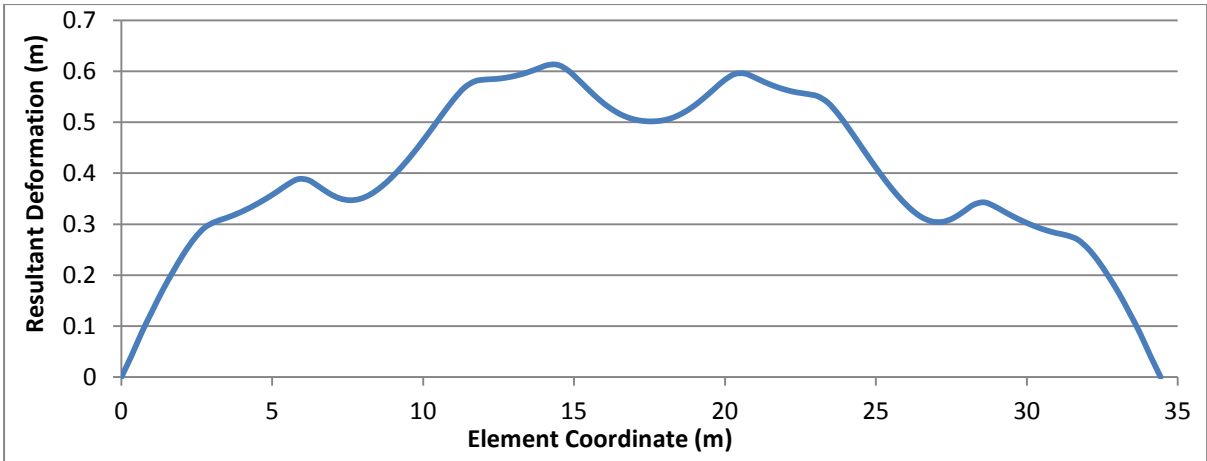
Figure 7.8 (b): Resultant curvature along length, developed from 2.0% axial strain.

So the snaking deformation phenomenon from tensioner effect, as suspected in Chapter 5.1.2 is not happening for Agbami.

7.1.4 Agbami Torsional Instability

According the analytical model presented in Chapter 4.1, residual curvature and opposite curvature has applied in this Agbami model to get torsional instability. Model has run with dynamic analysis in Bflex, as it shows convergence problem in static analysis of Bflex and in USAP. Existence of torsional instability that is zero torsion moment configurations has found for 2.5 meter residual curvature radius with 180 degree twisting rotation (Figure 7.9).
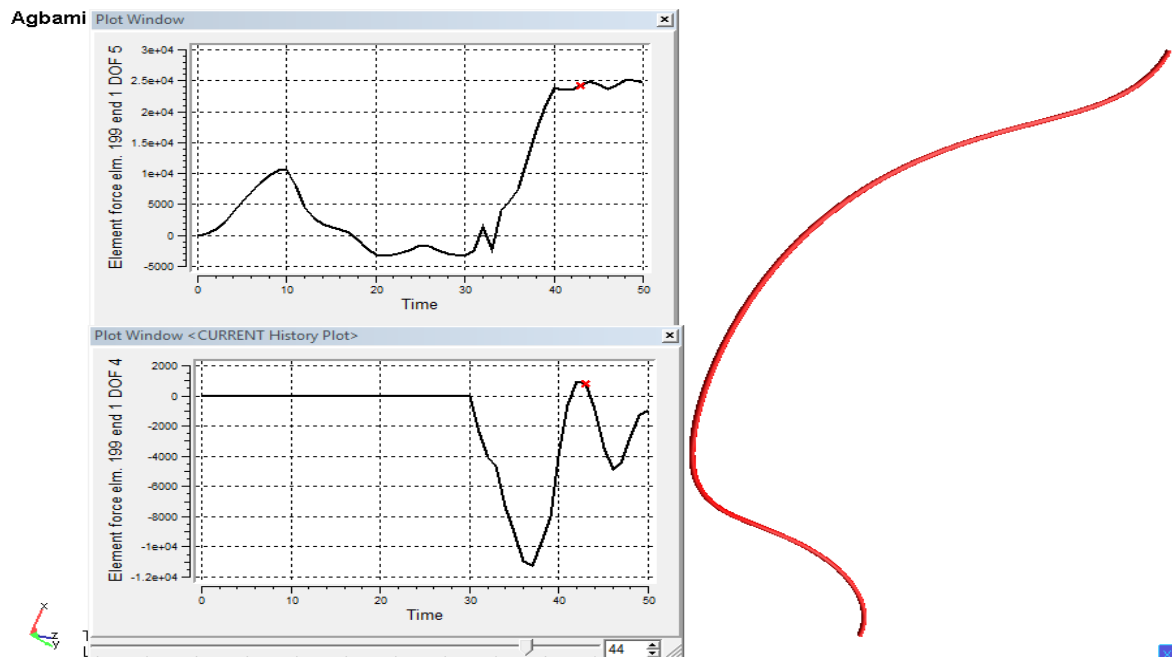

Figure 7.9: Torsional Instability configuration of Agbami model

Looking at the bending moment history (DOF 5) of above figure; it can be seen that residual curvature and curvature from gravity load has developed on the model within 30th second and gravity load curvature is more than the 2.5 meter radius residual curvature. No twisting (DOF 4) was present in that part, which means no torsion moment develops from the action of opposite directed bending curvatures. Twisting rotation has applied from 31st second to get twisting moment which has showed some upward and downward movement between 30 to 50 seconds. At the 42.5th second the twisting moment curve crossed up the zero moment and at the 44.5[th] second it again crossed the zero moment and moved down. So these two zero moment points are the torsional instability points found.

But the pitch length and amplitude of the deformation at torsional instability is very large. From Figure 7.10, which is the resultant deformation values along the model length, at 44.5[th] second, pitch length and amplitude found is 34.5 and 11.8 meter respectively, which are far higher than the values of Figure 5.2.

This suggests that although the Agbami model experiences torsional instability, but the deformation it experienced in real field (Figure 5.2) was not from torsional instability.
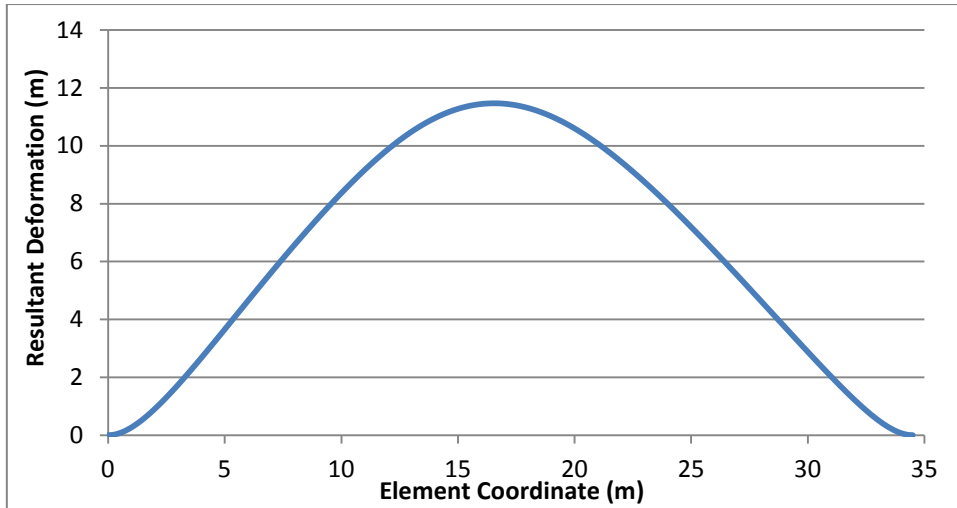
Figure 7.10: Deformation at torsional instability.

Simulations had done again to get deformation which will have similar pitch length and amplitude as of Figure 5.2 and it was found by changing the previous loading sequence. Previously it was residual curvature, gravity load and then twisting. In this case sequence is residual curvature, twisting and gravity load. Here helical deformation is found with pitch length and amplitude of 10.4 meter and 2.4 meter respectively (Figure 7.11). The deformation figure is found by taking the resultant of the deformations along Y and Z axis. Pitch length has measured as the distance between two consecutive peaks (marked with red circle) and height between trough and peak has taken as double amplitude.
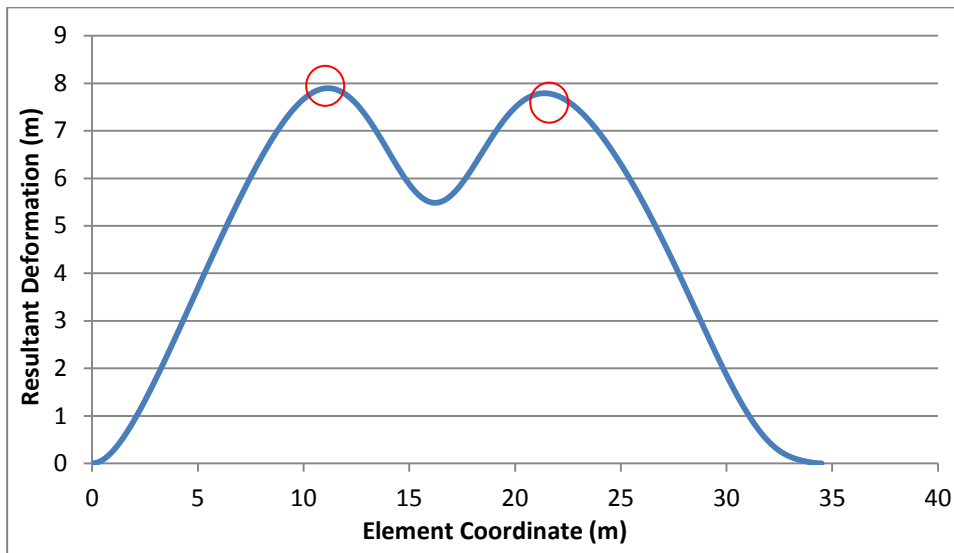

Figure 7.11: Deformation with changed loading sequence.

But in this case of deformation, torsion moment does not cross zero (Figure 7.12) which means there is no torsional instability configuration here. So the decision is standing as said above, the model is having helical deformation but not torsional instability.
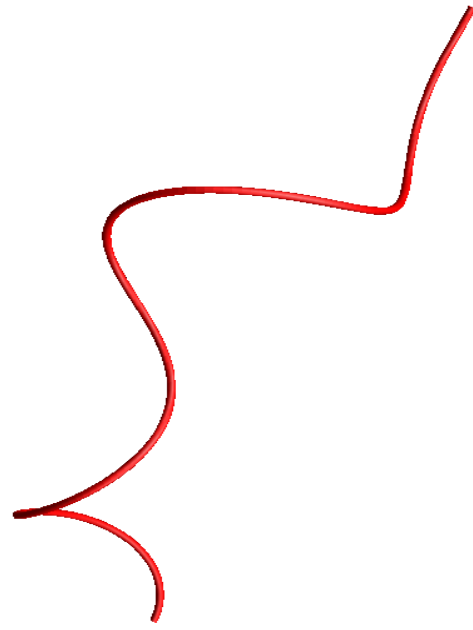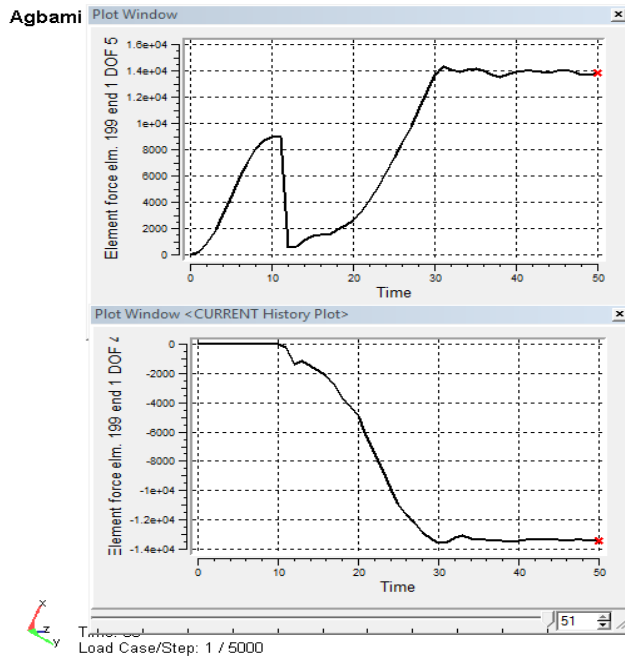
Figure 7.12: Deformation shape with changed loading sequence.

Looking the moment development in the latter case (Figure 7.12), the twisting moment has stated to develop from 11th second due to the application of twisting rotation. Gravity load was in action from 31st second, after which both the moments stopped their trend of changing and maintained their configuration throughout the time of gravity load action. In this loading sequence gravity load is not appearing strong enough to create opposite curvature.

So it is the sequence of loading, making such a difference in the nature of moment development and umbilical can experience loading by any of the sequences in the real installation field.

The same model with 2.5 meter radius of residual curvature but without gravity load and twisting shows deformation as in Figure 7.4. The difference in these two figures tells, how the deformation pattern can differs, due to the variation in number and nature of the applied loads.

7.1.4.1 Parametric Study

Some parametric study has performed with the latter loading sequence by changing model length, residual radius, twisting and tension to predict their effect in the deformation.

Length (m)	Residual Curvature radius (m)	Twisting Amount (degree)	Pitch length (m)	Amplitude (m)	Torsional Instability
Tension 2 KN					
34.5	2.5	90	10.3	2.3	No
		180	10.4	2.4	No
		270	34.5	12	No
	3.0	180	10.1	2.4	No
	3.5	180	34.5	12.4	Yes
20	3.5	180	20	1.6	No
50	3.5	180	50	10.2	No
Tension 10 KN					
34.5	2.5	180	34.5	6	No
	3.5	180	34.5	5.4	No

Table 7.1: Parametric study of changed loading sequence

The relevant input files has provided in the Appendix C. Pitch length and amplitude of the deformation has found by plotting figure similar to Figure7.12 and the existence of torsional instability has checked from the torsion moment plot of the models as like Figure 7.9 and 7.13.

The summery of the parametric study of Table 7.1 has got as:

1. With the increase of residual radius there is increment of deformation intensity as there is increase of both pitch length and amplitude. So length of umbilical spool in the outer radius of reel has the larger deformation.
2. With the increase of tension, deformation behavior is not regular, for 2.5 meter residual radius there happened increase of deformation but for 3.5 meter radius there happened decrease of deformation.
3. With the increase of twisting amount of pitch length and amplitude increases.
4. With the increase of model length, increase of amplitude and one pitch length in each case.
5. With the increased residual curvature, twisting and tension here is also have the tendency of having one pitch length over the length.

For no set of simulation, torsional instability configuration has found except the set of 34.5 meter length, 3.5 meter residual curvature, 180 degree twisting and 2 KN tension (Figure 7.13). But any change in model length, residual radius, twisting or tension amount do not repeat the incidence (olive greened rows of Table 7.1). This suggests an uncertain appearance of torsional instability. But again pitch length and amplitude of torsional instability model do not match with Figure 5.2.

The deformation picture of the set for which torsional instability happened has shown in Figure 7.13 below. It has lots of zero moment point so it is very unstable.
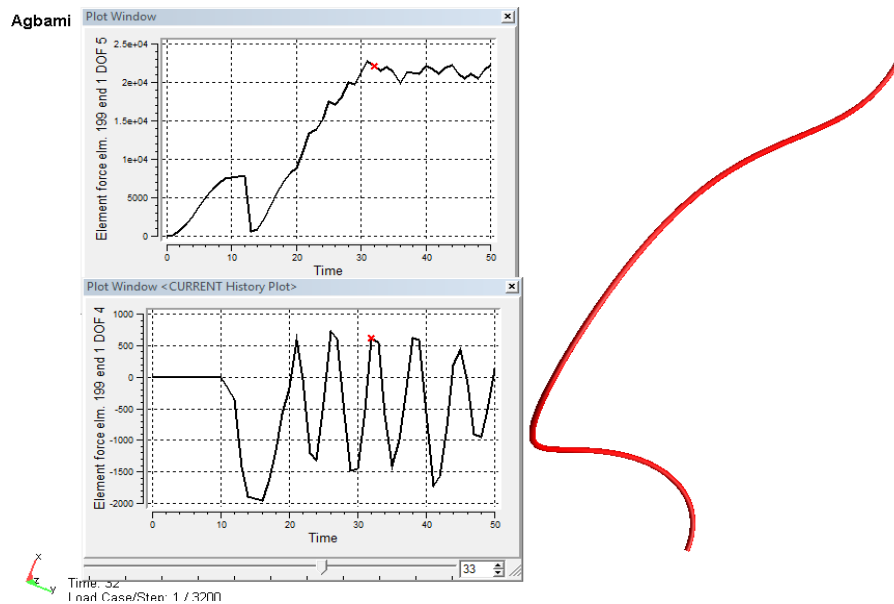

Figure 7.13: Torsional instability in second loading sequence.

Considering the uncertainty of appearing torsional instability in the second loading sequence, to check the stand of first sequence parametric study has done as in Table 7.2 below. Torsional instability is existing with every change of model length, curvature radius and twisting rotation. So uncertainty is found only in the second loading sequence.

Length (m)	Residual Curvature radius (m)	Twisting Amount (degree)	Torsional Instability
34.5	2.5	180	Yes
50	2.5	180	Yes
34.5	3.5	180	Yes
34.5	2.5	270	Yes

Table 7.2: Parametric study of first loading sequence

There is some weakness in this model of Agbami, in applying exact amount of required opposite curvature found from Equation 4.13. In the test model of Sævik presented in Chapter 4.1, opposite curvature has applied by bending moment, M=EIκ where everything is known and the required amount of curvature can be put.

Suppose with a 2.5 meter residual curvature radius (i.e. 0.4 curvature) in a 34.5 meter long model reversed curvature requirement from equation 4.13 is, $\Delta\kappa_\eta$= 0.42 per meter. This is applied by bending moment with curvature κ value of 0.02.

Equation 4.2 can give an idea about the intensity of gravity load. But this has strong limitations as it consider uniform load on straight beam, but the Agbami model here is curved with residual curvature (Figure 4.6). Boundary condition is not simply supported as well, as there is twisting in one end. Also Equation 4.13 needs to modify for consideration of tension loading.

7.2 Droshky

The expected pitch length and double amplitude of the deformation of Droshky model is 4.5 meter and 150 millimetres respectively. Similar range of values has got when the umbilical steel tubes has 30% of its initial curvature during bundling. Here initial curvature means the curvature that has applied in modelling chapter, where κ_0 value was 0.42. Here κ_0 value for equation 6.1 and 6.2 is 0.127 for 30% curvature. The deformation pattern has found as in Figure 7.14 below.
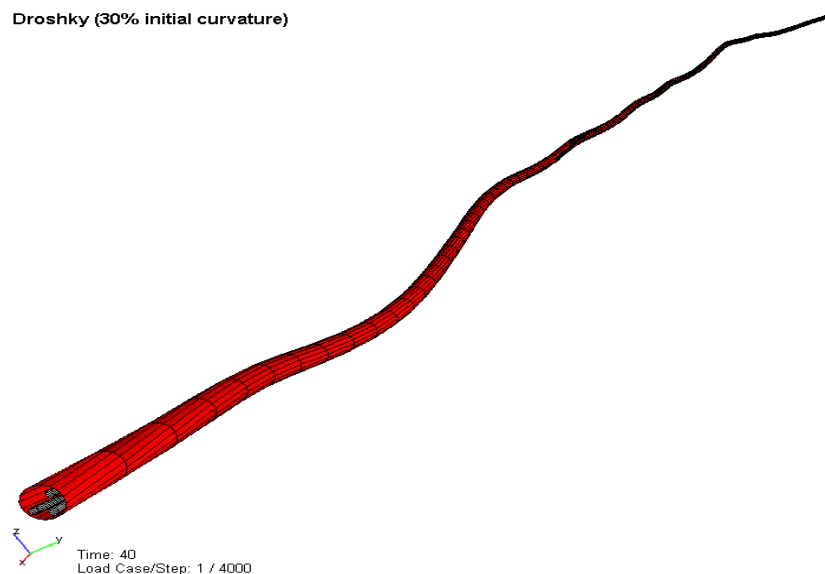

Figure 7.14: Deformation pattern at 30% curvature

To figure out the severity of deformation, pitch length and amplitude has calculated from the Xpost results. Y and Z coordinates of the curved models has extracted from Xpost and their resultant has calculated as in Figure 7.15.

But the variation of pitch length and amplitude in a deformation pattern is not so periodic or regular. So only the values of maximum deformation have taken (red circled in Figure 7.15). The real deformation pattern is slight different as it was kept on support.

Pitch length has measured as the distance between two consecutive peaks and the height between two consecutive peaks is the double amplitude.

Simulations have also made to find the amount of tension need to straighten these deformed umbilical models, keeping one end fixed and applying tension on the other end. Although, it is not possible to make an umbilical completely straight by only applying tension since it contains helical tubes. Some bending moment arises when a helical element is tensioned. So it requires some bending actions in opposite direction by roller to make it completely straighten.

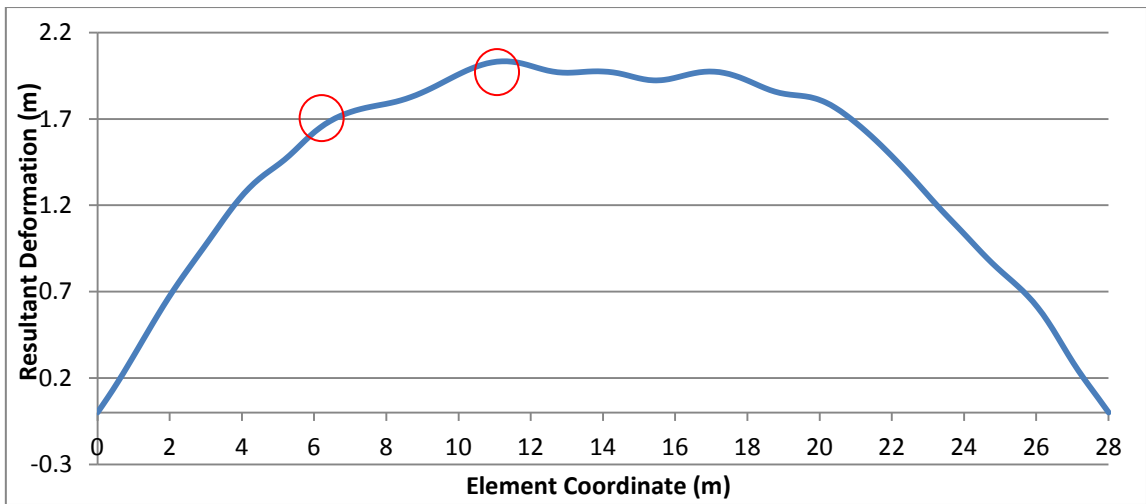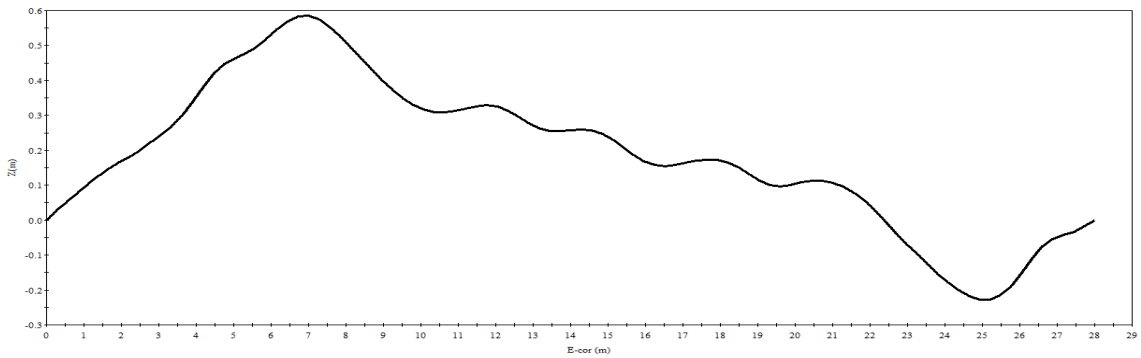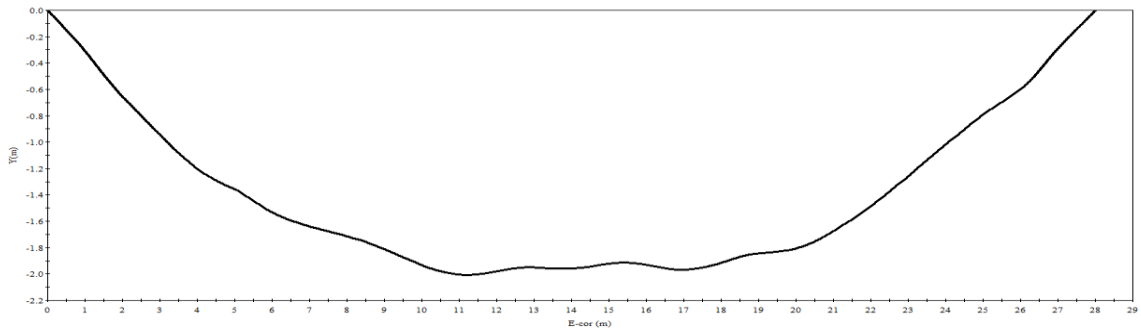The tension require to straighten the deformation of Figure 7.14 is found as 55 MN.

Figure 7.15: Resultant curvature along length at 30%

To observe the change in deformation pattern, with change in residual curvature amount some more simulations have done, whose results have presented in Table 7.3.

Initial Curvature (1/m)	Maximum Pitch Length (m)	Maximum Double Amplitude (mm)	Tension need to Straighten (MN)
0.211 (50%)	7.1	250	70
0.127 (30%)	4.5	140	55
0.084 (20%)	3.7	57	35
0.0422 (10%)	3.8	4.5	15
0.0084 (2%)	2.8	3.5	0.5

Table 7.3: Parametric study of Droshky.

The deformed shape at different curvatures has shown in Figure 7.16 and 7.18. As expected with the increase of applied curvature deformation was being severe.

The simulations also shows even a small amount of curvature say 2% introduce a considerable amount of distortion in the umbilical although its amount is not much severe. So the impact or functionality of straightener is very important from where umbilical can leave with curvature.

When the steel leave the straightener machine with big curvature say 50% then the deformation pattern is very inconvenient to handle.
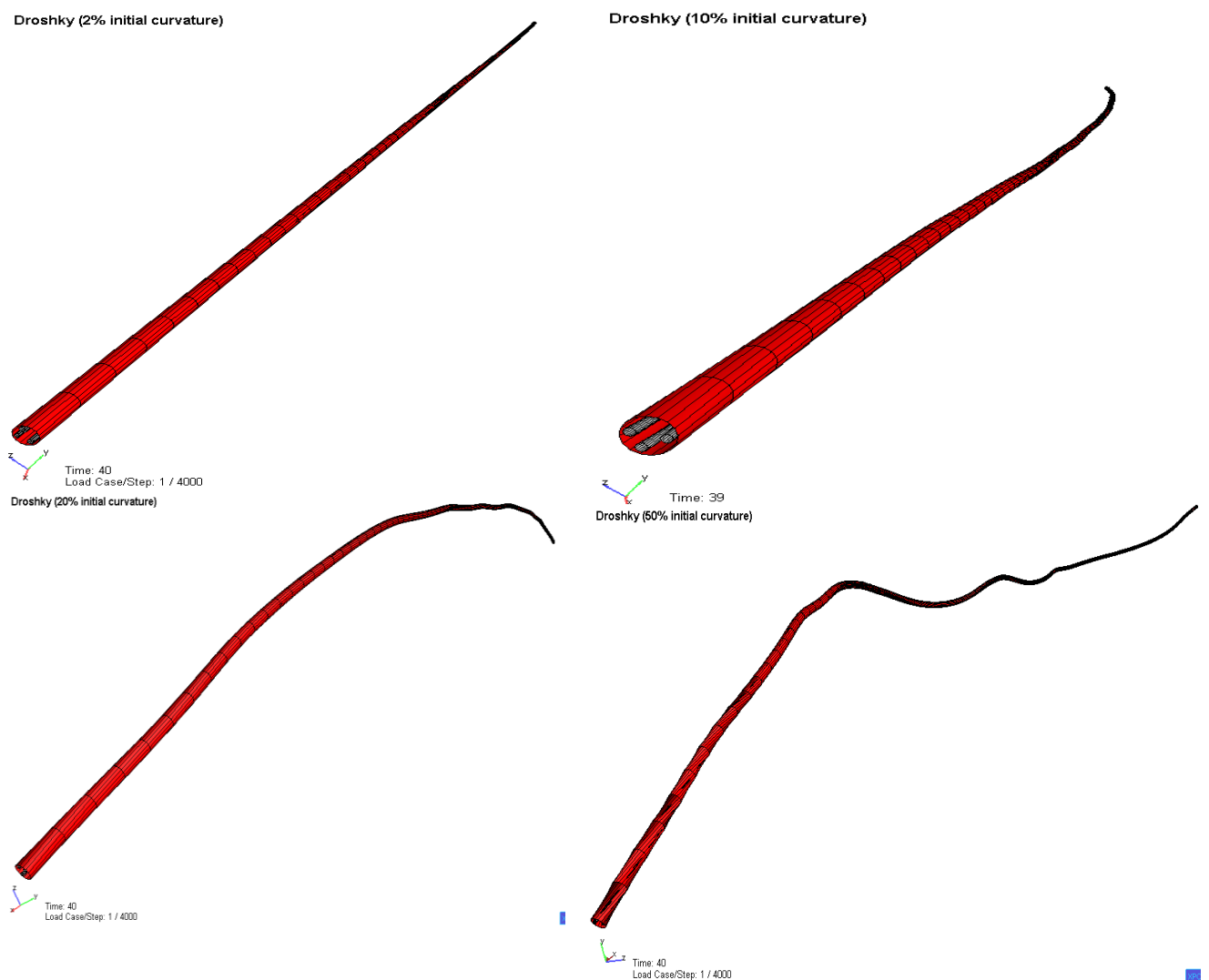

Figure 7.16: Deformed Droshky at 2% (top left), 10% (top right), 20% (bottom left), 50% (bottom right) residual curvature.
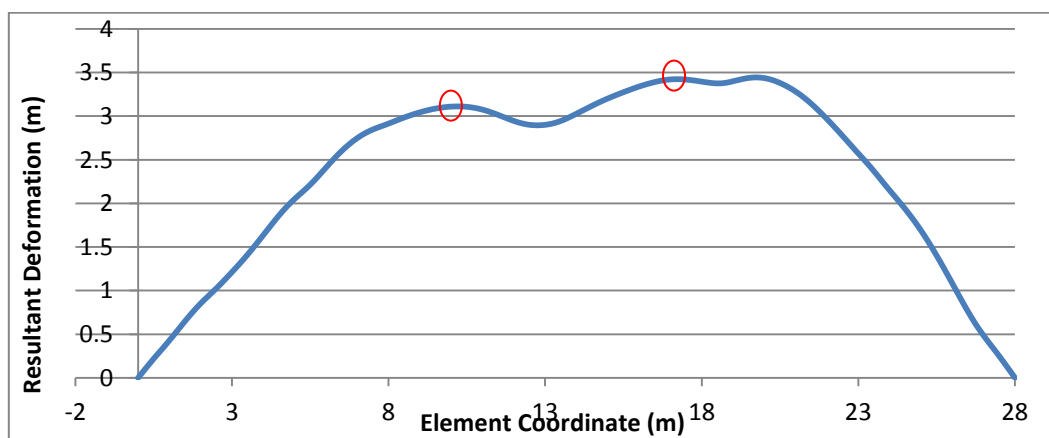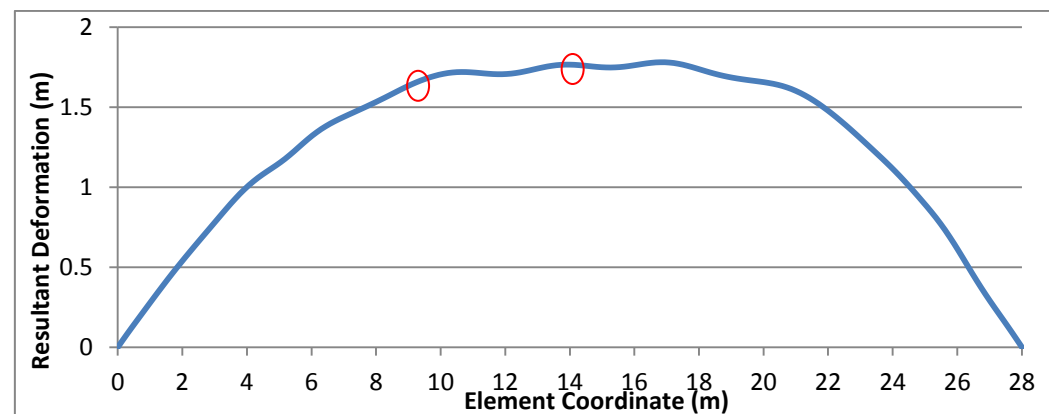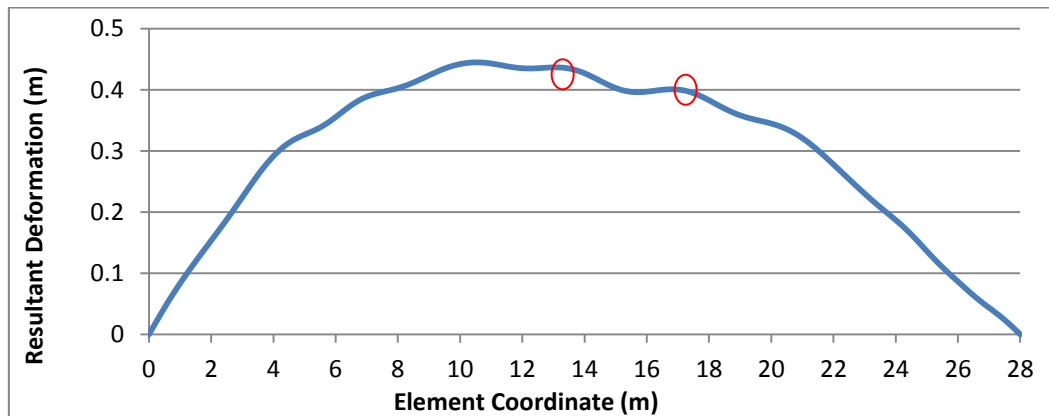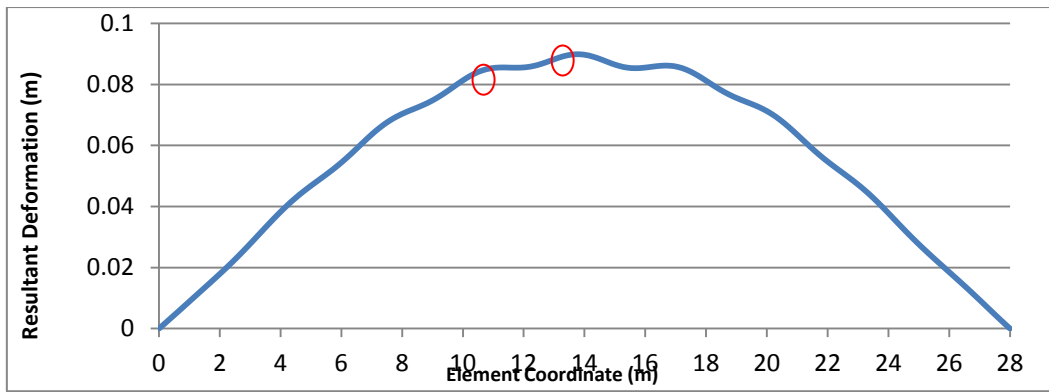
77

Figure 7.17: Resultant curvature along length at 2, 10, 20 and 50 percent (from top) residual curvature.

To investigate the effect of steel tube diameter on deformation severity, simulation has done on the model that has 30% residual curvature. The deformation picture of above Figure 7.14 and 7.16 was for steel tubes of 10.45 millimetre dia and 1.85 millimetre thickness.

For 14.45 millimetre dia and 2.0 millimetres thickness there happen Increment of deformation in form of pitch length (Figure 7.18, 7.20 and Table7.4). The reason is larger the dia , greater the unbalanced bending moment it introduces in the structure, so larger deformations occur.
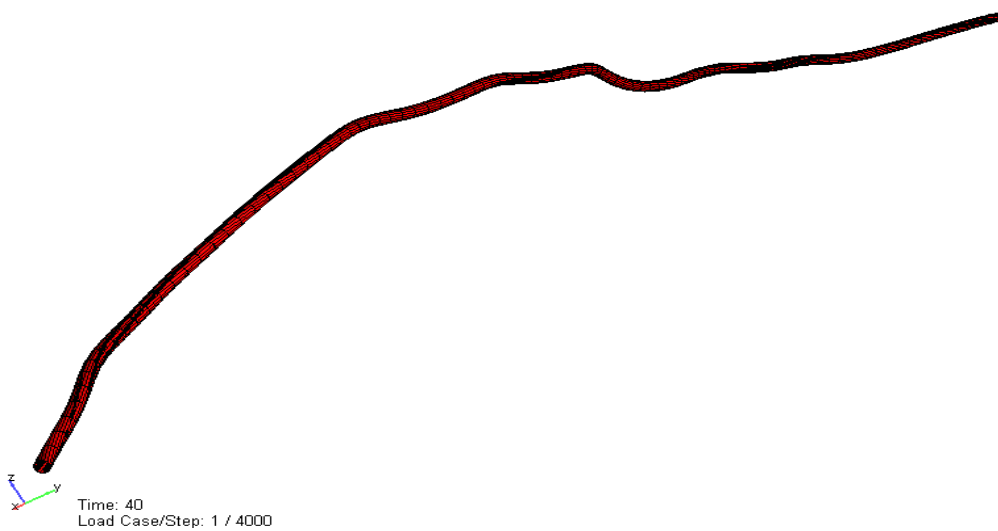

Time: 40
Load Case/Step: 1 / 4000

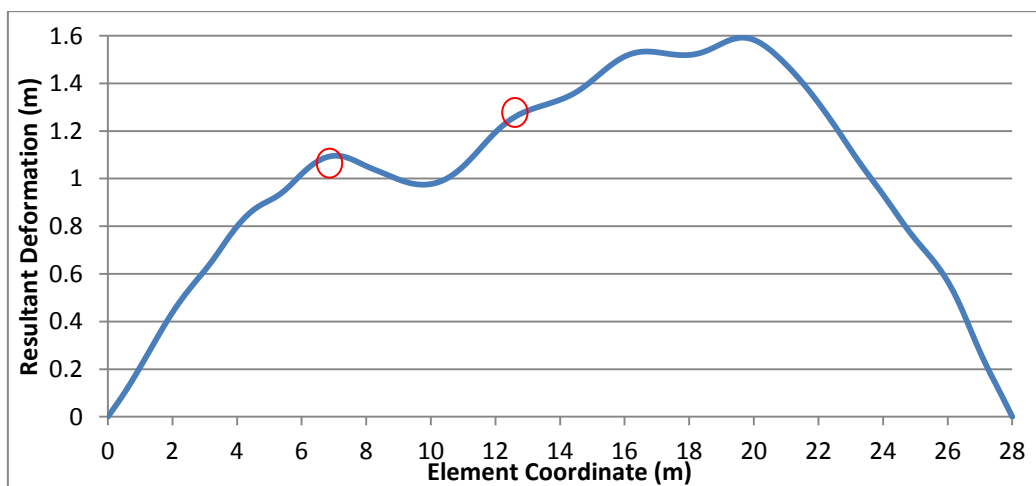*Figure 7.18: Deformation pattern at 30% curvature and larger dia*

Figure 7.19: Resultant curvature along length at 30% and larger dia

Dia (mm)	Maximum Pitch Length (m)	Maximum Double Amplitude (mm)
10.45	4.5	140
14.45	5	130

Table 7.4: parametric study of diameter at 30% curvature

7.3 Kipper

The phenomenon modelled here is reeling of kipper with residual axial strain. The modelling has been done to investigate deformation at two stages of operation. First one is when the kipper has wound on the turntable after extrusion and second one is when it has spool out from the storage reel. Modelling has done to investigate the existence and severity of friction effect on creating these deformations. As a way of introducing friction in the model axial strain has been developed on it before the start of rolling. Having axial strain means that, the model is squeezed to an extent and it has contact between the internal elements.

Deformation in the model start to create as it starts to roll on the reel. The deformation increases with rolling, as shown in Figure 7.20(a) to 7.20(d). The deformation picture after completing the spooling has found as in Figure 7.20(d), which is quite similar to the picture of kipper on turntable (Figure5.10). The deformation pattern is not like helix. It is like, some plastic hinges are forming after some interval of length and the umbilical is moving out from the contact with roller at that position. 6 plastic hinges has formed (marked with circle) on a full wound. High amount of stress is generated at the hinge point as found from the stress plot (Figure 7.21). Both compressive and tensile stress is resulted at hinge point.
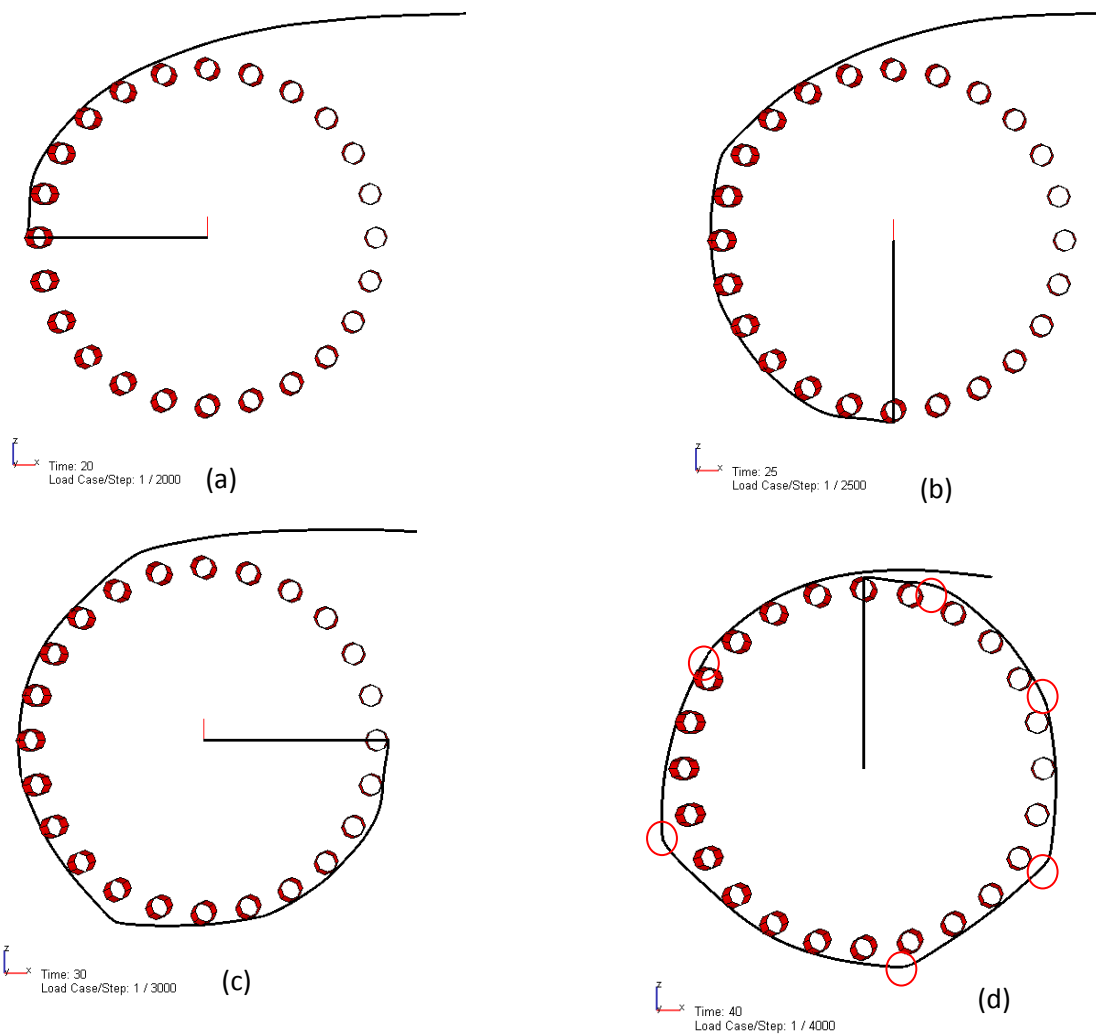

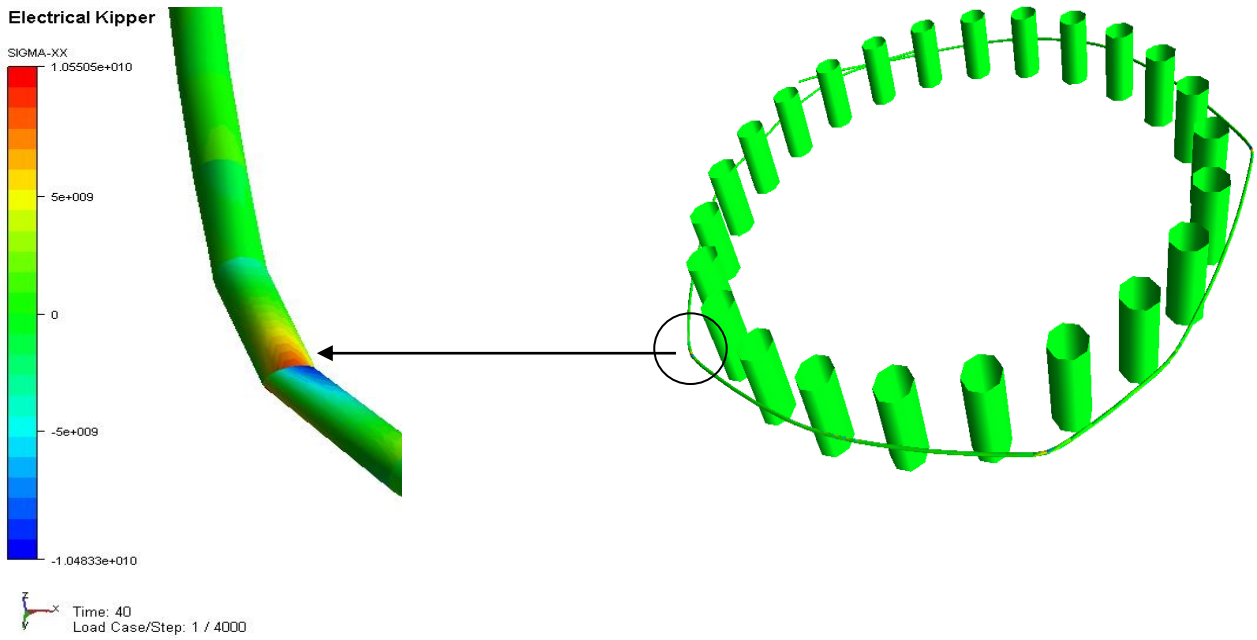Figure 7.20: Development of deformation with spooling in.

Figure 7.21: Axial stress distribution at plastic hinge point (both tension and compression)

The deformation formed in the model after spooling off has been found as in Figure 7.22. Here the pattern is like helix as that found in the real case of Aker's manufacturing plant (Figure5.10). Many twisted spot has been found along the length (marked with circle and zoomed in Figure 7.22) and the twisting was forming in both ways. Having low torsional stiffness might be the reason of twisted deformation. The helical shape of the deformation is not repeating and changing along the length. So it is having variable pitch length and amplitude along length.
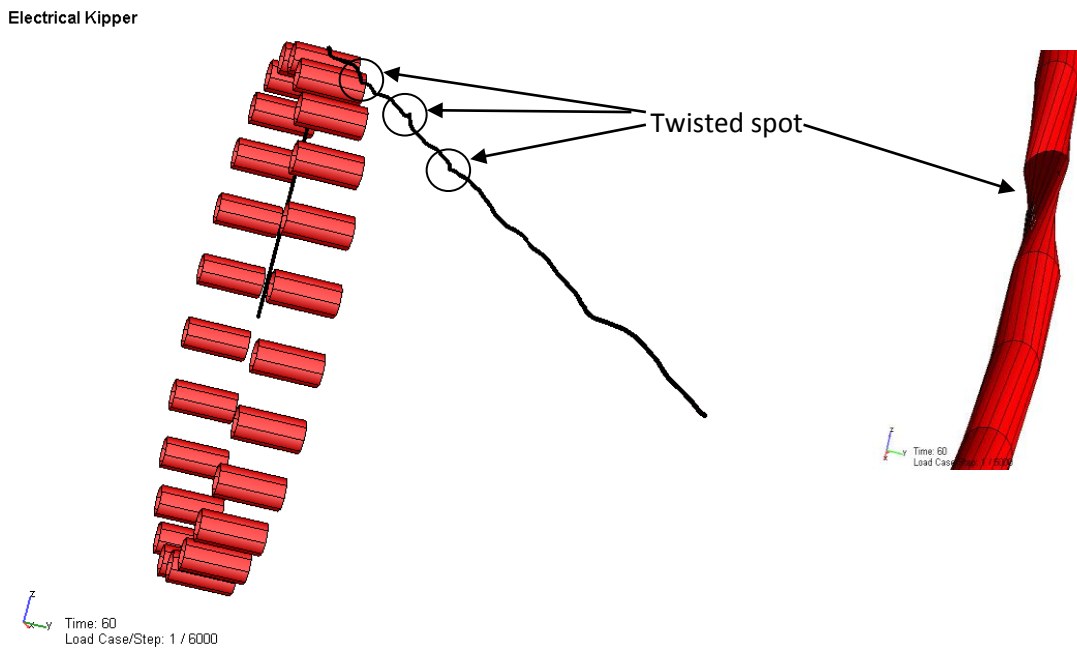

Figure 7.22: Snaking deformation, after spooling off.

Pitch length and amplitude of the deformation can be found from the curvature plot of the model along its length. Coordinate along Y and Z axis for the deformed model after spooling out has been found as in Figure 7.23. Z coordinate is coming very high as the umbilical is 8.4415 meter from the center of global coordinate system along Z axis. The resultant of these two pictures can be made by taking their square root. The calculation table of Figure 7.23 has attached in Appendix C.
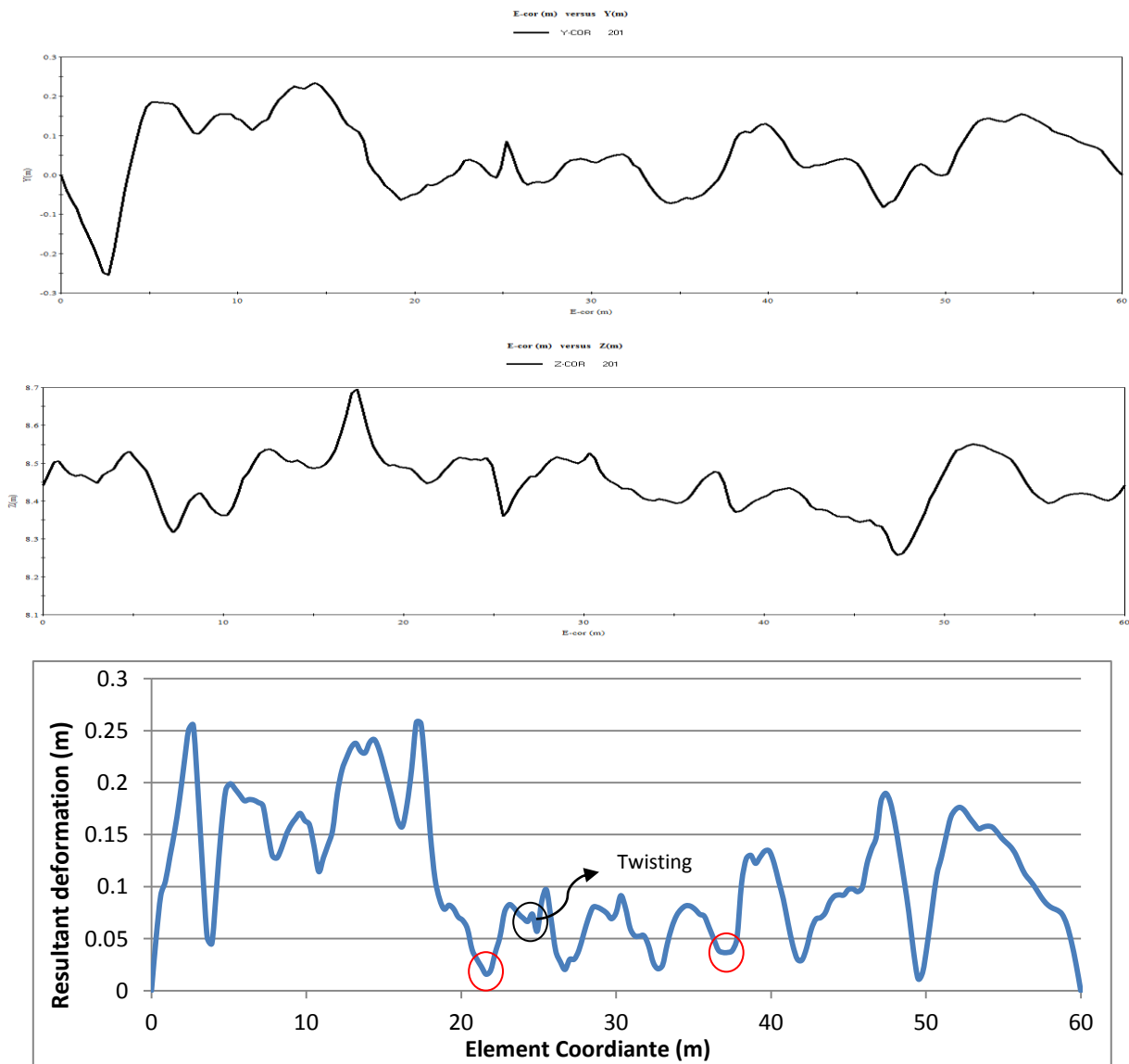

Figure 7.23: Curvature along Y axis (up), Z axis (middle) and resultant (bottom).

The model here has done reeling for a length of 49.64 meter. So the deformation is quite dense in this length. It is very hard to find pitch length and amplitude from this kind of deformation picture. The portion between 22 and 37 meter (red circled) is quite similar to the real picture (Figure5.10). It has three pitch lengths with twisted deformation. Average pitch length here is 5 meter with average double amplitude of 0.08 meter. Maximum deformation is 0.26 meter. Pitch length and amplitude values has difference with real picture but the deformation is quite similar in shape with the real picture. So it can say that friction in the internal structure is the reason of snaking in kipper, as suspected.

Formation of twist tells that twisting moment generating at the twisted spots is higher than the torsional stiffness of Kipper. This can be checked by observing the twisting moment generates in a twisted spot. Figure 7.24 shows the twisting moments at a twisted spot. The maximum moment generate is over 7000 Nm^2 , whereas the torsional stiffness is 980.7 Nm^2. So model kipper has low torsional stiffness and this is the reason of twist formation.
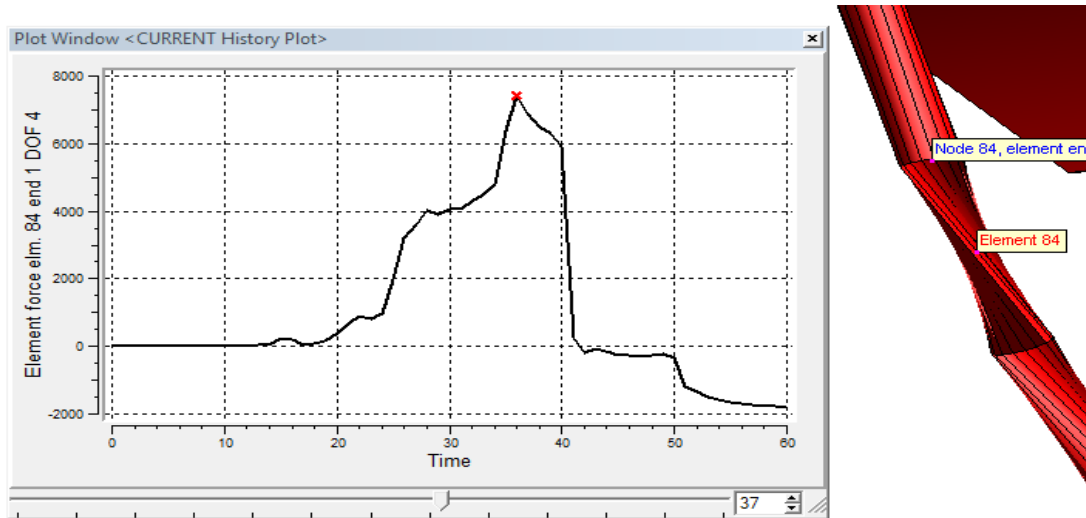

Figure 7.24: Twisting moment history at twisted spot

Moreover bending moment generates at the plastic hinge points can be checked, for instance as found in Figure 7.25 below.

Figure 7.25 Bending moment history at twisted spot

In this plastic hinge point bending moment generates is around 38000 Nm^2 and much higher than the bending moment of Kipper 5470 Nm^2. So umbilical kipper has low bending stiffness and this is the reason of plastic hinge formation.

7.3.1 Parametric Study

To introduce friction, 0.02% axial strain had applied in the tubes of the above model (Kipper1). A certain amount of tension was present in the spooling process to control it smoothly. The amount of tension required in this modelling was very high which is differing very much with the real field. The possible reason could be the low torsional stiffness of kipper, because of which plastic hinges and twisting was forming. Bflex was facing difficulties to overcome these deformations and high amount of tension needed to get convergence. So this modelling has been abled to trace out friction as the reason from the quality point of view not quantity.

Tension has been applied gradually to get numerical stability of the spooling process. In the model above (Kipper1), tension amount in spooling in process has increased from 10 to 70 KN and in spooling out process decreased from 1000 to 200 KN.

7.3.1.1 Tension

Tension applied in the spooling in process has effect on the shape of deformation. To figure out the tension effect parametric study has been done with two other sets of tension, one with 20 to 100 KN (Kipper2) and other with 5 to 30 KN tension (Kipper3) for spooling in. Since tension straighten out the curved section so with the increase of tension, intensity of deformation has reduced (Figure 7.26).
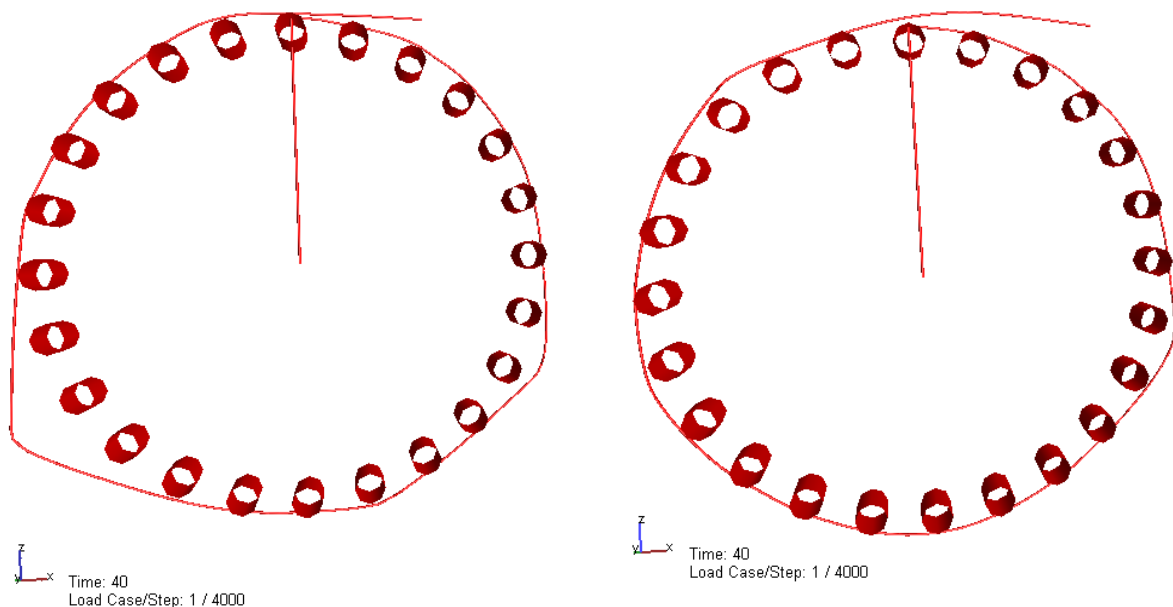

Figure 7.26: Deformation pattern after spooling in, Kipper3 (left) and Kipper2 (right).

For spooling out process the tension needed for Kipper2 is 1000 to 500KN and for Kipper3 is 1000 to 150KN. There curvature plot has found as in Figure 7.27 below
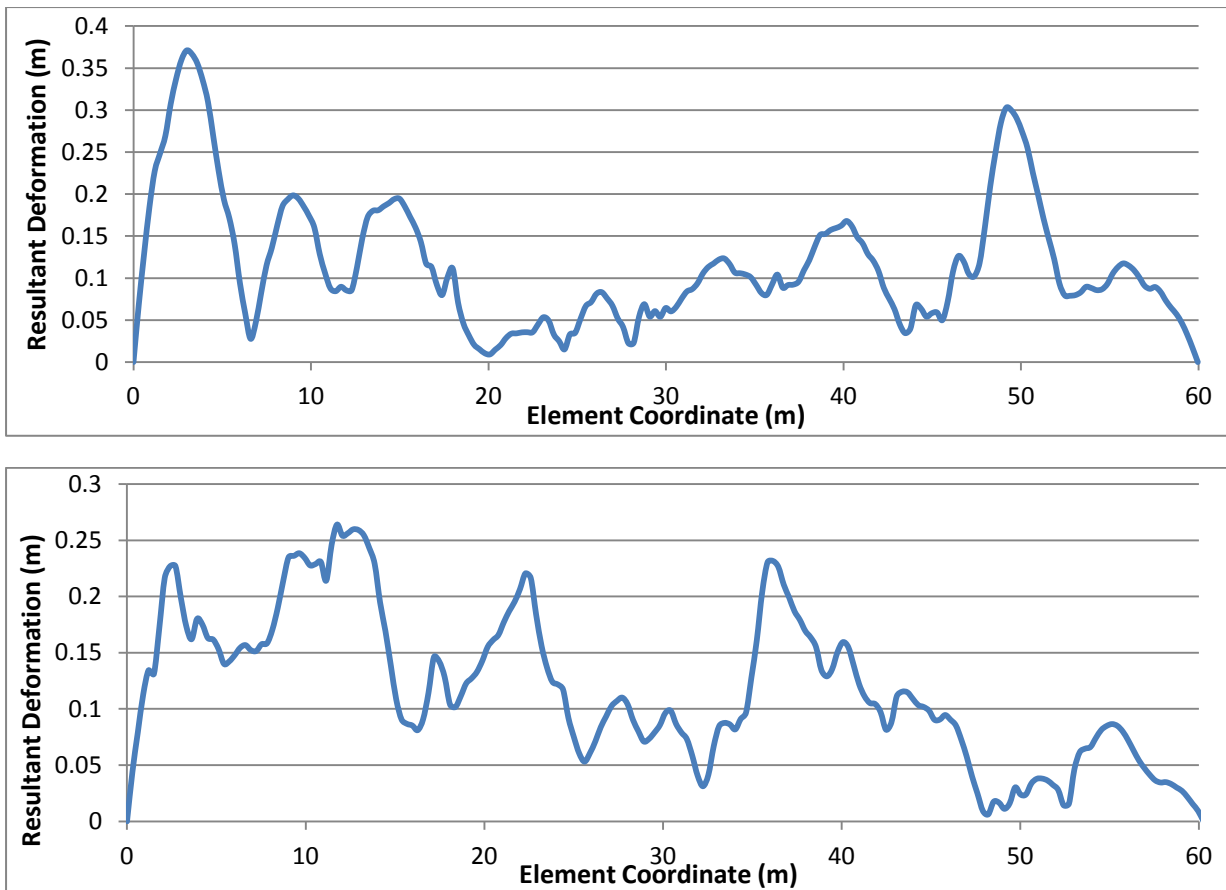
Figure 7.27: Resultant curvature along length after spooling out, Kipper3 (up) and Kipper2 (bottom).

Kipper2 is more regular and have less twisting than Kipper3. The Maximum deformations of them are 0.37, 0.26 meter respectively. So the results suggest that applying more tension lessen the severity of deformation. But too high tension also introduces internal friction in the helical umbilical structure, which in turn can increase the deformation and need to take in concern.

7.3.1.2 Friction

Friction amount can be changed by changing the axial strain value. More the axial strain more the contact between the elements and more the friction in the process. Yield strain of steel is 0.2%, so during modelling this value has taken in the consideration so that plasticity doesn't arise.

To find the behaviour of the model at different friction level one other axial strain level has applied on the Kipper1 model, that is keeping everything unchanged of the Kipper1 model axial strain has increased to 0.06% (Kipper4).
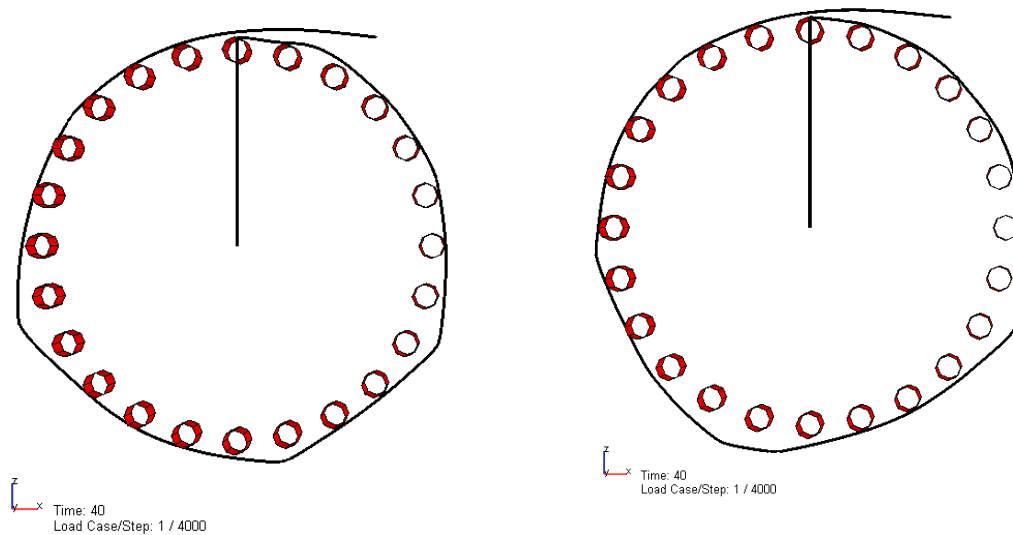
Figure 7.28: Deformation pattern after spooling in with 0.02 % (left) and 0.06% (right) axial strain.

Deformation pattern after reeling in is almost same for both friction level (Figure 7.28) but quite different after reeling out (Figure 7.29). With the increase of friction, magnitude of deformation has increased but density of deformation that is twisting amount was reduced. So with the increase of friction, severity of deformation increases in terms of magnitude and decreases in terms of twisting but it is confirmed that, friction effect introduce the deformation in the model.
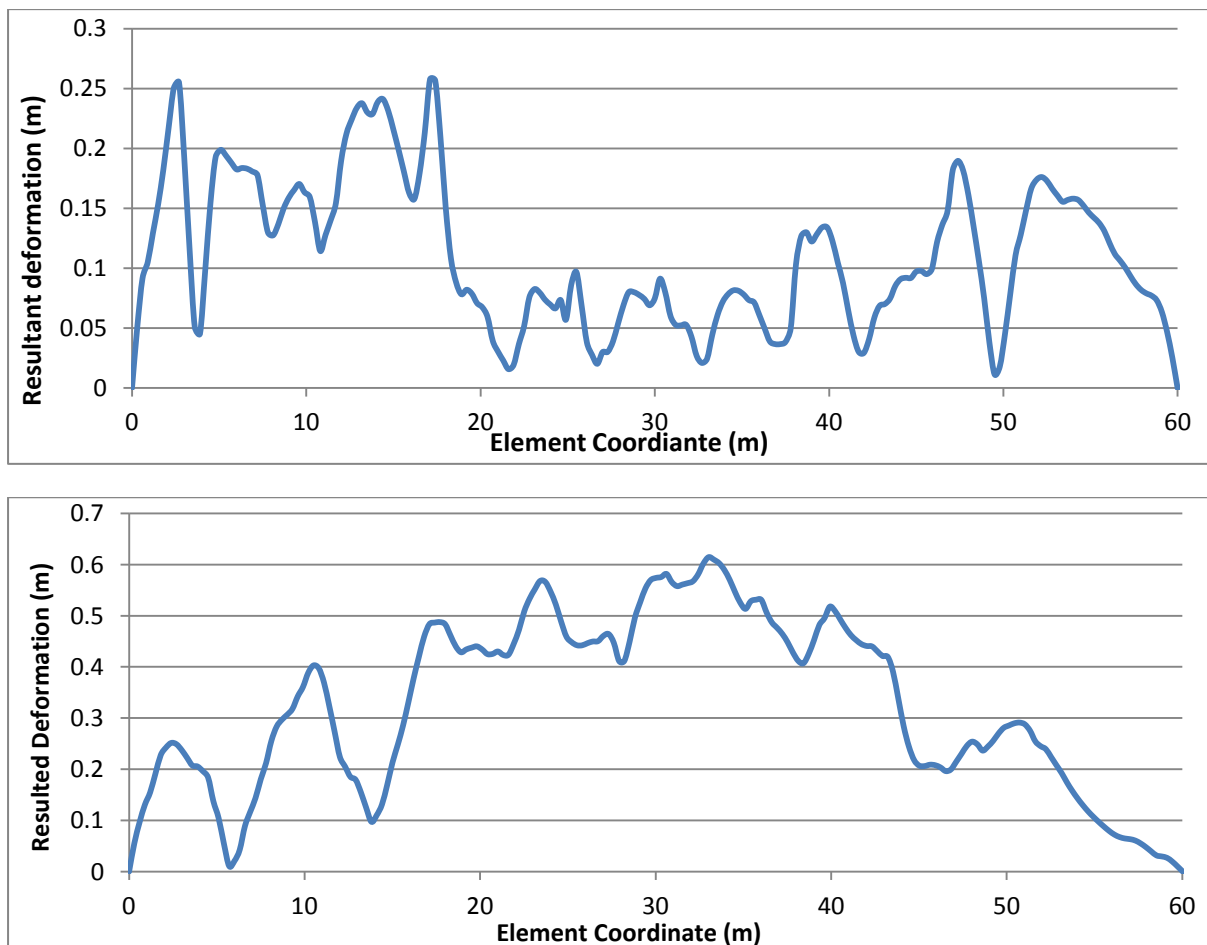

Figure 7.29: Resultant curvature along length after spooling out with 0.02 % (up) and 0.06% (below) axial strain.

7.3.1.3 Torsional Stiffness

Low torsional stiffness is the reason of forming twist, after spooling out. So increase of stiffness will reduce the intensity of twisting. To check this, keeping everything unchanged of Kipper1 model, torsional stiffness has increased to 2980.7 Nm^2 (Kipper5). Figure 7.30 shows their deformation pattern after spooling out, where it seen that Kipper1 has twisted spots much severe than Kipper5.
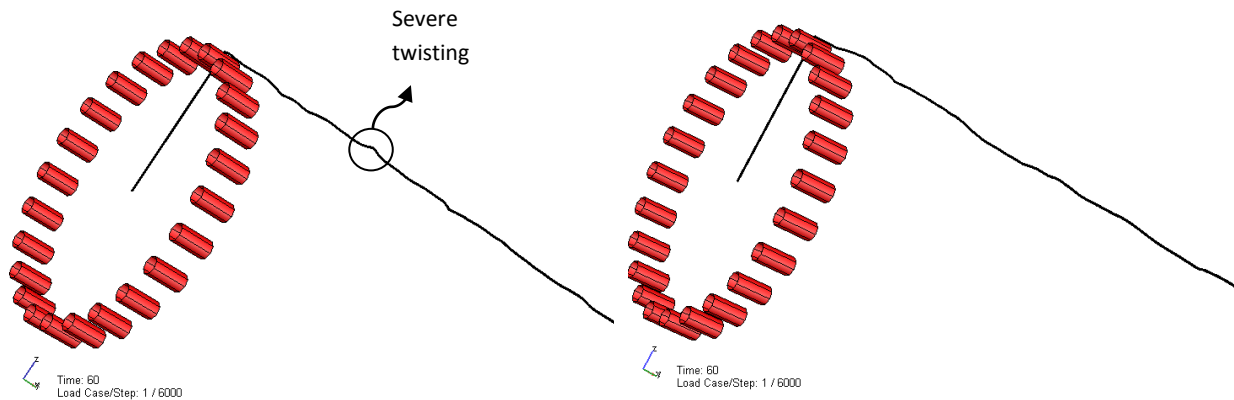

Figure 7.30: Snaking deformation, after spooling out with 980.7 Nm^2 (left) and 2980.7 Nm^2 (right) torsional stiffness.

Amount of twisting forms after spooling out can also be figure out by looking over the curvature plot along length (Figure 7.31). Here it is found that; model having high torsion stiffness has less twisting. Kipper1 has larger number of sharp and irregular peaks. So it is confirmed that torsional stiffness of original model of kipper is such a low that, it get twisted.
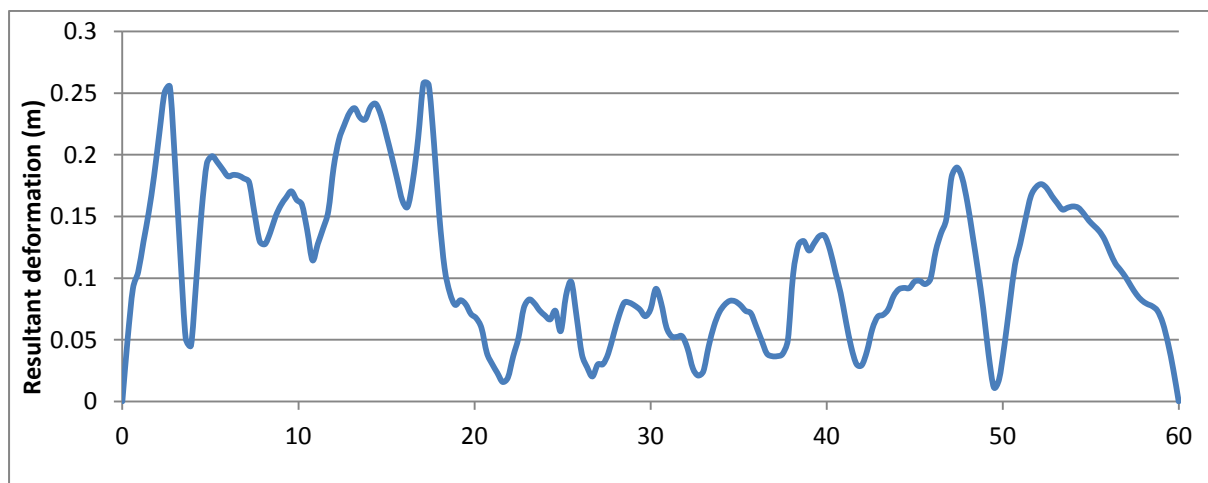

Figure 7.31 (a): Resultant curvature along length after spooling out with 980.7 Nm^2 torsional stiffness.
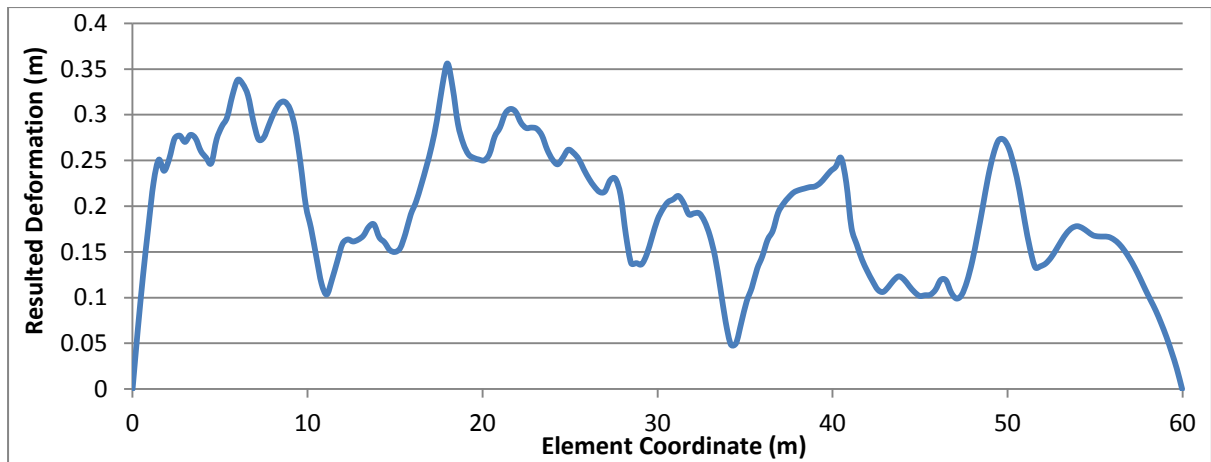
Figure 7.31 (b): Resultant curvature along length after spooling out with and 2980.7 Nm^2 torsional stiffness.

7.3.1.4 Bending Stiffness

Deformation of a flexible structure like umbilical is also related to its bending stiffness. Bending stiffness should be low so that it can be bent for reeling, but not so low that create deformation like plastic hinge.

Each umbilical has minimum bending radius (MBR) beyond which it cannot bend. In Figure 7.32, the model in left (Kipper3) has low bending stiffness then the right one (Kipper6) so it forms more severe plastic hinge. The model with high bending stiffness also shows less deformation after spooling out (Figure 7.33).

Plastic hinge point experiences very high bending moment. Tension applied in the reeling process and bending stiffness of umbilical is the two main factor of plastic hinge formation here.

Higher the bending stiffness, larger the resistance against being bent, so lower the bending amount generates which means lower intensity of plastic hinge (Figure 7.32).

Axial tension reduces the bending amount. So larger the tension lower the bending moment generation, so lower the intensity of plastic hinge (Figure 7.26).
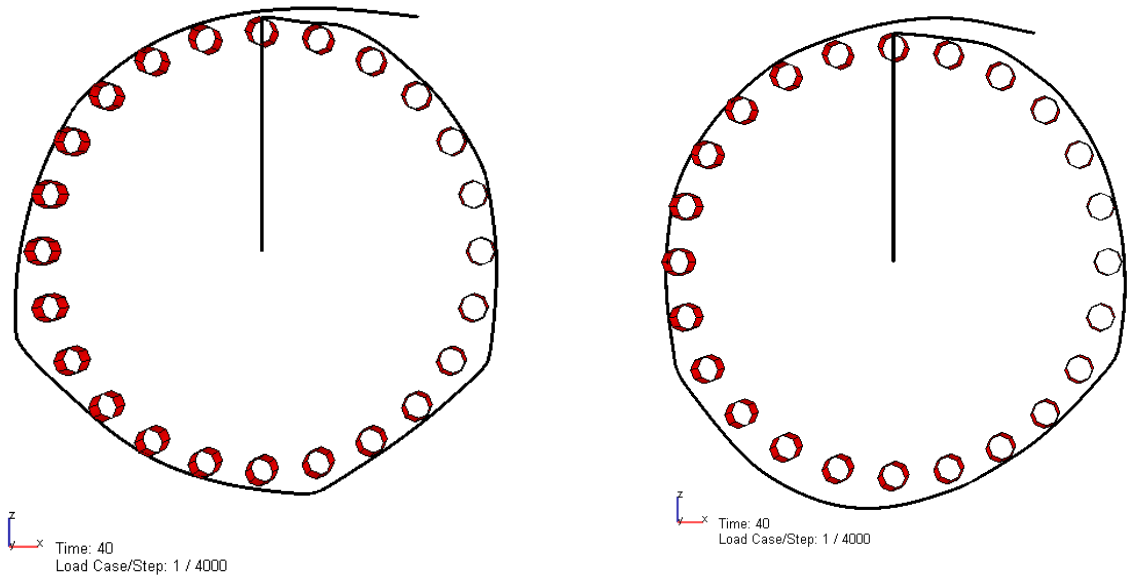
Figure 7.32: Deformation pattern after spooling in with 5470 Nm² (left) and 54700 Nm² (right) bending stiffness.
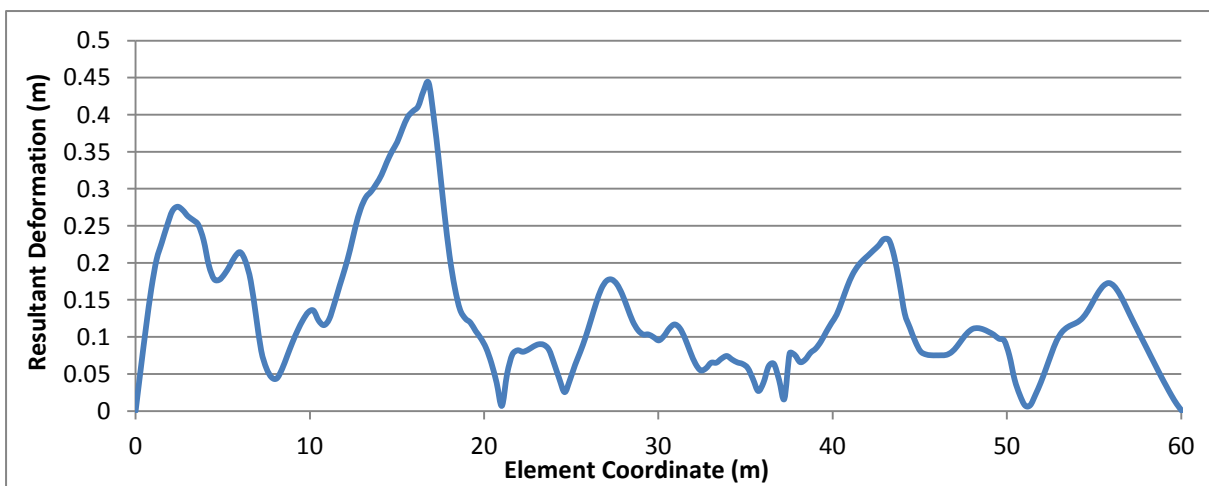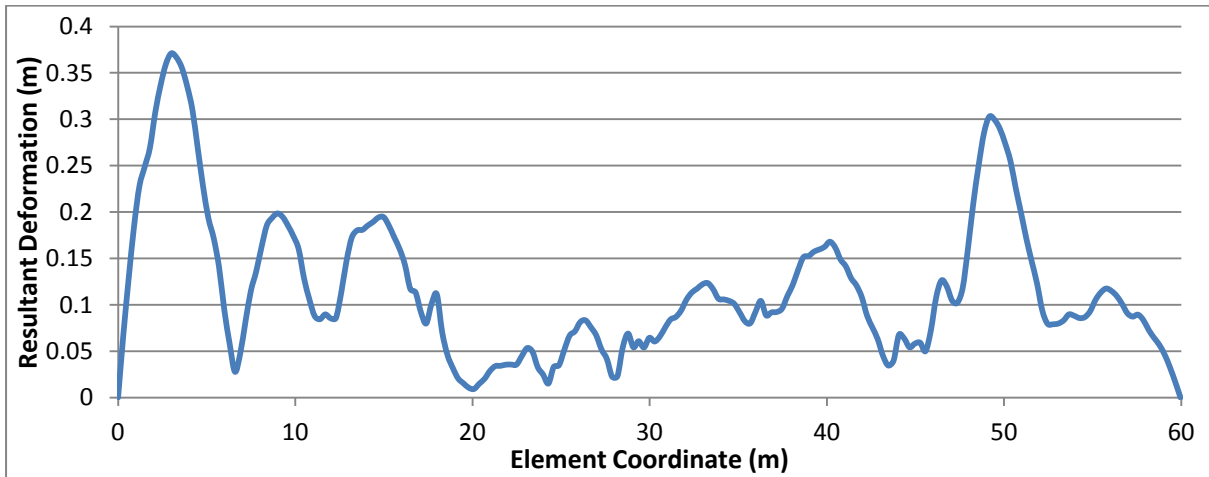

Figure 7.33: Resultant curvature along length after spooling out with 5470 Nm² (up) and 54700 Nm² (below) bending stiffness.

Table 7.5 below presents the all models discussed above and Table 7.6 presents the results of the above parametric studies.

Model Name	Tension, spooling in (KN)	Tension, spooling out (KN)	Strain (%)	Torsional Stiffness (Nm^2)	Bending Stiffness (Nm^2)
Kipper1	10 to 70	1000 to 200	0.02	980.7	5470
Kipper2	20 to 100	1000 to 500	0.02	980.7	5470
Kipper3	5 to 30	1000 to 150	0.02	980.7	5470
Kipper4	10 to 70	250 to 200	0.06	980.7	5470
Kipper5	10 to 70	550 to 150	0.02	2980.7	5470
Kipper6	5 to 30	400 to 150	0.02	980.7	54700
Parametric study of tension between Kipper 1, 2, 3					
Parametric study of friction between Kipper 1, 4					
Parametric study of torsion stiffness between Kipper 1, 5					
Parametric study of bending stiffness between Kipper 3, 6					

Table 7.5: Models of Kipper parametric analysis.

Parametric Study	Results
Increase of Tension	Decrease of snaking severity
Increase of Friction	Increase of magnitude, decrease of snaking twisting
Increase of Torsional Stiffness	Decrease of twisting, after spooling out
Increase of Bending Stiffness	Decrease of plastic hinge formation after spooling in

Table 7.6: Summery of parametric study of Kipper.

Chapter 8: Concluding Remarks

8.1 Conclusions

This thesis work has studied and analysed the loads and deformations in the umbilical structure in manufacturing and installation field in regard to three snaking scenarios. Modelling of six different phenomenon and corresponding simulations have done to find out the reasons of these scenarios. From the simulation results, reason of each snaking scenario has found as:

Agbami: Combination of residual curvature from creeping with gravity load and twisting.

Droshky: Residual curvature in the component steel tubes.

Kipper: Internal friction.

From the parametric study following conclusions have found regarding the deformation of umbilicals.

- It is expected that friction effect will always create some curvature in the umbilical after its reeling operation but the opposite might happen, there might not generation of curvature after reeling operation; as found from the Agbami reeling model.
- Internal friction arises from the orientation of umbilical components in its cross section, especially when the components have no gap with PVC profile and this creates deformation both during spooling in and spooling out on reel; as the Kipper simulations showed.
- The insufficient stiffness of umbilical structure will introduce deformation like creation of plastic hinges due to low bending stiffness and twisting from low torsional stiffness; as happened in Kipper model.
- The load arises on one of the component tube of umbilical during installing in water, due to not getting compression in tensioner might not large enough to create snaking in the whole umbilical as Agbami tensioner effect model showed.
- If two opposite curvatures appear in the same length then it is obvious to happen snaking deformation, presence of twisting rotation will intensify the snaking and can create torsional instability also; as found from Agbami torsional instability model.
- Presence and severity of snaking not only depend on the type and amplitude of load but also on the appearance sequence of loads; as found from Agbami torsional instability model.

The reason of snaking can be identified by knowing when and where it has appeared, if it appears in

- Manufacturing plant, then the reason is curvature of the component steel tubes which arises from straightener machine. The intensity of this snaking proportionally depends on the amount of curvature on tube and diameter of the tube; as showed by the Droshky model.
- During reeling operation, then development of internal friction in the reeling process is the reason beside residual curvature; as found from the simulations of Kipper.
- During unreeling after long time of storage, then creeping of outersheath is the reason. This has been confirmed from the Agbami reeling model, as friction did not generate any curvature.

To reduce the snaking deformation in umbilical, care need to take in it's designing so that less internal friction and unbalanced bending moment develops. Also cares need to put in the manufacturing plant operations, like:

- Estimation of storage time by considering the material property of outersheath and temperature of the storing place, to avoid creeping.
- Using bending shoe in the straightening process.
- Using a supporting structure while transferring from storage reel to installation work, which will guide the umbilical not creating any unsupported length.

8.2 Proposals for Future Work and Recommendations

1. The analysis of this thesis work is done by doing simulations in software USAP and Bflex. In few cases, simulations has faced convergence problem for example reeling simulation of Kipper.
   The reason of the problem needs to find and need improvement in the solution algorithm.
2. The phenomenon of not finding friction effect in Agbami reeling is not what supposed to be happen. So it needs some more investigation and analysis like modelling in Bflex etc.
3. Improvement in the analytical model of torsional instability, for the consideration of curvature from gravity load.
4. For each umbilical more information is needed to make complete evaluation of their deformation reasons. Like deformation history starting from straightening, then extrusion, transferring to reel, storage and transferring for installation work, when and where other deformation had found.

   Also it is quite hard to measure the pitch length and amplitude of deformation from their pictures so deformation need to measure in the real field when it is appears.

References

1. *S. Sævik and O.D.Okland and J.K. Gjosteen., USAP - User Manual. MARINTEK, Trondheim, Norway, 2014.*
2. *S. Sævik and J.K. Gjosteen, USAP - Theory Manual.* MARINTEK,Trondheim, Norway, 2010.
3. Gjosteen, S.S.a.O.D.O.a.G.S.B.a.J., *Bflex2010 - Users Manual.* MARINTEK,Trondheim, Norway. Marintek Document, 2009.
4. Sævik, S., *Bflex2010 - Theory Manual.* MARINTEK,Trondheim, Norway, 2010.
5. *Aker Solutions*. Available from: http://www.akersolutions.com/en/Global-menu/Products-and-Services/Subsea-technologies-and-services/Subsea-production-systems-and-technologies/Umbilicals-and-power-cables/.
6. Heggdal, O., *The Integrated Production Umbilical (IPU®) and Design Tools for Deep Water.* Proceedings of the Offshore Technology Conference. Houston, TX. OTC17157, 2005.
7. *Technip*. Technip's presentation of Umbilicals; Available from: http://www.technip.com/en/our-business/subsea/umbilicals
8. *Glossary of terms and abbreviated terms for use with umbilical systems*. UMF-GN02-03, October 2011.
9. Josef, H.F. and W. Karlheinz, *Roller straightening machine*. 1969, Google Patents.
10. Sævik, S., *Lecure notes in offshore pipeline technology*. Institute of Marine Technology 14th February, 2013.
11. Ekeberg, K.I.,Ottesen, T., Aarstein .J, Sævik, S., Ye, N., Igland, R.T., *Predicting, Measuring and Implementing Friction- and Bending Stresses in Dynamic Umbilical Design.* Proceedings of the Offshore Technology Conference, OTC 17986, Houston, 2006.
12. Dixon-Stubbs, P.J., *Creep behaviour of polyethylene and polypropylene.* Journal of Materials Science, February 1981,. **Volume 16**(2): p. 389-396.
13. *Wikipedia* Available from: http://en.wikipedia.org/wiki/Medium-density_polyethylene.
14. Sævik, S., Bruaseth, S., *Theoretical and experimental Studies of the Axisymmetric Behaviour of Complex Umbilical Cross-sections.* Applied Ocean Research 27(2005): p. 97-106.
15. Sævik, S., Gjøsteen, J.K., Figenschou, A., *Comparison between Predicted and Measured Umbilical Bending Stresses during Manufacturing.* Proceedings of the 25th International Conference on Offshore Mechanics and Arctic Engineering, ISBN: 0-7918-4746-2, OMAE2006—92563, June 4-9, Hamburg, Germany, 2006.
16. Sævik, S., *Theoretical and experimental studies of stresses in flexible pipes.* Comput. Struct., 2011. **89**(23-24): p. 2273-2291.
17. Fylling, I., Larsen, C. M., Sødahl, N., Ormberg, H., Engseth, A., Passano, E., and Holthe, H., *Riflex - theory manual.* Technical Report STF70-F95219, SINTEF Structural Engineering, 1995.
18. Amdahl, J.a.S., T., *Usfos - Theory Manual.* SINTEF, Trondheim, Norway, 1993.
19. Mathisen, K.M., *Large Displacement Analysis of Flexible and Rigid Systems Consdiering Displacement-Dependent Loads and Non-Linear Constraints.* PhD thesis, Norwegian Institute of Technology, Trondheim, Norway, 1990.
20. Sævik, S., Thorsen, M.J., *Techniques for predicting tensile armour buckling and fatigue in deep water flexible pipes.* Proceedings of the 31th International Conference on Ocean, Offshore and Arctic Engineering, OMAE2012-83563, July 1-6, 2012, Rio de Janeiro, Brazil.

Appendix A: Calculation of Material Properties of the Models

Agbami Tensioner effect:

<u>Whole umbilical:</u>

EA = 4.62E8 N

EI = 2.68E4 Nm^2

GI$_t$ = 2.06E4 Nm^2

Weight in air (empty) = 400 N/m

Inner Dia of big steel tubes = 25.4 mm

Inner Dia of small steel tubes = 12.7 mm

Outer dia of Agbami = 178 mm

Hollow area of tubes = $4 \times \left[\pi \left(\frac{25.4}{2} \right)^2 \right] + 22 \times \left[\pi \left(\frac{12.7}{2} \right)^2 \right] = 4813.7$ mm^2

Filling factor F$_f$ = 0.95

So, solid area of umbilical A = $\pi (\frac{178}{2})^2 \times 0.95 - 4813.7 = 18826.68$ mm^2

Density = $\frac{400}{9.81 \times 18826.68 \times 10^{-6}} = 2166$ Kg/m

<u>Helix:</u>

Solid Area = $\left[\pi \left(\frac{15.38}{2} \right)^2 \right] - \left[\pi \left(\frac{12.7}{2} \right)^2 \right] = 59.1$ mm^2

I = $\left[\frac{\pi}{4} \left(\frac{15.38}{2} \right)^4 \right] - \left[\frac{\pi}{4} \left(\frac{12.7}{2} \right)^4 \right] = 1469.6$ mm^4

I$_t \approx$ 2I = 2939.2 mm^4

Mass = $7850 \times 59.1 \times 10^{-6} = 0.46$ kg/m

Mean structure radius = 14.125 mm

Thickness = 2.85 mm

$E = 2E11$ N/m^2

$G = 8E10$ N/m^2

υ = 0.3

EA =1.18E7 N

EI = 293.9 Nm^2

GI$_t$ = 235.14 Nm^2

Core pipe:

EA = $4.62 \times 10^8 - 1.18 \times 10^7 = 4.502 \times 10^8$ N

EI = $2.68 \times 10^4 - 293.9 = 2.65 \times 10^4$ Nm^2

GI$_t$ = $2.06 \times 10^4 - 235.14 = 2.04 \times 10^4$ Nm^2

$E = 2.33E10$ N/m^2

υ = 0.4

$G = 0.896E10$ N/m^2

Droshky:

Whole umbilical:

EA = 1.99E8 N

EI = 8.58E3 Nm^2

GI$_t$ = 6.6E3 Nm^2

Weight in air (empty) = 154 N/m

Inner Dia of big steel tubes = 19.05 mm

Inner Dia of small steel tubes = 12.7 mm

Outer dia of Droshky = 115 mm

Hollow area of tubes = $5 \times \left[\pi \left(\frac{19.05}{2}\right)^2\right] + 7 \times \left[\pi \left(\frac{12.7}{2}\right)^2\right] = 2311.86$ mm^2

Filling factor F$_f$ = 0.95

So, solid area of umbilical A = $\pi(\frac{115}{2})^2 \times 0.95 - 2311.86 = 8075.06$ mm^2

Density = $\frac{154}{9.81 \times 8075.06 \times 10^{-6}} = 1944.04$ Kg/m

Each Helix:

Solid Area = $\left[\pi \left(\frac{22.75}{2}\right)^2\right] - \left[\pi \left(\frac{19.05}{2}\right)^2\right]$ = 121.47 mm^2

I = $\left[\frac{\pi}{4}\left(\frac{22.75}{2}\right)^4\right] - \left[\frac{\pi}{4}\left(\frac{19.05}{2}\right)^4\right]$ = 6684.38 mm^4

I$_t$ ≈ 2I = 13368.76 mm^4

Mass = $7850 \times 121.47 \times 10^{-6} = 0.954$ kg/m

Mean structure radius = 10.45 mm

Thickness = 1.85 mm

$E = 2E11$ N/m^2

$G = 8E10$ N/m^2

υ = 0.3

EA =2.43E7 N

EI = 1336.9 Nm^2

GI$_t$ = 1069.5 Nm^2

Core pipe:

EA = $1.99 \times 10^8 - 3 \times 2.43 \times 10^7 = 1.26 \times 10^8$ N

EI = $8.58 \times 10^3 - 3 \times 1.34 \times 10^3 = 4.56 \times 10^3$ Nm^2

GI$_t$ = $6.6 \times 10^3 - 3 \times 1.07 \times 10^3 = 3.39 \times 10^3$ Nm^2

$E = 4E8$ N/m^2

υ = 0.4

$G = 1.43E8$ N/m^2

Kipper:

Whole umbilical:

EA = 1E8 N

EI = 5.49E3 Nm^2

GI$_t$ = 1E3 Nm^2

Weight in air (empty) = 106 N/m

Outer dia of Kipper = 83 mm

Filling factor F$_f$ = 0.95

So, solid area of umbilical A $\approx \pi(\frac{83}{2})^2 \times 0.95 = 5140$ mm^2

Density = $\frac{106}{9.81 \times 5140 \times 10^{-6}} = 2102$ Kg/m

Each Helix:

Dia of each wire = 3.64 mm

Outer radius of bundle = 6.5 mm

Helix Thickness = 1. 5 mm

Mean structural radius = 5.75 mm

Area = $7 \left[\pi \left(\frac{3.64}{2} \right)^2 \right] = 72.84$ mm^2

Mass = $7850 \times 72.84 \times 10^{-6} = 0.57$ kg/m

I = $7 \left[\frac{\pi}{4} \left(\frac{3.64}{2} \right)^4 \right] = 60.34$ mm^4

I$_t$ = 2I = 120.68 mm^4

$E = 2E11$ N/m^2

$G = 8E10$ N/m^2

υ = 0.3

EA = 1.46E7 N

EI = 12.068 Nm^2

GI$_t$ = 9.65 Nm^2

Core pipe:

EA = $10 \times 10^7 - 2 \times 1.46 \times 10^7 = 7.08 \times 10^7$ N

EI = $5.49 \times 10^3 - 2 \times 12.068 = 5.47 \times 10^3$ Nm^2

GI$_t$ = $1 \times 10^3 - 2 \times 9.65 = 0.9807 \times 10^3$ Nm^2

$E = 4E10$ N/m^2

υ = 0.4

$G = 1.43E9$ N/m^2

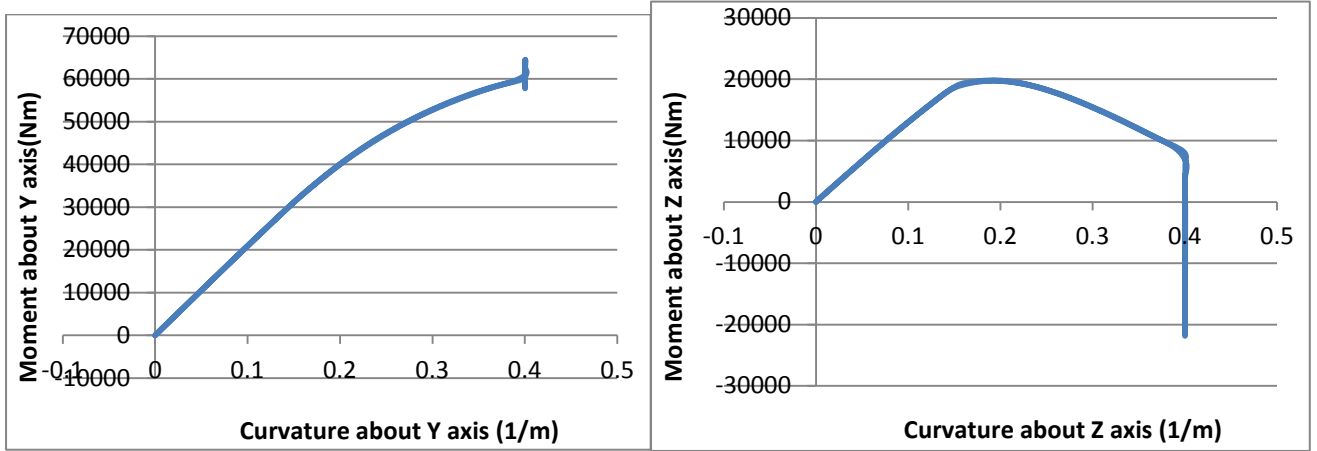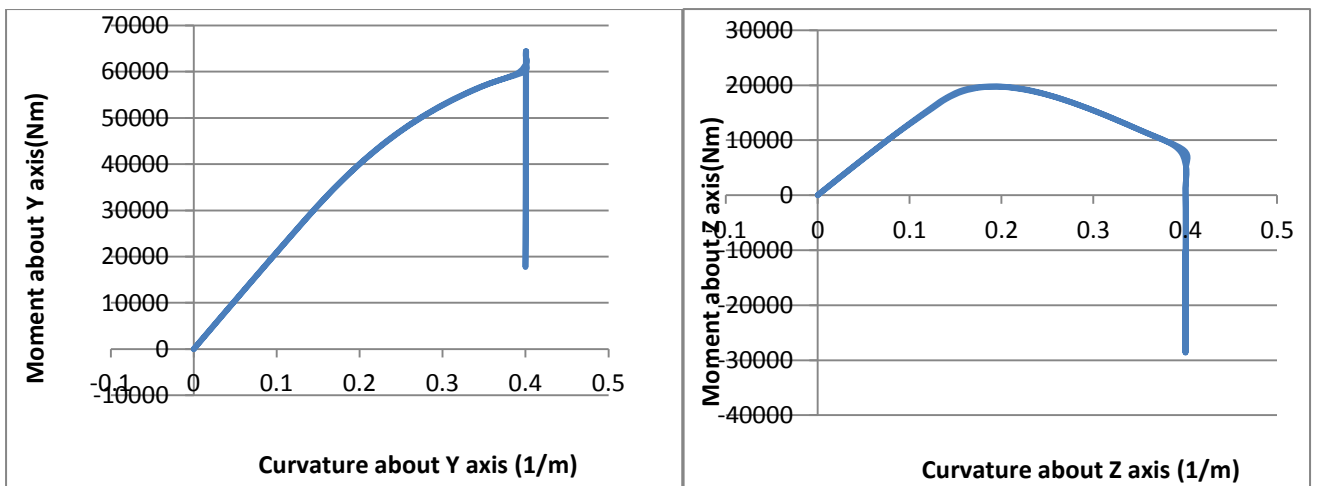# Appendix B: Agbami Reeling of 180 and 270 Degree

Figure: 180 deg.

Figure: 270 deg.

Appendix C:

Soft copies of

1. Input files of all models.
2. Calculation of all the figures and tables.